DESIGN AND DEVELOPMENT OF A STERILIZATION BOX AND ITS VARIANTS WITH DIFFERENT FUNCTIONALITIES

A Thesis Submitted in Partial Fulfillment of the Requirements for the Degree of

DOCTOR OF PHILOSOPHY

by

Nilkamal Mahanta

(Roll number: 176103015)

Department of Mechanical Engineering
Indian Institute of Technology Guwahati
Guwahati 781039
INDIA

April 2024

DECLARATION

I declare that,

a. The work contained in this thesis is original and has been done by me under the guidance of my supervisor.
b. The work has not been submitted to any other institute for any degree or diploma.
c. I have followed the guidelines provided by the institute in preparing the thesis.
d. I have confirmed the norms and guidelines given in the ethical code of conduct of the institute.
e. Whenever I used materials (data, theoretical analysis, figure and text) from other sources, I have given due credit to them by citing them in the text of the thesis and giving their details in references.

Signature of the student

(Nilkamal Mahanta)

CERTIFICATE

It is certified that the work contained in the thesis entitled "Design and Development of a Sterilization Box and its Variants with Different Functionalities" is submitted by Mr. Nilkamal Mahanta to the Indian Institute of Technology Guwahati for the award of the degree of Doctor of Philosophy. The work has been carried out under my supervision in the Department of Mechanical Engineering, Indian Institute of Technology Guwahati. This work has not been submitted elsewhere for the award of any other degree or diploma.

Dr. Uday Shanker Dixit
Professor
Department of Mechanical Engineering,
Indian Institute of Technology Guwahati,
Guwahati-781039, INDIA

Date: April 18, 2024

Dedicated to Almighty GOD, My Parents and My Teachers

Acknowledgements

The journey is eternal when we are fortunate enough to have blessings from Almighty. I would like to start by thanking Almighty for giving me strength during this journey. Started with trust and faith; I would like to extend my sincere gratitude to my supervisor Prof. Uday Shanker Dixit, Department of Mechanical Engineering, IIT Guwahati, for his ideas, suggestions, encouraging interactions, and constructive criticism. Without his expert guidance and patience, it would not have been possible for me to carry out this research work. I shall always be grateful to him.

I would also like to extend my gratitude to Dr. Lalit Mohan Pandey for his enormous support and encouragement to carry out research in the Department of Biosciences and Bioengineering (BSBE), IIT Guwahati. I express my sincere gratitude to my doctoral committee members, Prof. Debabrata Chakraborty (Chairperson), Prof. Anoop K. Dass, and Prof. Chitralekha Mahanta for their valuable suggestions and comments. I am also grateful to the former and present heads of the Department of Mechanical Engineering, Prof. A.K. Dass, Prof. S.K. Dwivedy, Prof. S. Senthilvelan, and Prof. K.S.R. Krishnamurthy. I would like to thank the staff members of the Central Workshop and Department office. A special thanks to Mr. Gwmchar Baro, Mr. Dilip Chetry, Mr. Mrinal Sarma, Mr. Manoj Baishya, Mr. Gautam Gogoi, and Mr. Sontosh Gogoi for helping me to work in the Central Workshop. Also, I am thankful to the Central Instrument Facility (CIF), IIT Guwahati for letting me perform my experiments. Also, the financial assistance provided by the Ministry of Human Resource Development (MHRD), Government of India, is greatly acknowledged.

I express my sincere thanks to my seniors Dr. Polash Pratim Dutta, Dr. Rajkumar Shufen, Dr. Vikash Kumar, Dr. Amit Raj, Dr. Faladrum Sharma, Mr. Sujoy Tikader, and my friends Dr. Nitish Bhardwaj, Mr. Nilavjyoti Sarmah, Dr. Pranjyoti Saikia, Dr. Kaustabh Chatterjee, Dr. Bappa Das, Mr. Bhanu Prakash Bonthala, and Mr. Biswajeet Barman. I would specially want to thank Dr. Swati Sharma, Dr. Varun Saxena, Dr. Priyanka Batra, and Mrs. Laipubam Gayatri Sharma for extending a helping hand to carry out my experiments in the Department of BSBE, IIT Guwahati. Thanks to all my IIT Guwahati friends and childhood friends for their great encouragement and best wishes.

Finally, my deepest gratitude goes to my beloved parents, my father Mr. Nanimadhab Adhikary and my mother Mrs. Swapna Adhikary for their encouragement and moral support throughout my life. My sister Miss Shyamali Mahanta and brother Mr. Kamallochan Mahanta deserve my wholehearted thanks for sharing all of my family's responsibilities while I was pursuing my PhD. I take the opportunity to thank my grandfather Late Kaliram Kalita, who drove me to my first school and my paternal uncle Late Sukhamoy Datta Adhikari, who looked after my education all the time.

Once again, I would like to thank Almighty for everything. I apologize for the unintentional moments when I could not recognize your presence in my life. May the thankfulness and love I feel for you be reflected in my choices and actions as well. I will always indebted for your profound lessons of consciousness that you have bestowed upon me. Everything I have, I owe to you.

With sincere appreciation

Nilkamal Mahanta

IIT Guwahati

Abstract

The purpose of design and development of a new product is to transform ideas into tangible products. Product design and development is an exciting adventure that integrates several sectors of engineering with creative vision and user-centric thinking. Severe acute respiratory syndrome coronavirus 2 (SARS-CoV-2) emphasized the researchers to design and develop a sterilization box equipped with an efficient approach for the prevention of coronavirus disease 2019 (COVID-19).

A sterilization box is designed with both ultraviolet-C (UV-C) radiation and incandescent bulb heating facilities. For performance assessment, two studies were carried out. Firstly, unfolding of Immunoglobulin G (IgG) glycoprotein (a model protein similar to that of spike glycoprotein of SARS-CoV-2) and secondly, antibacterial efficacy for the clinically relevant *E. coli* bacteria as well as for bacteria collected from daily use items. IgG was incubated under UV-C and heat sterilization. An incubation with simultaneous UV-C at 70 °C for 15 min was found to be effective in unfolding and aggregation of the protein. The experimental parameters were optimized using a statistical tool. At optimized condition, the hydrodynamic size of the protein increased to ~171 nm from ~5 nm of the native protein. Similarly, the optical density at 280 nm (OD_{280}) values also increased from 0.17 to 0.78 indicating the exposure of more aromatic moieties and unfolding of the protein. The unfolding and aggregation of the protein were further confirmed by the intrinsic fluorescence measurement and Fourier Transform Infrared Spectroscopy (FTIR), showing a 70% increase in the β-sheets and a 22% decrease in the α-helixes of the protein. The designed box was effective in damaging the protein's native structure indicating the effective inactivation of the SARS-CoV-2. Furthermore, the incubation at 70 °C for 15 min inside the chamber resulted in 100% antibacterial efficacy for the *E. coli* bacteria as well as for bacteria collected from daily use items. It is the first detailed performance study on the efficacy of using simultaneous UV-C irradiation and heat for disinfection against virus and bacteria.

Next, another product is designed to develop minimum viable products (MVPs). MVP is a product built with the few sets of features as well as extensive research incorporating the product's aesthetics, market fit, and usability. Infrared (IR) radiation of high energy efficiency, uniform heating, and more penetration power, is used in the newly designed sterilization box

combined with UV-C irradiation. It is tested for its disinfection ability against pathogenic bacteria and SARS-CoV-2 spike protein. The killing of a Gram-positive, namely, *S. aureus* and a Gram-negative namely, *S. typhi* bacteria was studied followed by the inactivation of the spike protein. For the broad-spectrum antibacterial activity, the optimum condition was holding at 65.61 °C for 13.54 min. The killing of the bacterial pathogen occurred via rupturing the cell walls as depicted by electron microscopy. Further, the unfolding of SARS-CoV-2 spike protein and RNase A was studied under IR and UV-C irradiations at the aforesaid optimized condition. The unfolding of both the proteins was confirmed by changes in the secondary structure, particularly an increase in β-sheets and a decrease in α-helixes. Remarkably, the higher penetration depth of IR waves up to subcutaneous tissue resulted in lower optimum disinfection temperature, less than 70 °C in vogue. Thus, the combined UV-C and IR radiation is effective in killing the pathogenic bacteria and denaturing the glycoproteins.

Showing different functionalities, sterilization box is used to disinfect N95 filtering face-piece respirators (FFRs). Degradation of FFRs was studied for five disinfection methods, viz., incandescent bulb heating, UV-C irradiation, air drying after alcohol immersion, exposing to steam, and incandescent bulb heating combined with UV-C irradiation. Effects of these methods on fiber diameter, surface roughness (R_a), ultimate tensile strength (UTS), and scratch resistance of the disinfected fibers were compared. Fibers treated with incandescent bulb heating, steam exposure, and incandescent bulb heating combined with UV-C irradiation became thinner and smoother. On the other hand, alcohol and UV-C treatment made fiber rougher (and consequently increased fiber diameter), although the effect was statistically not much significant. Incandescent bulb heating combined with UV-C irradiation caused lesser reduction in UTS and scratch resistance than that in other methods. X-ray diffraction (XRD) analysis did not indicate any significant chemical changes in the surface after disinfection. Overall, the minimal effect on degradation was observed in incandescent bulb heating combined with UV-C irradiation.

Further, sterilization box is transformed into a pedagogical gadget to develop MVPs. Pedagogy is the art and science of teaching-learning approaches. The gadget was designed for teaching the basic concepts of heat transfer by conducting experiments, increasing the students' engagement in hands-on practices, developing the team spirit by making them work in a group

and attracting students towards a career in mechanical engineering. Five possible experiments with the help of developed gadget are described. A survey was carried out among students and teachers of different levels using a set of written questions and statements in a feedback form. Participants involved in this survey were from seven different institutions. Feedback from the participants provided important information related to the gadget viz., its pedagogical usefulness and required modifications in the gadget. The enthusiasm of the participants towards hands-on activities was revealed through the survey. A study for assessing the impact of pedagogical gadget was conducted among a group of newly graduated mechanical engineering students. In general, the potential users found the developed gadget very useful for improving teaching-learning activity.

Furthermore, sterilization box is used for artificial ageing of rice, showing its another functionality. Artificial ageing positively impacts the cooking and eating qualities of rice, but natural ageing takes years. Artificial ageing of rice was carried out at 70 ºC using simultaneous IR radiation heating (3.18×10^4 W/m^2) for 1, 3, 5, and 7 h as well as UV-C irradiation (49.24 J/cm^2-h). IR heating at 70 ºC combined with UV-C irradiation for 5 h was the optimized condition for artificial ageing. At optimized conditions, the proportionate change of rice was the highest as 0.21, followed by that for naturally aged (0.15) and non-aged (0.08). The values of elongation ratio and actual elongation after cooking were the highest in artificial ageing, followed by those for naturally aged and non-aged rice. Water uptake (%) value was also the highest for artificial ageing (89.62%), followed by that for naturally aged (68.45%) and non-aged (59.93%) rice. Furthermore, nutritional values, microstructure, and antimicrobial studies were carried out at optimized conditions. No significant changes in nutritional values viz., starch, protein, and fat were observed in artificially aged rice in comparison to one year old naturally aged rice. Electron microscopy analysis showed no changes in the structure of starch granules, which further revealed no adverse effect of IR radiation heating on the microstructure of rice. Results from the spread plate assay showed no growth of bacterial colony indicating the antibacterial effectiveness of artificial ageing. Thus, simultaneous artificial ageing as well as surface disinfection of rice can be carried out by combining IR radiation heating and UV-C irradiation. These observations endorsed the effectiveness of the designed box for the artificial ageing of rice without compromising the cooking and nutritional qualities. A conceptual design of an artificial ageing box is also presented for handling large amount of rice. A preliminary

sensory test was conducted. Overall, an efficient, inexpensive, and easy-to-handle artificial ageing combined with surface disinfection of rice was accomplished.

Overall, this comprehensive study contributes to the essence of product design and its MVPs with different functionalities. A product with many variants has been developed. Performance study of a newly designed sterilization box, its variants as well as its applications in different field of engineering are discussed thoroughly. The findings provide valuable insight of the designed products for industrial application.

Table of Contents

Chapter 3

Design of a Sterilization Box Using Combination of Heat and Ultraviolet Light Irradiation and Its Performance Study

Chapter 4

Design of a Sterilization Box having Both IR Radiation Heating and UV-C Irradiation Facilities and Its Performance Assessment

List of Figures

List of Tables

Nomenclature

List of Symbols

β_i	Biot number
ρ	Density
τ_t	thermal time constant
A_s	surface area
B	breadth
C tape	carbon tape
C or C_p	specific heat
D	UV-C dose
D_i	dilution factor
d	distance from heat source to surface to be sterilized
G_i	growth inhibition in percentage
h	convective heat transfer coefficient
k	thermal conductivity
k_d	death rate
L	length
L_c	characteristic length
m	mass
N	number of bacterial colonies
n	sample size
P	UV bulb power
pI	isoelectric point
R^2	coefficient of determination
R_0	correction factor
R_a	surface roughness
S	standard deviation
T	temperature
ΔT	temperature difference
T_i	initial temperature

T_∞	ambient temperature
T_m	melting point
t	time
t-value	critical value for t-distribution
V	volume
W	weight

List of abbreviations

3D	Three-dimension
AAD	Ambient Air Drying
ACE 2	Angiotensin Converting Enzyme
AE	Actual Elongation
AFM	Atomic Force Microscope
ANOVA	Analysis of Variance
BSA	Bovine Serum Albumin
BCA	Bicinchoninic acid
CD	Circular Dichroism
CDC	Centers for Disease Control and Prevention
CFU	Colony-forming Unit
COVID-19	Coronavirus Disease 2019
DAQ	Data Acquisition
DLS	Dynamic Light Scattering
DNA	Deoxyribonucleic Acid
DTC	Digital Temperature Controller
DUV-LED	Deep Ultraviolet Light Emitting Diode
ER	Elongation Ratio
FESEM	Field Emission Scanning Electron Microscopy
FFR	Filtering Facepiece Respirator
FIR	Far Infrared
FTIR	Fourier Transform Infrared Spectroscopy
GI	Galvanized Iron

HAD	Hot Air Drying
HTFAM	High Temperature Formaldehyde Alcohol Mixture
IgG	Immunoglobulin G
IR	Infrared
IRD	Infrared Drying
LB	Luria Bertani
LED	Light Emitting Diode
LTSF	Low Temperature Steam Formaldehyde
MCQ	Multiple Choice Question
MRE	Mean Residue Ellipticity
MVP	Minimum Viable Product
NB	Nutrient Broth
OD	Optical Density
PBS	Phosphate Buffer Saline
PC	Proportionate Change
PDA	Potato dextrose agar
PjBL	Project Based Learning
PPE	Personal Protective Equipment
QAC	Quaternary Ammonium Compound
RBD	Receptor Binding Domain
RL	Remote Laboratory
RNA	Ribonucleic Acid
RPM	Revolutions Per Minute
RSM-CCD	Response Surface Methodology with Central Composite Design
SA	*Staphylococcus aureus*
SARS-CoV-2	Severe Acute Respiratory Syndrome Coronavirus 2
ST	*Salmonella typhi*
STEM	Science, Technology, Engineering and Mathematics
UTM	Ultimate Tensile Machine
UTS	Ultimate Tensile Strength
UV	Ultraviolet

UVGI	Ultraviolet Germicidal Irradiation
VHP	Vaporized Hydrogen Peroxide
WEW	Work Experience Week
WU	Water Uptake
XRD	X-ray Diffraction

Chapter 1
Background and Scope

1.1 Introduction

The rapid spreading of the novel coronavirus disease 2019 (COVID-19) has affected the entire world and brought it to a lockdown. The World Health Organization (WHO) has referred it as 'pandemic' and identified the virus as severe acute respiratory syndrome coronavirus 2 (SARS-CoV-2). The pandemic causes company closures, lead to job losses, travel restrictions, and disruptions in worldwide supply chains followed by significant economic recessions. The COVID-19 has highlighted the critical need of maintaining a sterile environment to prevent its transmission from aerosols and contacting surfaces. Thus, the resurgence of studying the sterilization methods is a direct response to the unprecedented challenges caused by the COVID-19 pandemic. The implementation of effective sterilization methods is crucial in controlling the spread of the virus, safeguarding healthcare environments, maintaining the safety, and well-being of individuals across the world. Researchers are investigating innovative sterilization methods in order to provide effective and rapid sterilization, addressing the critical need for infection control.

The SARS-CoV-2 comprises inner Ribonucleic acid (RNA) and outer surface spike glycoprotein (Zeng et al., 2020). The spike glycoprotein on the surface is responsible for binding as well as fusion of the virus to the host cell membrane (Pandey, 2020a). The glycoprotein Immunoglobulin G (IgG) is a model protein similar to that of spike glycoprotein in SARS-CoV-2 and used as a model material in lieu of SARS-CoV-2 (Fischer et al., 2020; Schmidt et al., 2020; Salazar et al., 2020). The inactivation of the coronavirus is achieved by unfolding of the spike protein (Pandey, 2020b). The unfolding of the protein prevents entry of the virus into host cells by disabling its binding with surface receptor (Li and Hirst, 2020; Lokman et al., 2020). It is recommended as the preventive measure against COVID-19. The schematic of a SARS-CoV-2 with spike protein is shown in Figure 1.1. Several physical (e.g., heat and radiation) and chemical (e.g., pH, disinfectants and surface modification) methods have been investigated to test the unfolding of the spike protein (Pandey, 2020b). Thus,

researchers have always emphasized the importance of sterilizers with efficient sterilization techniques during the COVID-19 pandemic.

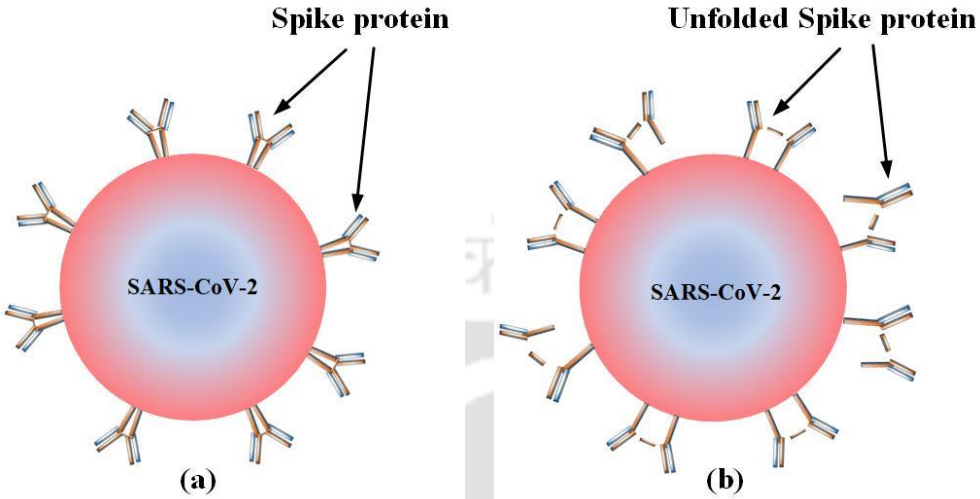

Figure 1.1 Schematic of the SARS-CoV-2 with **(a)** spike protein and **(b)** unfolded spike protein

The market for sterilization box was flourishing amid the COVID-19 urgency. However, it had suffered a drop-in demand after the pandemic due to many reasons viz., successful vaccination campaign, consumer behavior towards less usage as well as craving for return to pre-pandemic practices. As the world navigates the post-pandemic period, sterilization industries must adjust to some new dynamics in order to stay robust in the face of changing customer needs. Thus, various innovative products based on same concept for different functionalities are explored in this thesis.

One of the fundamental elements of successful innovation is being able to come up with an excellent idea and then perfectly document it in a product brief. Product brief outlines the theoretical concepts, broad applications, and present as well as future scopes. Purpose of design and development of a new product is to transform ideas into tangible products. The process of designing and developing a product requires meticulous planning, creative thought, and a keen awareness of user requirements. Applications for a product should be as diverse as its capacity to adapt new concepts. Specification of a product design defines summary of ideas, information, and concepts as well as the aim of the completed product.

Prime concern during early stage of design is to transform the vague concept for a new product idea into something more concrete that improves our lives and pushes the boundaries of what is conceivable. In this crucial stage of the design process, doing anything wrong will lead to loss of time, money as well as resources, and ultimately ineffective development stage. At this early stage, it is also necessary to decide whether a single product would satisfy market demand or if a variety of items are needed. For this purpose, different versions of minimum viable products (MVPs) are developed. The concept of MVP suggests a forward-thinking and customer-focused methodology. MVP is defined as that variety of a newly designed product that enables a team to gather the greatest amount of validated learning about users with minimum amount of effort (Ries, 2009). Validated learning by a team is referred as a process of learning significant truths about a startup's current and future commercial prospects with the help of experimental demonstration (Ries, 2011). To put it another way, MVP is a product created with the few set of features as well as extensive research to encompass the aesthetics, market fit, usability for the product, understand customers need, and uncover emerging ideas. By focusing on a product's essential components, designers and developers improve their concepts using prototyping and testing to make the finished product efficient as well as optimized one.

Several product design researchers have suggested a reverse process of finding applications for a developed technology, rather than developing a technology for a specific application (Lee et al., 2020). Lee et al. (2020) discussed three different alternative design processes— (1) problem-first design, (2) co-evolution of problem and solution, and (3) solution-mapping. In problem-first design, finding and understanding a problem in initial phase is followed by finding a solution. In the co-evolution of problem and solution design, simultaneous development of problem and solution takes place. In solution-mapping, a technology is developed first and then the problems are identified to which the technology can be applied. In the process of solution mapping, a number of problems can be identified. For each problem, a slight modification of the product may be needed, thus, producing the MVPs. Developing a number of MVPs based on the same technology provides continuous innovation and stability to industry that captivate customers.

The realm of product design and development is a fascinating journey that combines different fields of engineering with artistic vision as well as user-centric thinking. Embracing the idea of MVPs, possibilities for transformation of a product are limitless. Combining MVP as a guiding principle and solution mapping as a design process, designers and developers bring their ideas to life in a modernized, simplified and efficient manner to solve real life problems and shape the future of innovation. Following are the products designed in this thesis:

- Product 1: Sterilization box equipped with incandescent bulb heating and ultraviolet type C (UV-C) irradiation
- Product 2: Sterilization box equipped with infrared (IR) radiation heating and UV-C irradiation
- Product 3: Pedagogical gadget for teaching heat transfer
- Product 4: Artificial ageing box

Motivations for each product are discussed in following sections.

1.2 Motivation for Developing Sterilization Box Equipped with Combined Incandescent Bulb Heating and UV-C Irradiation

Severe acute respiratory syndrome coronavirus 2 (SARS-CoV-2) has affected millions of lives and created global pandemic all over the world by spreading a very contagious disease called coronavirus disease 2019 (COVID-19). The virus gets transmitted by contacting surfaces and aerosols (Pandey, 2020b). Personal protective equipment (PPE) becomes crucial element to stop spreading the disease. Throwing away of infected PPE kits creates wasting of large amount of money. Furthermore, it is hazardous to disposing PPE kits and other infected things in environment as soil and water will get infected by the contagious SARS-CoV-2 (Conde-Cid et al., 2021a; Conde-Cid et al., 2021b; Núñez-Delgado, 2020). Therefore, sterilizing the infected surfaces before disposing them to the environment is critically important. The design of a low-cost sterilization device becomes immediate requirement for the society to sterilize contacting surfaces as well as day-to-day life accessories.

Temperature based sterilization has been a potential choice for many applications. According to reports, SARS-CoV-2 can be inactivated by heating at a temperature higher than 65 °C for more than 5 min despite being stable on various surfaces (Abraham et al., 2020).

Researchers gave significant attention to sterilizers as an important area of research for disinfection (Boudam and Moisan, 2010; Darmady et al., 1961; Hugo, 1991). The COVID-19 pandemic has further prioritized the design and development of an efficient sterilization technique (Liao et al., 2020; Ludwig-Begall et al., 2020; Rubio-Romero et al., 2020; Sivakumar et al., 2021). Additionally, it has been found that UV based sterilization is especially efficient for particular surfaces. The effectiveness of UV-C based sterilization is influenced by surface roughness. This method is more efficient to sterilize smooth surfaces of fruits and vegetables viz., apples and tomatoes (Abdussamad et al., 2016). In contrast, heating method of sterilization is effective for pathogens in pores and unexposed surfaces. Thus, it is essential to design a sterilization chamber that is easy to use, inexpensive and has both heating as well as UV irradiation facilities. The combination of heat and UV-C can be used for sterilizing small items like wallet, mask, belt, wrist watch as well as other day-to-day items before being reused or disposal to the environment. However, there is still a lot of research being carried out on the synergistic effects of UV irradiation and temperature. Thus, a product, sterilization box equipped with both incandescent bulb heating as well as UV-C irradiation facilities was designed. Its effectiveness was tested to fight against COVID-19 and bacteria inactivation. The primary focus of designing this product was to provide an inexpensive, simple, and easy to use sterilization box with efficient heating as well as UV-C irradiation method.

1.3 Motivation for Developing Sterilization Box Equipped with IR Radiation Heating and UV-C Irradiation

Researchers used IR radiation heating as a significant way of sterilization. Fibrous filters contaminated with bioaerosols were sterilized using IR radiation (Damit et al., 2011). A device was developed to inactivate the spores with the help of IR radiation (Molin and Östlund, 1975). IR radiation heating possesses many advantages viz., uniform heating, high energy efficiency, lower heating time, easy to use, compactness, more penetration depth, and higher heat transfer coefficients. These advantages make it superior to other conventional heating methods. Thus, another product to develop MVPs, a sterilization box equipped with both IR radiation heating as well as UV-C irradiation facilities was designed. The main focus of this product was to provide an easy to handle, efficient, and rapid sterilization method by combining IR radiation

heating and UV-C irradiations. Furthermore, its performance against contagious infections by viruses as well as broad-spectrum antibacterial activity were studied. This may lead to use of sterilization box for several purposes in healthcare sectors.

1.4 Motivation for Developing Pedagogical Gadget for Teaching Heat Transfer

Pedagogy is the science and art of teaching-learning methods. Teachers-students interaction, learning environment, learning task and hands-on practices are the key elements of pedagogy. In engineering pedagogy, a lot of research activities have been carried out in recent years. Pedagogical gadgets are one of the significant developments in the field of engineering pedagogy. These gadgets have the potential to improve the teaching method of engineering concept as well as to understand with the help of hands-on practices and active engagement of students. It shapes complex concepts of engineering more enjoyable and interesting one by providing concrete representation of the concepts, allowing students to visualize as well as experiment with them. Deeper comprehension as well as retention of theoretical concepts are improved by hands-on practices using these gadgets. Students from different disciplines get encouraged for group learning and cooperation by working together, exchanging perspectives as well as ideas while using these gadgets for experimentation. These gadgets bridge the gap between theory and application and prepare students to solve real-life problems in the constantly developing engineering field. Thus, with advancement of technology, design, development, and implementation of pedagogical gadgets will play significant role in making engineers for future. Thus, another product to develop MVPs, a pedagogical gadget was designed. This pedagogical gadget has been transformed from a heat-based sterilization box with small modification. Using it, a number of hands-on experiments related to heat transfer can be carried out. Furthermore, survey and educational assessment were carried out to check the pedagogical efficacy of the gadget for teaching heat transfer.

1.5 Motivation for Developing Artificial Ageing Box for Rice Ageing

Ageing of rice is a process that improves cooking, milling, and eating qualities by altering nutritional contents as well as physical properties throughout storage (Keawpeng and Venkatachalam, 2015). There are two types of ageing viz., natural and artificial. Artificial ageing is a less time-consuming method, carried out using IR radiation heating in a temperature

range of 35–110 ºC (Khir et al., 2014; Faruq et al., 2015). Furthermore, effectiveness of UV-C irradiation for the fungal decontamination without affecting color and cooking properties of rice was reported (Ferreira et al., 2021). Thus, another product variant of the sterilization box equipped with IR heating and UV-C facility was artificial ageing box. Artificial ageing box was tested for simultaneous artificial ageing and surface disinfection of rice. Cooking quality, nutrient values, and moisture removal content were investigated. Antimicrobial activity was also tested to study the surface disinfection of rice.

1.6 Scope of the Present Thesis

The COVID-19 pandemic has emphasized the researchers for innovative sterilization methods to prevent the transmission of the virus. The primary objective of the present thesis is to design and development of a sterilization box followed by its variants and to discuss their functionalities. A sterilization box is designed having efficient, easy to handle as well as inexpensive methods viz., incandescent bulb heating and UV-C radiation. Performance study of this product for the prevention of COVID-19 is discussed. In addition, bacterial inactivation is discussed in bacterial cells collected from various day-to-day life items viz., belt, watch, and wallet along with clinically relevant *Escherichia coli* (*E. coli*) bacteria. *E. coli* is commonly found in the lower intestine of warm-blooded organisms and most of its strains are harmless, however, some can cause serious food poisoning. To develop MVPs, another sterilization box with both IR radiation heating and UV-C radiation facilities is designed. Its performance assessment is based on broad-spectrum antibacterial activity against Gram-negative bacteria viz., *Salmonella typhi* (*S. typhi*) and Gram-positive bacteria viz., *Staphylococcus aureus* (*S. aureus*) as well as antiviral activity. Gram-negative bacteria possess thin layered cell wall, while, Gram-positive bacteria possess thick layered cell wall. For antiviral study, unfolding of SARS-CoV-2 spike glycoprotein is discussed as it provides the major stability to the virus. Another product variant, a pedagogical gadget is designed and discussed its pedagogical effectiveness. Five possible experiments related to heat transfer are discussed using the gadget. A survey is carried out among teachers and students of different standard with a set of written questions as well as statements to know its pedagogical usefulness. An educational test is conducted among a group of newly graduated mechanical engineering students for assessing the impact of gadget to learn heat transfer.

To show different functionalities, sterilization boxes are used for sterilizing N95 filtration fiber and simultaneous artificial ageing as well as surface disinfection of rice. Mechanical properties viz., fiber diameter, surface roughness (R_a), ultimate tensile strength (UTS), and scratch resistance along with X-ray diffraction (XRD) analysis of the sterilized fiber are presented in this thesis. Furthermore, cooking quality, nutrient values (starch, protein, and fat), and moisture removal contents are discussed to show the usefulness of the sterilization box. Results of antimicrobial activity shows the potential of the box for surface disinfection of rice. Finally, the thesis proposes the industrial value of a sterilization box and its MVP with different functionalities. Developing a number of MVPs based on same technology offers stability to the industry by captivating customers with ongoing innovative ideas.

1.7 Organization of the Thesis

The work performed in this thesis comprises eight chapters, which are organized as follows:

- The present chapter briefly introduces product design and its MVPs along with the scope of the thesis and organization of the thesis.
- Chapter two presents the survey of existing literature, identifies research gaps and detailed objectives of the present thesis.
- Chapter three presents the design of a sterilization box equipped with both incandescent bulb heating and UV-C irradiation facilities. Performance study of this designed sterilization box for the prevention of COVID-19 is described. Optimized temperature and time duration for denaturation of a glycoprotein and inactivation of clinically relevant Gram-negative bacteria, *E. coli* are described. Moreover, inactivation of bacterial cells collected from various day-to-day life items viz., belt, watch, and wallet are described.
- Chapter four presents design of a sterilization box equipped with both IR radiation heating and UV-C irradiation facilities. Its sterilization ability against pathogenic bacteria (Gram-positive viz., *S. aureus* and Gram-negative viz., *S. typhi*) and denaturation of SARS-CoV-2 spike protein is described. Optimized temperature and time duration for denaturation of SARS-CoV-2 spike protein and inactivation of bacteria are described.

- Chapter five presents change in properties of N95 respirator after disinfecting it by various techniques. Mechanical properties viz., fiber diameter, R_a, UTS, and scratch resistance of the disinfected fibers are discussed. X-ray diffraction (XRD) analysis is described to indicate any chemical changes in the surface after disinfection.
- Chapter six presents design of a pedagogical gadget for teaching heat transfer. Survey and educational assessment were described to know the pedagogical efficacy of the gadget.
- Chapter seven presents analysis of cooking quality, nutrient value as well as moisture removal content of combined IR heat and UV-C treated rice using a sterilization box.
- Chapter eight summarizes the overall conclusion of the work and scope for further work. This is followed by references.

Chapter 2
Literature Review and Detailed Objectives

2.1 Introduction

Product design is the process of transforming information about a product's demands and requirements into knowledge about that product as well as its underlying processes. Transformation of ideas into a new product needs imaginations, creative thinking, and consumer requirements. The key to successful product design is its ability to solve real life problems for people as well as to adapt new concepts based on different applications. Different researchers define product design in different way. Stoll (1999) defined product design as a process that starts with the identification of a requirement and concludes with a concrete product that customers accept due to its satisfactory service. It is a learning process that comprises design-making decisions, investigating their acceptability followed by necessary modifications. This design-investigation-redesign process is a fundamental characteristic of design process, often called as “iterative nature of design”. Magrab et al. (2009) defined product design as an activity that (1) outlines the aims or purposes of the products and (2) evaluates as well as generates their form with respect to their aims. Researcher reported the five aspects of a successful product development viz., product quality, product cost, development time, development cost, and development capability (Eppinger and Ulrich, 1995). Four primary aspects of design described by Magrab et al. (2009) are as follows:

- Problem definition: advancing from an uncertain collection of facts and myths to a clear presentation of the issue.
- Creative process: process of creating a concrete embodiment of the solution that relies on the particular expertise of the participants.
- Analytical process: evaluates the correctness of the proposed solution; providing a method of assessing “good” and “bad” solutions.
- Ultimate check: verification of the design fulfilling the original demands.

Survival of a product in market is the primary concern in the field of product design and development. A single product may not be able to satisfy the market demand. Thus, designer proposes variety of products to fulfill the market demand. Thus, minimum viable

products (MVPs) are developed and introduced in the market. The idea of MVP suggests a futuristic and customer-centered methodology. Lenarduzzi and Taibi (2016) defined MVP as "a version of a new product, which allows a team to collect the maximum amount of validated learning about customers with least effort". In other words, MVP is a product that has a limited set of features and has undergone comprehensive research to include pleasant design, market fit, functionality, consumer requirements and to uncover emerging concepts. Prototyping and testing assist designers and developers to refine their concepts assuring the final product to be efficient and optimized one. MVPs are being used in a variety of contexts including startups, industry-academia collaborations, universities, and established enterprises. Alonso et al. (2023) emphasized the significance of bridging the gap between the theory and the practical use of MVPs in software engineering to benefit both professionals from business and academia.

While developing new products using new technology, certain design processes may prioritize finding solutions before focusing on problems. Lee et al. (2020) described three different design processes: (a) problem-first design, (b) co-evolution of problem and solution, and (c) solution-mapping as shown in Figure 2.1. In problem-first design, initial exploration of problem is followed by identifying a solution. Process of problem exploration guides the designers' quest for a solution. In co-evolution of problem solution design, problem and solution grow simultaneously. Designers refine their knowledge of the problem depending on their investigation of potential solutions and these potential solutions further refocus the problem as well as lead to new design criteria. A potential solution influences the change in definition of the problem and new problem drives a fresh perspective on the progress of solution. In solution-mapping, a new technology has been developed followed by identification of the problems that can be solved with newly designed technology. Designers create a new technology as a solution followed by exploring, identifying, and considering the problems that the new technology might solve, finally choosing a problem application.

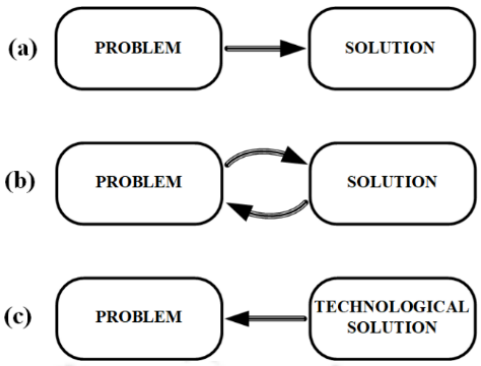

Figure 2.1 Three design processes with different stages of problem and solution: **(a)** problem-first design **(b)** co-evolution of problem and solution and, **(c)** solution-mapping

Product design and development is an enchanting area that blends several sciences as well as engineering fields with creative vision and user-centric thinking. Designers convert their ideas into modernized as well as efficient concrete products to address real-world issues by combining MVP as a guiding concept with solution mapping as a design process. The pandemic due to the coronavirus disease 2019 (COVID-19) motivated the researchers for the design and development of an easy to handle, low cost sterilization box with efficient sterilization methods.

Severe acute respiratory syndrome coronavirus 2 (SARS-CoV-2) spread a highly contagious disease COVID-19, leading to a worldwide pandemic as well as disruption of daily lives in most of the country. Several studies reported survival of coronavirus for hours or even days on skin as well as nonliving surfaces (Hiep et al., 2023; Xu et al., 2022). Droplets in the air and surfaces that come into touch with the virus can transmit it (Pandey, 2020b). Thus, usage of personal protective equipment (PPE) became necessary to prevent the spreading of the disease. As PPE kits get infected after usage, throwing away of such kits to environment may lead to contamination of soil as well as water. The presence of SARS-CoV-2 in wastewater has been verified by recent investigations (Conde-Cid et al., 2021a). Conde-Cid et al. (2021b) mentioned development of scientific methodology for the measurement of SARS-CoV-2 and other pathogens in liquid samples related to soil. Researchers reported the possibility of transmission of SARS-CoV-2 from waste water and sewage sludge to soils (Conde-Cid et al., 2021b; Núñez-Delgado, 2020), leading a deep attention to the affected planet and its ecosystem (Cela-Dablanca et al., 2021). Thus, sterilization of infected PPE kits before their disposal becomes utmost necessary to prevent the spreading of contagious COVID-19.

Moreover, there are many COVID-19 vaccinations available currently. However, prevention is widely acknowledged as the key to halting the spread of this pandemic (Anand et al., 2021; Watanabe et al., 2023). Keeping all this in mind, finding practical solutions is crucial to minimizing the virus's negative effects on human health as well as environment.

2.2 Sterilization Methods

Sterilization is a treatment method to deactivate viable microorganisms from objects or inanimate surfaces. In this context, a microorganism's viability is determined by its potential to reproduce in a suitable environment (Jildeh et al., 2021). Sterilization methods come in a wide variety. Heat, chemical, and radiation are the three primary methods of sterilization. Dry heat and moist heat (autoclave) are two types of heat-based sterilization methods. Chlorine and their compounds, ethylene oxide (EtO), ozone (O_3), hydrogen peroxide (H_2O_2), quaternary ammonium compounds (QACs), formaldehyde, glutaraldehyde, nitrogen dioxide (NO_2), alcohol, and peracetic acid are chemical based sterilization methods. X-rays, gamma rays, ultraviolet (UV) rays, microwave, and infrared (IR) are some of the radiation based widely used methods (Govindaraj and Muthuraman, 2015; Liao et al., 2020). Detailed classification of sterilization methods is shown in Figure 2.2. Different sterilization methods are described in sequel.

2.2.1 Heat Sterilization

Moist heat or autoclaving was the earliest and safest sterilization method applied in medicinal products. Moist heat under pressure in saturated steam form is the most popular and reliable method of sterilization among all the available sterilization methods (Rutala and Weber, 1999). Majority of the autoclaves are metallic containers that can endure high temperatures and pressure. Basic principle of this sterilization is the direct use of steam to the products at required temperature and pressure for a specific time. Thus, steam, temperature, pressure, and time are the four parameters of this sterilization method. Sterilization is accomplished by directly exposing the material to full steam at 121 °C (250 °F) or 132 °C (270 °F) in a sterilization chamber with a pressure rating (Rutala and Weber, 1999). Metabolic and structural elements required for microbe growth are destroyed in this sterilization methods.

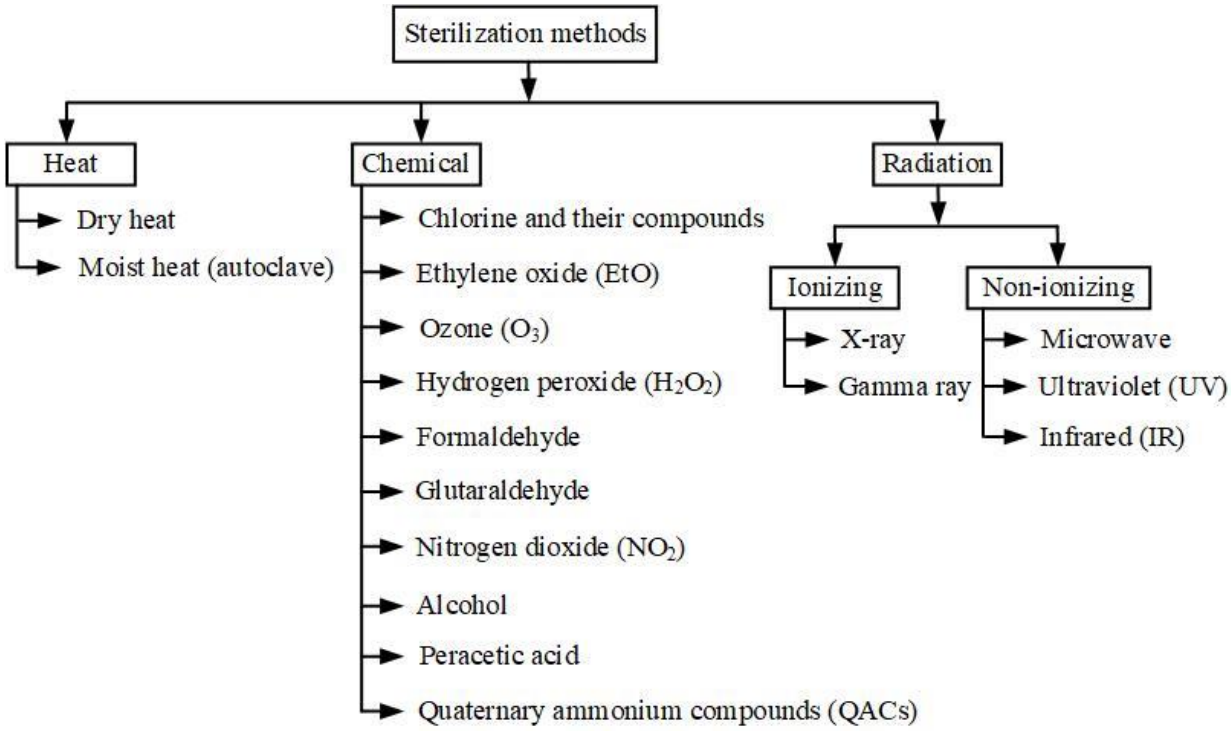

Figure 2.2 Classifications of sterilization methods

Dry heat sterilization is accomplished by increasing the temperature of materials to extreme temperatures (>140 °C) through heat transfer using a heat source. Using hot air sterilizers, the standard temperature-time correlations for dry heat sterilization are 170 °C for 60 min, 160 °C for 120 min, and 150 °C for 150 min. The main fatal mechanism during dry heat sterilization is considered to be cellular oxidation (Govindaraj and Muthuraman, 2015).

2.2.2 Chemical Sterilization

In 1968, Borick initially defined the term chemo sterilizer, which was eventually replaced by the term chemical sterilants (Bharti et al., 2022). A chemical sterilant refers to a chemical agent or its derivatives with microbicidal properties like interfering with genetic material viz., Deoxyribonucleic acid (DNA) or Ribonucleic acid (RNA), leading to death of the microorganism due to deactivation of cellular functions (Jildeh et al., 2021). The chemicals are mostly used to sterilize medical devices since high temperature steam has adverse effect on them. Some of widely used chemical sterilization methods are discussed in sequel.

Since 1950s, ethylene oxide (EtO) has been utilized as a chemical sterilant for moisture as well as temperature sensitive devices. Combination of EtO with other gases viz.,

hydrochlorofluorocarbons, carbon dioxide, immersion in peracetic acid, and gas plasmas are also used as alternatives to EtO. It is a common chemical sterilization method with fungicidal, sporicidal, bactericidal as well as virucidal properties (Bharti et al., 2022). It is clear and transparent liquid below its boiling point temperature of 11 °C. Alkylation of amine groups in microbial nucleic acids is the major cause of lethal effect. It alters the microbes' metabolism and reproduction, leading to death (Govindaraj and Muthuraman, 2015).

The recent development in chemical methods of sterilization is chlorine and their compounds. Chlorine and their compounds are used to destroy vegetative microorganism including fungi. The most accepted chlorine disinfectant is hypochlorite, which is available in both solid i.e., calcium hypochlorite ($Ca(ClO)_2$) as well as liquid form i.e., sodium hypochlorite (NaOCl) (Bharti et al., 2022). NaOCl is usually known as bleach and extensively used for surface cleaning in healthcare facilities and medical equipment (Racioppi et al., 1994). Chloramine-T., sodium dichloroisocyanurate, and chlorine dioxide (ClO_2) are the alternatives of hypochlorite showing bactericidal effect for longer period. The ideal working conditions for ClO_2 are 298–303 K for 6 hours with its low concentration (Govindaraj and Muthuraman, 2015).

Ozone (O_3) is very unstable on the surface of the earth. It is the result of collision between O_1 molecules with energized O_2 molecules (Govindaraj and Muthuraman, 2015). It has pleasant clean smell at low concentration, however, it is highly irritating and dark blue in color at higher temperature. It shows bactericidal, sporicidal, and mycobactericidal activities as well as effective against yeast, fungi, viruses, and amoebae. It is extensively used in disinfection of drinking water and deodorization (Bharti et al., 2022). O_3 is commonly employed to inactivate harmful bacteria in the air, water, and wastewater due to its potent oxidizing properties (Crini and Lichtfouse, 2019; Martinelli et al., 2017; Mecha and Chollom, 2020). In case of viral disinfection in surfaces and aerosols, it has been used efficiently (Hiep et al., 2023). Organic and inorganic materials get oxidized while exposed to O_3; thus, sterilization occurs. It penetrates the membranes of microbial cells, lading to their rupture. By adding humidity or vacuum pressure, penetration of ozone is controlled (Patel, 2003).

Hydrogen peroxide (H_2O_2) is mainly used for medical equipment sterilization. It is popular as a sterilant, disinfectant, preservative, fumigant, and household antiseptic. It is

considered to be environment-friendly as it degrades into water and oxygen. It deactivates various microorganisms viz., bacteria, yeast, fungi, viruses, and spores (Bharti et al., 2022). At 20 ℃, a 0.5% accelerated H_2O_2 showed the bactericidal and virucidal activity as well as fungicidal and mycobactericidal activity within 1 min and 5 min, respectively (Omidbakhsh and Sattar, 2006). Pathogens with higher cellular catalase activity (*Serratia marcescens, S. aureus, and Proteus mirabilis*) need 30–60 min of 0.6% H_2O_2 exposure for a reduction of 10^8 to <1 colony forming unit per ml. However, pathogens with lower cellular catalase activity (*E. coli, Streptococcus species, and Pseudomonas species*) need 15 min of exposure (Schaeffer et al., 1980). H_2O_2 damages the outer wall of bacteria cell or virus cell by oxidizing it, leading to inactivate their function (Bharti et al., 2022). H_2O_2 also attacks membrane lipids, DNA as well as other critical structural components of cell, thus, disinfection occurs (Rutala and Weber, 2008).

Peracetic acid is an extensively used low-temperature sterilization method, controlled by a microprocessor. It is a colorless liquid with a pungent odor and a high degree of corrosion. In 1955, it was launched as a bactericide. At low concentrations (~0.3%), it is more effective than H_2O_2 in virucidal, sporicidal, fungicidal as well as bactericidal activity (McDonnell and Russell, 1999). It can inactivate yeast, fungi as well as gram-positive, and gram-negative bacteria within less than 5 min with lower dose. However, doses required for yeast and viruses are relatively larger (Hiep et al., 2023). It oxidizes sulphur bonds and sulfhydryl in proteins, enzymes as well as other metabolites leading to protein denaturation, and cell wall disruption (Govindaraj and Muthuraman, 2015).

Quaternary ammonium compounds (QACs) are extensively used as a disinfectant agent (Kampf et al., 2020a; Sozzi et al., 2019). These compounds comprise a halide or a sulphate as an anion and an amino group as a cation. Alkyl didecyl dimethyl ammonium chloride, alkyl dimethyl benzyl ammonium chloride, and dialkyl dimethyl ammonium chloride are a few chemical compounds of QACs used in medical facilities (Rutala and Weber, 2008). Interacting with the cell wall, QACs penetrate it and start reacting with the cytoplasmic membrane followed by disorganization of membrane as well as leakage of intercellular material leading to nucleic acid and protein degradation (Gerba, 2015).

Alcohol is the oldest disinfectant still used in hospitals for both intact as well as broken skin. A variety of alcohols are used in many chemical and industrial processes. The most efficient alcohol for destroying the microorganism is ethyl alcohol. Methyl alcohol is hardly utilized in healthcare due to its lesser antibacterial activity (Tilley and Schaffer, 1926). Combining alcohol with water makes alcohol more effective against germs as water helps in denaturation proteins in cell membrane (Block, 2001). Antibacterial action of alcohol destroys the cell membranes as well as denaturation of vital microbial proteins, showing rapid denaturation of protein in presence of water (Al-Sayah, 2020). Ethanol destroyed *Pseudomonas aeruginosa* with 30 to 100% of concentration range, whereas *Serratia marcescens, Salmonella typhosa,* and *E. coli* were destroyed with 40 to 100% within 10 s. Isopropyl alcohol exhibits better bactericidal activity than ethyl alcohol to deactivate *S. aureus* and *E. coli* (Coulthard and Sykes, 1936). The recommended alcohol concentration for everyday use on hands to reduce the risk of disease transmission is between 70 to 80% (Bharti et al., 2022).

Formaldehyde is used for preservation, disinfection, and sterilization in both liquid as well as gaseous form. It has a very unpleasant odor. Two sterilization techniques, low temperature steam formaldehyde (LTSF) and high temperature formaldehyde alcohol mixture (HTFAM) have been widely applied, which used formaldehyde as a gas. LTSF is an active, economical, and simple to monitor sterilization method, used in automated sterilization procedures particularly in medical facilities (Bharti et al., 2022). In general, formaldehyde gas requires more humidity for the best biocidal effect, especially for bacterial and fungal spores. Formaldehyde exhibits fungicidal, bactericidal and virucidal action (Rubbo et al., 1967; Spicher and Peters, 1976). It is an alkylating agent that results in alkylation of nucleic acid as well as inhibits the germination process (Trujillo and David, 1972). HTFAM technique uses heat combined with formaldehyde (0.23%) and alcohols (<4% methanol and 72% ethanol). A mixture of distilled water, formaldehyde, and alcohol is vaporized using heat at 132 ℃ and pressure of 138 kPa in a sterilizer. HTFAM, a low humidity technique with little corrosion and rusting, demonstrated superior material compatibility than steam sterilization. This fast process has the ability of broad-spectrum activity (Bharti et al., 2022).

Glutaraldehyde is a low-temperature disinfectant used in liquid form to disinfect variety of medical instruments. It is also used as a surface disinfectant and mainly used for temperature sensitive medical equipment viz., thermometers, endoscopic equipment, plastic or rubber equipment. As industrial application, it is used as a fixative in electron microscopy (Bharti et al., 2022). Glutaraldehyde solutions in water are acidic in nature and show no sporicidal action due to the presence of two aldehydes groups. The solution shows sporicidal action, when it is activated using alkalinating agents to a pH level of 7.5 to 8.5. Once solution get activated, polymerization of glutaraldehyde molecules takes place at alkaline pH values. This polymerization prevents the functioning of two aldehydes groups in glutaraldehyde molecules. New formulations of glutaraldehyde viz., potentiated acid glutaraldehyde, glutaraldehyde-phenol-sodium phenate, and stabilized alkaline glutaraldehyde have sustained microbial action (Rutala and Weber, 2008). Alkaline glutaraldehydes have better anticorrosion and microbicidal capabilities compared to acid glutaraldehydes (Babb et al., 1980; Collins and Montalbine, 1976). The carboxyl, sulfhydryl, hydroxyl, and amino groups of microorganisms are alkylated by glutaraldehyde, which leads to alteration of DNA, RNA as well as protein synthesis, resulting in biocidal activity (Rutala and Weber, 2008).

Nitrogen dioxide (NO_2) gas has the capability of sterilization as well as disinfection. It is a deployable, dependable, inexpensive, durable, and easy to use sterilization method with low settings of resource as well as no electrical power. Since NO_2 is a gas at normal temperature rather than a vapor, it may quickly penetrate packaging and challenging spaces in medical equipment. Fungi (*Candida albicans, Tricophyton mentagrophytes*), mycobacteria (*Mycobacterium terrae*), bacterial spores (*Bacillus atropheus, Geobacillus stearothermophilus, Clostridium sporogenes, Bacillus pumilus*), vegetative spores (*Staphylococcus aureus, Psuedomonas aeruginosa, Typhimurin*), lipid viruses (*Herpes simplex virus* Type 1) as well as non-lipid viruses (*Porcine parvovirus*) were tested to demonstrate the microbicidal efficiency of NO_2. All of these microbes displayed quick mortality while exposing to NO_2. Breaking of single-strand in DNA has been the microbicidal mechanism of NO_2. Additionally, it has been noted that breaking of DNA single-strands increases with increase in NO_2 exposure time (Shomali et al., 2015).

2.2.3 Radiation Sterilization

Radiation is a natural process, when an unstable atom of an element emits excess amount of energy in the form of electromagnetic waves or particles. There are two types of radiations viz., ionizing and non-ionizing radiation. Ionizing radiation is a form of radiation with higher energy than non-ionizing radiation. In contrast to ionizing radiation, non-ionizing radiation does not remove electrons from atoms or molecules of materials. X-ray and gamma ray are the ionizing types of radiation. Microwave, UV and IR are the non-ionizing radiations, used for sterilization and disinfection.

2.2.3.1 X-ray/Gamma ray radiation

X-ray and gamma ray are ionizing radiations with high energy electrons, useful for sterilization (Bharti et al., 2022). Gamma rays are mainly used to sterilize solid, liquid, gaseous objects, and medical instruments viz., syringes and needles. Sterilization of medical equipment using high energy X-ray was initially suggested in 1960s and put into use in the 1990s. Enzyme malfunctioning, increased permeability of cellular membrane and the production of radiotoxins were reported to be the destruction mechanism of gamma ray against treated cell. However, the harmful effects of gamma radiation are mostly caused due to DNA damage, either by damaging the DNA helix or by producing free radicals to destroy chemical bonds within DNA (Harrell et al., 2018). Both these interactions have the potential to kill the cell by breaking down the RNA/DNA double strands (Hiep et al., 2023). The ability of microorganisms to repair single strand break is a key factor to their gamma radiation resistance. In comparison to bacterial spores, which themselves are more resilient than yeasts, molds, and vegetative bacteria, viruses are more radiation resistant. Helminths and parasites require high radiation doses of 4–6 kGy, as they are more radiation resistant than bacteria (Harrell et al., 2018). It is interesting to observe a noticeable variation in radiation resistance within same type of microorganism. Viruses with single stranded DNA are more radiation sensitive than the one with double stranded. Yeasts are more radiation resistant than molds. Similarly, gram-positive bacteria have higher radiation resistance than gram-negative bacteria (Halls, 1992). To eliminate parasites and bacteria from dry products or frozen foods, gamma radiation of higher dose was used (Harrell et al., 2018).

2.2.3.2 UV radiation

The traditional method of UV sterilization uses medium and low-pressure mercury (Hg) vapor lamps (Oppenheimer et al., 1997). UV radiations are rapidly absorbed by both glass and plastic, whereas it exhibits reduced penetration power for solids (Bharti et al., 2022). UV radiations have been extensively used for sterilizing hospital facilities, virus contaminated places as well as biological laboratories. There are three types of UV light depending on wavelength, viz., UV-A (380–320 nm), UV-B (320–290 nm), and UV-C (290–190 nm). UV-C with the shortest wavelength, are the most lethal against microorganism (Coohill and Sagripanti, 2008; McDevitt et al., 2007). The maximum absorbance of the DNA bases is around 254 nm, produced by low-pressure Hg lamps. UV light cannot pass through solid, opaque, and light absorbing substances. It is mostly beneficial for air disinfection, drinking water disinfection, surfaces as well as sterilizing platelet concentrates (Linden et al., 2019; Szeto et al., 2020; Mohr et al., 2009). It also used for cabinet disinfection against microorganism (Reed, 2010). UV light emitting diodes (UV-LEDs) are toxic-free and have a high energy efficiency. UV-LEDs are efficient technology to destroy *E. coli* in water by emitting light in the wavelengths of 250 to 270 nm (Chatterley and Linden, 2010; Vilhunen et al., 2009). UV radiation primarily targets the DNA of UV treated bacteria, leading to destruction (Sinha and Häder, 2002). UV radiations detrimentally impacts numerous viral components, including proteins (Schuit et al., 2022; Wigginton et al., 2012). The genetic material receives energy from the absorbed photons, which damages the chemical bonds and causes genetic damage. This prevents the virus from spreading or infecting others.

2.2.3.3 Microwave

The wavelength of microwave ranges from 1 mm to 1 m. It is also considered as heat sterilization method due to its rapid generation of heat from water. It gets generated at a frequency of around 2500 MHz in commonly used oven. Its efficiency for antibacterial activity is higher in presence of water (Bharti et al., 2022). It completely inactivates bacterial cultures, viruses, G. stearothermophilus spores as well as bacterial cultures within 60 s to 5 min (Rutala and Weber, 2008).

2.2.3.4 IR radiation

IR radiation is an environment friendly, energy efficient, and less water-consuming method compared to other conventional heating method. IR radiation mainly used for surface disinfection with a temperature range of 50–1000 ℃. Based on wavelength range of IR radiations, it is categorized into three types viz., near-IR (0.75–1.4 μm with temperature less than 400 ℃), mid-IR (1.4–3 μm with temperature range 400–1000 ℃), and far-IR (3–1000 μm with temperature more than 1000 ℃) (Aboud et al., 2019). Among these three, near IR is the most popular one and can be used for mass sterilization. In both solid and liquid foods, IR radiation is effective to inactivate bacteria, yeasts, mold as well as spores. Increasing the IR source capacity results in more heating, followed by more microbial inhibition due to more energy absorbed by microorganisms. Compared to conductive heating, IR heating is more destructive to proteins, RNA, and cell walls of microorganism (Aboud et al., 2019).

2.3 Study of Sterilization Methods Against SARS-CoV

COVID-19 pandemic has highlighted the study of sterilization methods to deactivate novel human coronavirus such as SARS-CoV-2. Efficient methods are required for proper sterilization of infected inanimate surfaces viz., glass, plastic or metal to prevent spreading of contagious disease. Some of the sterilization methods against coronavirus is described below.

Starting from the heat sterilization method, temperature range of 60 to 80 ℃ effectively reduced the infectivity of coronaviruses within 1 to 30 min of contact time (Kampf et al., 2020b). Aggregation of the membrane protein due to thermal treatment resulted in their functional loss, followed by inactivation of SARS-CoV (Lee et al., 2005). SARS virus lost complete infectivity at around 55 ℃ as SARS nucleocapsid protein (one of the major structural proteins) started unfolding at 35 ℃ and denatured completely at around 55 ℃ in 10 min (Wang et al., 2004). Chin et al. (2020) evaluated the stability of SARS-CoV-2 at various temperatures, surfaces, and pH levels. The virus is quite stable at 4 °C, whereas its infectivity can be destroyed by incubating it at 70 °C for 5 min. It was more stable on smooth surfaces as well as across a wide range of pH values (3–10) at ambient temperature. Inactivation of SARS-CoV at 56 °C within 30 min and 80 °C within 1 h was reported (Rabenau et al., 2005a; Patterson et al., 2020).

In case of chemical sterilization method, ethanol (78% to 90%) exposure for 30 s reduced the viral infectivity of SARS-CoV (Rabenau et al., 2005a; Rabenau et al., 2005b). Ethanol at 70–75% concentration level acts as a biocidal agent against SARS-CoV-2, which reduces the viral activity after 60 s of exposure (Lauritano et al., 2020). In suspension experiments, isopropanol inactivates coronaviruses and ethanol eliminates coronaviruses at 70% to 95% level within 30 s of exposure time (Kratzel et al., 2020; Rabenau et al., 2005b). In biocidal test, ethanol (62–71% level) show viral infectivity against coronavirus within 60 s (Kampf et al., 2020a). Concentration range of 62% to 80% of ethanol and isopropanol inactivate human coronavirus on tile surfaces within short exposure time of 15 s (Meyers et al., 2021). 2-propanol with 70% to 100% concentration showed virucidal activity against SARS-CoV in 30 s of exposing time (Rabenau et al., 2005a). Hand rubs (alcohol based) inactivated the SARS-CoV below detection limit within 30 s (Rabenau et al., 2005b). Moreover, 0.5% concentration of H_2O_2 for 1 min exposure time resulted in reduction in viral infectivity against human coronaviruses (Omidbakhsh and Sattar, 2006). 1–3% concentration of H_2O_2 was biocidal as well as more potent in the gaseous phases and effective in inactivation of coronavirus in 1 min (Goyal et al., 2014; Herzog et al., 2012). One active chemical, NaOCl with 0.1% was used for surface disinfection against coronavirus within 1 min (Henwood, 2020). Chloramine B solution of 0.1% level was used in Vietnam to disinfect domestic surfaces, ambulances and cars to fight against coronavirus (Duong et al., 2021). Formaldehyde (0.7% to 1%), povidone iodine (0.23% to 1%) and glutardialdehyde (0.5% to 2.5%) easily inactivated SARS-CoV within 2 min, 1 min and 2–5 min, respectively (Kariwa et al., 2006; Rabenau et al., 2005a; Eggers et al., 2018). QACs had emerged as a crucial method for deactivating and preventing SARS-CoV-2 on surfaces. It was widely used in commercial surface cleaning products (DeLeo et al., 2020). Baker et al. (2020) reported antiviral activity of QAC (ammonium chloride) compound against coronavirus. Ijaz et al. (2021) reported QAC based microbicidal formulations as per standard methodologies and inactivated SARS-CoV-2 as well as other coronaviruses on high-touch environmental surfaces or in suspension. Another chemical, O_3 is potential disinfectant for inactivating coronavirus with 10 to 20 parts per million (ppm) doses within 10–15 min (Quevedo et al., 2020). Lee et al. (2021) disinfected face mask contaminated with a surrogate of SARS-CoV-2 (human coronavirus-229E) using 120 ppm of O_3 gas in 10 s, without any functional or structural degradation of filter layer of

mask. Tizaoui (2020) showed the effectivity of O_3 against SARS-CoV-2 using molecular modeling. By attacking the lipids and proteins of virus's envelope and spikes, O_3 destroyed the infectivity mechanism of the virus. Zucker et al. (2021) carried out inactivation test of pseudovirus SARS-CoV-2-spike for different levels of O_3 incubation viz., low, medium, and high with 30 min exposure time. Results showed 90%, 94%, and 99% inactivation for low, medium, and high O_3 levels, respectively. Cai et al. (2023) reported the disinfection mechanism of ozonated water by degradation of the viral envelope, followed by inactivation of SARS-CoV-2. Additionally, peroxyacetic acid was proposed as anti-coronavirus chemical with 10 min of contact time.

Different radiation sterilization methods have also been used against SARS-CoV. Sabino et al. (2020) reported the use of UV-C light for successful deactivation of SARS-CoV-1 and other RNA-based coronaviruses transmitted through liquid, air, and other inanimate surfaces. Takamure et al. (2022) inactivated SARS-CoV-2 virus below the detection limit using deep ultraviolet light-emitting diode (DUV-LED) with 280 nm wavelength. Device with DUV-LED facility with 38 mJ/cm^2 amount of dose prevented the spreading of the virus through contaminated objects as well as air (Inagaki et al., 2020). UV radiation more than 0.04 J/cm^2 dose inactivated the SARS-CoV-2 virus (Patterson et al., 2020). Pulsed-xenon UV also reduced the exposure to SARS-CoV-2 virus on N95 respirator as well as hard surfaces within 1–5 min (Simmons et al., 2021). Pendyala et al. (2020) reported UV-C dose sensitivity for 90% inactivation of SARS-CoV-2 as 21.5 J/m^2. Heilingloh et al. (2020) reported the much more effectiveness of UV-C irradiation for inactivation of SARS-CoV-2 compared to UV-A. Dose required to inactivate SARS-CoV-2 completely reported as 1048 mJ/cm^2 for exposure time of 9 min. Another research reported the inactivation of SARS-CoV virus infected tissues with 10 kGy dose of gamma irradiation emitted by cobalt-60 source (Feldmann et al., 2019).

2.4 Industrial Application of Sterilization Methods

Sterilization is a method to render any product or inanimate surface without viable microorganisms. In general, various industrial sectors viz., (1) pharmaceutics, (2) food and beverages, (3) cosmetics, and (4) medical and health care utilize sterilization methods for a range of goals. Industrial sectors categorized sterilization methods into two processes, viz., low-temperature processes (e.g., EtO and H_2O_2) and high-temperature processes (e.g.,

autoclave) (Wallace, 2016). In pharmaceutics, critical products are produced and sterilized to avoid biocontaminants, which can create health issues to the user. Critical products are those that come into contact with user's sterile tissue directly or indirectly (Jildeh et al., 2021). In food and beverages, products are sterilized to have a long shelf life (without adding conservatives), preserve organoleptic qualities, and prevent encountering of disease-causing microorganisms with the consumer. Gamma rays, x-rays, electron beams, UV rays, microwave heating, IR, radiofrequency are some of the sterilization methods, used to extend the shelf life of fresh (fruits and vegetables) as well as processed foods (milk and dairy products, meat products) without compromising nutrient content (Ashraf et al., 2019; Indiarto and Qonit, 2020; Singh et al., 2021a). IR method was used in food industries for manufacturing of juice and bread, drying, heating, peeling, boiling, freeze drying, microbial inhibition as well as sterilization of grains. It improved food safety and product quality (Aboud et al., 2019). It is extensively used in rice kernel drying by removing the moisture content (Khir et al., 2014; Pan et al., 2011; Khir et al., 2011). Abdussamad et al. (2016) reported the extension in shelf life of UV-C treated cucumber by reducing bacterial population as well as slowing down in quality. In cosmetics, sterilization is used to produce biologically sensitive products to avoid biocontaminants and maintain hygiene standards for critical instruments viz., creams, eyeliner, and lipsticks (Jildeh et al., 2021).

In medical and healthcare facilities, low-temperature sterilization processes are mostly used for medical equipment that cannot resist high temperature (over 60 °C) and high humidity. However, some of medical and surgical equipment used in hospitals are typically made up of heat-resistant materials. Thus, heat (dry or autoclave) sterilization is used for such heat stable medicinal equipment (Rutala et al., 2020). Hard objects, surgical instruments (which are moisture insensitive), wrapped products, vented containers with liquid, garbage, and glassware can all be sterilized using autoclave sterilization (Mubarak et al., 2019). Medical equipment, wound dressings, and syringes are sterilized to prevent the spreading of microbes and illness to the patients. Peracetic acid is also used for sterilizing surgical and dental instruments (Govindaraj and Muthuraman, 2015). Microwaves are also widely utilized for disinfection of dentures, dental equipment, soft contact lenses as well as urine catheters (Rutala and Weber, 2008). During recent SARS-CoV-2 epidemic, people all across the world are compelled to use N95 filtering face-piece respirators (FFRs) in order to prevent the virus from spreading through

aerosols and contacting surfaces. Infected FFRs are sterilized before reuse or disposal to prevent the financial loss as well as contamination of soil and water. Ludwig-Begall et al. (2020) studied the effect of three disinfection treatments, viz., UV irradiation, vaporized hydrogen peroxide (VHP), and dry heat, on the SARS-CoV-2 surrogate virus infected face mask and filtering respirators. Liao et al. (2020) investigated the filtration efficiency of the N95 respirators after disinfecting it by five user-friendly methods viz., dry heating at 75 °C, steam exposure, ethanol (75%) immersion, chlorine based (2%) spraying, and ultraviolet germicidal irradiation (UVGI). Disinfection of the mask by soaking in 56 °C hot water for 30 min followed by drying was reported (Wang et al., 2020). Banerjee et al. (2021) reported the use of moist heat in presence of UV-C exposure for industrial, medical, and personal sterilization purposes. Respirators, PPEs, and face shields exposed to 20 ppm ozone at 21–24 °C and >70% relative humidity for more than 40 min resulted in 99.99% reduction in viral infection (Blanchard et al., 2020). Bopp et al. (2020) carried out moist heat autoclave disinfection of N95 FFRs in four ways— 115 °C for 60 min, 121.1 °C for 30 min, 130 °C for 2 min, and 130 °C for 4 min. Viscusi et al. (2009) observed the changes in odor, penetration of aerosol, and physical appearance of N95 FFRs after disinfecting it by UVGI, VHP, ethylene oxide (C_2H_4O), bleach, and microwave oven irradiation. Disinfection methods involving UV radiation and H_2O_2 (vapour and liquid) produced the least damage in filtration performance of FFRs (Viscusi et al., 2007).

2.5 Advantages and Disadvantages of Different Sterilization Methods

Several methods are applied for sterilizing different types of materials or surfaces. Every sterilization method possesses some advantages and disadvantages based on their working condition, toxicity, rapidity, cost, efficiency, and application. Table 2.1 summarizes the advantages as well as disadvantages of various sterilization methods.

Table 2.1 Advantages and disadvantages of different sterilization methods

Sterilization methods	Advantages	Disadvantages	References
Dry heat	• Easy installation • Operational simplicity	• Time consuming • Slower procedure • Restricted to heat-sensitive materials	Chin et al., 2020; Govindaraj and Muthuraman, 2015; Jinia et al.,

	• No need for pressure and vessels • No need for an outside jacket • No corrosion • Light weight • High penetration capability • Eco-friendly and nontoxic • Economical	• Causes distortion, oxidation, and softening of some materials • Damages styrene, acrylics, polyethylene terephthalate, plasticized polyvinyl chloride, and low-density polythene	2020; Kampf et al., 2020b
Moist Heat	• Nontoxicity • Simplicity in process • Easy control • Reliability • Rapidity • Ability to penetrate fabrics • Efficacy	• Heat-sensitive products cannot be sterilized • Increases cytotoxicity of rubber bands in teeth • Corrosion is possible • May hydrolyze certain plastics • Polymers cannot be steam sterilized	Govindaraj and Muthuraman, 2015; Pithon et al., 2010; Rutala and Weber, 2008
EtO	• It is a low temperature sterilization process • It can be widely used in packaging materials • High penetration ability • Eco-friendly • High microbial activity	• Pure EtO is flammable, toxic, and carcinogenic • Costly • Complex process • Residues left even after degassing	Govindaraj and Muthuraman, 2015; Rutala and Weber, 2008
Chlorine and their compounds	• Rapidity • Inexpensive • Non-flammable • Can be used as critical disinfectant • Bactericidal, fungicidal, virucidal, and tuberculocidal • Gas concentration can be easily controlled • Efficacy	• Corrosive to metal surfaces • Hazardous reaction with ammonia and acids • Stained or discoloration of fabrics • Leaving salt residues • Irritating at higher contents	Govindaraj and Muthuraman, 2015; Henwood, 2020; Singh et al., 2021b

	• No need for post-sterilization aeration	• Irritating to eye and skin	
O_3	• Highly efficient • Low temperature process • No need of manual handling • Non-toxic residues • Can be used for moisture and heat-sensitive materials • Compact size of chamber	• Corrosive • Limitation of data against microbicidal activity • Limitation of materials compatibility	Hiep et al., 2023; Mecha and Chollom, 2020; Rutala and Weber, 2013
H_2O_2	• Bactericidal, fungicidal, virucidal, and tuberculocidal • Nontoxicity • Rapidity • Non-flammable • Non-staining • Eco-friendly • No irritation or odor issues	• Limited data of clinical use • Hazardous to respiratory system, skin, and eye • Cannot be used for cellulose, powders, liquid, and linen materials • Less penetration ability than EtO • Damages nylon-based products	Banerjee et al., 2021; Govindaraj and Muthuraman, 2015; Hiep et al., 2023; Rutala and Weber, 2008
Peracetic acid	• Low temperature sterilization process • Nontoxicity • Rapidity • Highly efficient than EtO	• Pungent odor • Corrosive	Govindaraj and Muthuraman, 2015
QACs	• Effective against enveloped viruses • Non-staining • Fair priced • Can be used as cleaning agents • Surface compatibility	• Not effective against nonenveloped viruses • Some can cause eye burning and allergic skin rashes • Causes nose and throat irritation	Baker et al., 2020; Bharti et a., 2022; DeLeo et al., 2020
Alcohol	• Bactericidal, fungicidal, virucidal, and tuberculocidal • Rapidity • Non-staining • Non-corrosive	• Flammable • Rapid evaporation • Slow activity against nonenveloped viruses • Can damage some instruments	Al-Sayah 2020; Hiep et al., 2023; Yoo, 2018

	• No toxic residues • Suitable for small surfaces	• Not suitable for large surfaces	
Formaldehyde	• Fungicidal, bactericidal, and virucidal • Low temperature sterilization process • Simplicity in monitoring • More rapid than EtO • Inexpensive per cycle • Material compatibility	• Unpleasant odor • Carcinogenic and mutagenic to humans • Less penetration power than EtO • Inadequate temperature and humidity control	Bharti et al., 2022; Govindaraj and Muthuraman, 2015
Glutaraldehyde	• Low temperature sterilization process • Used as surface disinfectant • Non-corrosive • Excellent microbicidal activity	• Highly irritating • Time consuming • Increases cytotoxicity of orthodontic elastics	Bharti et al., 2022; Govindaraj and Muthuraman, 2015
NO_2	• Inexpensive • Durable • Low settings of resources • Proper penetration rate • More efficient than other gaseous methods under vacuum settings	• Toxic residues • Potential health hazard • Costlier than heat sterilization process	Bharti et al., 2022
X-ray	• High penetrating power • Machine generated source of irradiation • No toxic residue • Uniform dosage • No harm to plastic material • Required smaller chamber	• Higher safety required • Large amount of energy wastage	Hiep et al., 2023; Yoo, 2018
Gamma ray	• High penetrating power • Process simplicity	• High processing cost • Higher safety required	Bharti et al., 2022; Molina-Chavarria et al., 2020

	• Easy control • Rapidity • Can be used for large surface sterilization	• Large amount of energy wastage • Cannot be used for radiation sensitive material	
UV radiation	• Simple process • Low temperature sterilization process • Virucidal, bactericidal, fungicidal activity against enveloped viruses • Effective for flat and smooth surface • Inexpensive	• Antimicrobial activity varies from material to material • Less penetrating power to solids • Ineffective for rough surface • Hazardous to skin and eye	Hiep et al., 2023; Martins et al., 2022
Microwave	• Cost effective • Efficient	• Non-uniform heating • Cannot be used for large quantities	Bharti et al., 2022
IR radiation	• More penetrating power • High energy efficiency • Uniform heating • Proper control • High heat transfer coefficient • No toxic residue • Compactness of the equipment	• High heat may cause burning issue	Yadav et al., 2020

Based on the literature surveys of various sterilization methods as well as their advantages-disadvantages, design of a heat and UV based sterilization box is presented in this thesis. Further, to develop MVPs, sterilization box is transformed into a pedagogical gadget. In recent years, there have been intense research activities in the field of engineering pedagogy. Pedagogy is the art and science of teaching-learning approaches. It refers to the interaction between teachers and students, learning environment, and learning task. Different pedagogical gadgets viz., toys, doll-shaped robots, and inexpensive experimental setups are used for understanding some basic concepts of mechanical engineering (Billard, 2003; Paul and Dixit, 2011; Meng et al., 2019). Such pedagogical gadgets help in developing scientific spirit among

the students. Unfortunately, there is a dearth of consumer products in the form of pedagogical gadgets. Educational institutions have either high-cost experimental setups in the laboratories or no experimental setup for clarifying certain concepts. There is a strong need for developing easily affordable products for teaching the scientific principles in a simplified manner. Thus, a pedagogical gadget for teaching heat transfer is designed in this thesis.

Moreover, different industrial applications of sterilization methods are reported in literature survey. Uses of various sterilization methods viz., alcohol, dry heat, UV, VHP, autoclave, gamma radiation, and microwave to sterilize FFRs are reported (Banerjee et al., 2021; Cramer et al., 2020; Saini et al., 2020; Viscusi et al., 2007). In addition, sterilization methods are widely used in food industries. IR heat is used for manufacturing of juice and bread, drying, microbial inhibition as well as sterilization of grains. IR heat is extensively used for artificial ageing of rice grain (Khir et al., 2011; Khir et al., 2014; Pan et al., 2011). UV rays are also used to extend the shelf life of fresh products as well as processing of solid and liquid foods (Singh et al., 2021a). Thus, applications of the designed sterilization box to sterilize FFRs and drying as well as surface disinfection of rice are discussed in this thesis.

2.6 Gaps in the Literature

The information gathered from the published literature reveals a few research gaps with possibilities of further examination. The gap observed in the literature review are summarized as follows:

- Heat-based sterilization has shown potential in a variety of applications in different industries. UV-based sterilization has also been discovered to be quite effective for a variety of surfaces. However, the synergistic impact of simultaneous heat and UV is scant.
- A low-cost sterilization box equipped with both incandescent bulb heating and UV-C facilities have not been designed. Performance study of a sterilization box to fight against COVID-19 as well as its antibacterial activity have not been reported yet.
- IR radiation heating and UV-C facilities have not been used together in a sterilization box. Effectiveness of a sterilization box against COVID-19 along with broad-spectrum antibacterial activity have not been reported yet.

- The design transition of a sterilizing box into a pedagogical device to develop MVPs has yet to be documented.
- Sterilization of N95 mask using a sterilization box with simultaneous heat and UV-C treatment has not been reported. Change in mechanical properties of sterilized N95 filtration fiber viz., fiber diameter, surface roughness, ultimate tensile strength as well as scratch resistance, and any chemical changes are not presented till date.
- Application of a sterilization box for artificial ageing as well as surface disinfection of rice has not been reported yet.

2.7 Detailed Objectives of the Present Thesis

Based on literature survey the main objective was defined as design and development of a sterilization box and its variants using MVP for different field of applications. To accomplish the main objective, different products and applications of these products were investigated. Four sub-objectives were adopted to accomplish the main objective of the present thesis. The detailed objectives are as follows:

- **Design and development of a sterilization box equipped with incandescent bulb heating and UV-C irradiation as well as its performance study**

  The first objective of this thesis is to design an efficient, low cost and easy to handle sterilization box. For performance study, two assessments were performed. First, Immunoglobulin G (IgG), a model protein in lieu of spike glycoprotein of SARS-CoV-2 was incubated under heat and UV-C irradiation. The experimental conditions are determined using a statistical tool Response Surface Methodology with Central Composite Design technique (RSM-CCD). Unfolding of the protein is studied by measuring hydrodynamic size and optical density at 280 nm (OD_{280}). Further, it is confirmed by the intrinsic fluorescence measurement and Fourier Transform Infrared Spectroscopy (FTIR) analysis. Furthermore, antibacterial activity is carried out on clinically relevant *E. coli* bacteria as well as for bacteria collected from daily use items viz., wrist watch, belt, and wallet.

- **Design of a sterilization box having IR radiation heating and UV-C irradiation as well as its performance study**

  The second objective of this thesis is to design a sterilization box with IR radiation heating and UV-C irradiation facilities. For performance assessment, inactivation of both Gram-positive viz., *Staphylococcus aureus* (*S. aureus*) as well as Gram-negative viz., *Salmonella typhi* (*S. typhi*) bacteria is studied. A statistical tool, RSM-CCD is used to optimize the experimental conditions. Microscopic evaluation is carried out to confirm the inactivation of bacterial pathogen. Furthermore, unfolding of SARS-CoV-2 spike protein and a model protein RNase A is investigated experimentally. FTIR, Circular Dichroism (CD) spectroscopy, and intrinsic fluorescence is carried out to study the secondary structure of protein.

- **Study on the degradation of N95 respirator after disinfecting it using designed sterilization box**

  The third objective of this thesis is to study the changes in properties of N95 filtration fiber, disinfected by designed sterilization box. Five well established disinfection methods, viz., incandescent bulb heating, UV-C irradiation, air drying after alcohol immersion, exposing to steam, and incandescent bulb heating combined with UV-C irradiation are studied. Effects of these methods on fiber diameter, surface roughness (R_a), ultimate tensile strength (UTS), scratch resistance, and any chemical changes of the disinfected fibers are presented. Field emission scanning electron microscopy (FESEM), atomic force microscope (AFM), universal testing machine (UTM), scratch tester, and X-ray diffraction (XRD) are used to study the changes. A hypothesis testing is carried out to understand the significance of changes in fiber diameter and R_a.

- **Design and development of a variant for teaching heat transfer**

  The fourth objective of this thesis is to design a pedagogical gadget and illustrating its effectiveness for a better teaching-learning process. It is designed for teaching the basic concepts of heat transfer by conducting experiments, increasing the students' engagement in hands-on practices, developing the team spirit by making them work in a group and attracting the students towards a career in mechanical engineering. Five possible experiments with the help of developed gadget are described. A survey among students as

well as teachers of different levels is carried out using a set of written questions and statements in a feedback form. Feedback from the participants provides important information related to pedagogical usefulness as well as required modifications in the gadget.

- **Design and development of a variant for artificial ageing of rice**

  The fifth objective of this thesis is to study the cooking quality, nutrient value (carbohydrate, protein, fat), and moisture removal contents of treated rice. Electron microscopy analysis are carried out to study the microstructure of rice. Spread plate assay is carried out to study antimicrobial activity of combined IR radiation heating as well as UV-C irradiation. Preliminary survey with questionnaire is carried out to compare the taste and appearance of treated rice.

The research plan of the thesis is represented in a flow chart as shown in Figure 2.3.

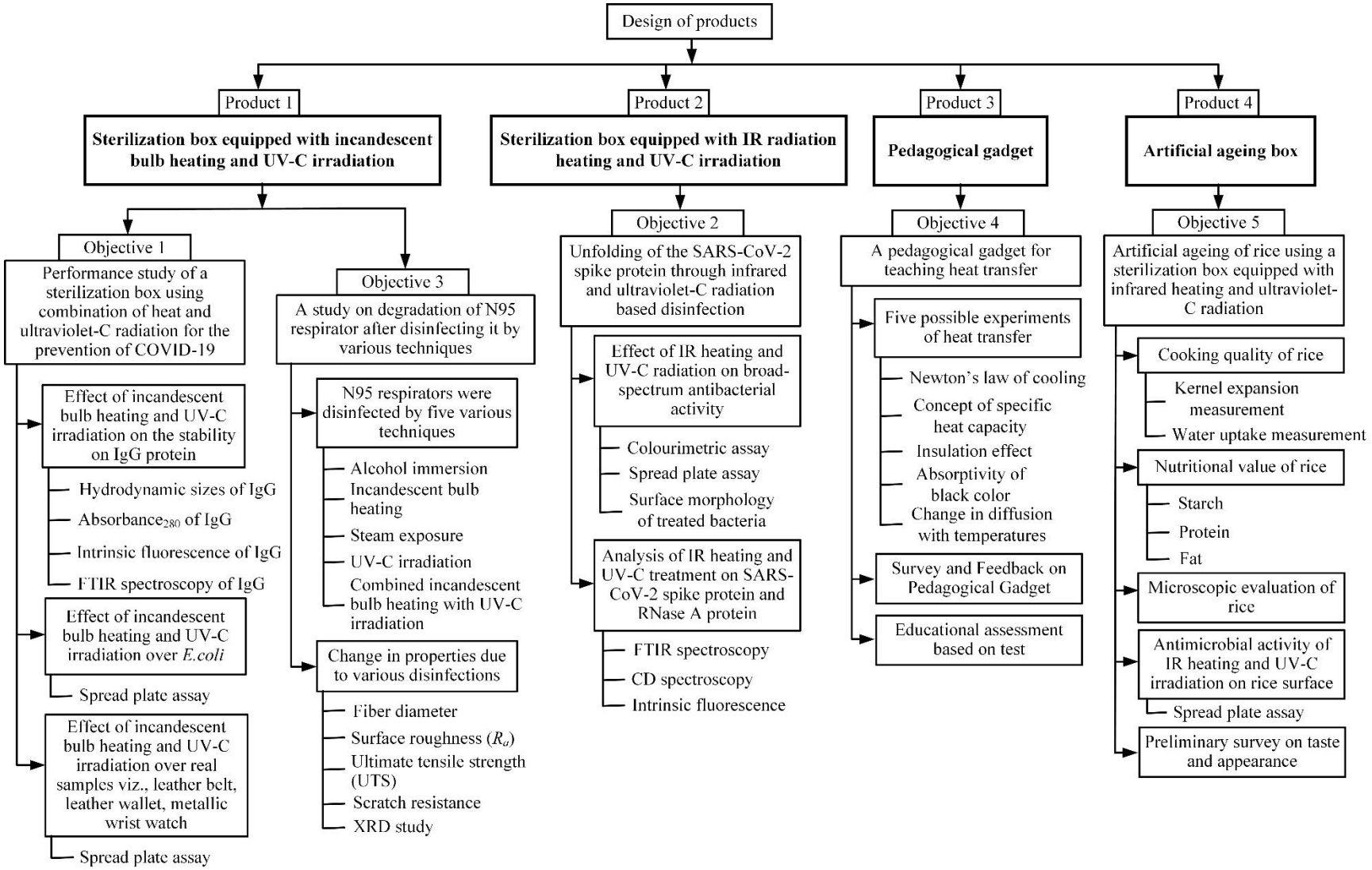

Figure 2.3 Flow chart of research plan

Chapter 3

Design of a Sterilization Box Using Combination of Heat and Ultraviolet Light Irradiation and its Performance Study

3.1 Introduction

Sterilization methods have been the captivating topic among researchers and the coronavirus disease 2019 (COVID-19) pandemic further highlighted the need of designing and developing a sterilization box equipped with an adequate approach. To study on severe acute respiratory syndrome coronavirus 2 (SARS-CoV-2), a glycoprotein Immunoglobulin G (IgG) was used as a model material in lieu of SARS-CoV-2 (Fischer et al., 2020; Salazar et al., 2020; Schmidt et al., 2020). The major stability of SARS-CoV-2 is due to the presence of the surface spike-glycoprotein, which is a three-domain protein with an isoelectric point (pI) of ~5.9 (Pandey, 2020b). The virus can be inactivated by altering the stability of this protein. Various physical (e.g., temperature and adsorption) and chemical (e.g., pH, disinfectants, and surface modification) methods have been explored to test the stability of the spike protein (Narita et al., 2021; Pandey, 2020a; Pandey, 2020b).

It has been reported that SARS-CoV-2 remains stable on different surfaces but can be inactivated by heating at a temperature greater than 65 °C for more than 5 min of duration (Abraham et al., 2020). Sarada et al. (2020) described the technologies of the International Advanced Research Center for Powder Metallurgy and New Materials (ARCI), India, in developing various disinfection systems to combat COVID-19 (Sarada et al., 2020). ARCI used physical, chemical, and dry heat processes to disinfect surfaces effectively. The duration and temperature required for sterilization of SARS-CoV-2 are not sufficient for inactivating the potentially harmful bacteria viz., *Escherichia coli* (*E. coli*), which are commonly present on the surfaces of objects (Bang et al., 2011; Bari et al., 2009; Choi et al., 2016). In this context, an effective ultraviolet type C (UV-C) based killing of bacteria have been reported (Gayán et al., 2012; Unluturk et al., 2008), which was also efficient for decontamination from SARS-CoV-2 (Cadnum et al., 2020; Maris et al., 2020). Heilingloh et al. (2020) carried out a comparative study between ultraviolet type A (UV-A) and UV-C irradiation for complete

inactivation of SARS-CoV-2 and found that UV-C is more effective in inactivating viruses. Complete inactivation of SARS-CoV-2 after 9 min of UV-C exposure was also mentioned (Heilingloh et al., 2020). Gayán et al. (2014) demonstrated the combined effect of UV and heat treatment in liquid foods (apple juice and orange juice), vegetable, and chicken broth from *Staphylococcus aureus* (*S. aureus*) disinfection (Gayán et al., 2014). Cheon et al. (2015) studied the degree of deactivation of foodborne pathogens on powdered red pepper under the combined treatment of UV-C irradiation and mild heat (Cheon et al., 2015). It was concluded that the combination of UV radiation and mild heat treatment is more effective than UV radiation alone for deactivating *E. coli* O157:H7 and *Salmonella typhimurium* (*S. typhimurium*). The existence of the synergistic effect of UV and heat treatment process was studied by Gouma et al. (2015) in apple juice for microbial inactivation (Gouma et al., 2015). To predict the effect of temperature on UV inactivation kinetics of microorganisms viz., *E. coli*, *S. typhimurium*, *L. monocytogenes*, and *S. aureus*, mathematical models were also developed (Gouma et al., 2015). Although these techniques are sufficient alone or in combination for the effective killing of bacteria, the synergistic effect on the microbiome over surfaces is still under scrutiny. Thus, it is necessary to design an easy to handle, simple, and cost-effective sterilization box with proper sterilization method. Both heating as well as UV-C irradiation facilities are included as UV-C irradiation is more effective in killing the pathogens in the surfaces and heat is effective in sterilizing the unexposed areas and pores.

In this chapter, a sterilization box is designed and presented its effectiveness for denaturation of glycoprotein IgG and inactivation of bacteria. The effects of heat and UV-C, individually and in combination, are presented. The required temperature and duration, with as well as without UV-C are optimized to denature the IgG and disinfect bacterial strain. In order to analyze the actual effect of the optimized conditions on day-to-day life accessories, the real samples are also sterilized at the optimized conditions.

3.2 Design of a Low-cost UV-C and Heat-based Sterilization Box

The sterilization box comprised a wooden box of size 58 cm × 25 cm × 19 cm, two 100 W incandescent bulbs, two 11 W UV-C lamps, one DTC, one timer, and one limit switch. Plywood of 8 mm thickness was used for making the wooden box. A small part of the wooden box was used as a compartment for electrical equipment and the other part was used as a

sterilization chamber. Electrical wires were placed inside the compartment of electrical equipment to avoid contact with users. Incandescent bulbs manufactured by Crompton were used for heating whereas UV-C lamps manufactured by Philips were used for radiation. Two-sided linear lamp holders (manufactured by EVERLITES in China) were used for holding the UV-C lamp in the wooden sterilization box. Aluminium lamp holders were used in the UV-C lamps because of its lightweight. Two switches were used for turning on/off the incandescent bulbs and UV-C lamps. Incandescent bulbs were connected with a DTC (manufactured by Robocraze) which measured the inside temperature of the sterilization chamber with the help of a thermocouple and showed it in the light emitting diode (LED) display. It also maintained the temperature inside the sterilization chamber. Once the temperature inside the box crossed the set value in DTC, it would automatically turn off the heating source i.e., incandescent bulb. DTC would turn on the incandescent bulb again, when the temperature lowered by 2 ºC with respect to the set value. A timer manufactured by Selec 800XA was also placed inside the chamber of electrical equipment. It was connected with the main supply to turn off after sterilizing an item for a pre-decided time. A limit switch controlled top cover was used to prevent the direct exposure of UV light to the human eye and skin. Incandescent bulbs were covered all around with a fencing net to safeguard against burning due to direct contact. To reduce the heat loss through the walls of the box, the inner surfaces were covered by a high reflecting galvanized iron (GI) sheet; the thin layer of air between the surfaces of the wooden box and GI sheet acted as a thermal insulator. Further, to increase the reflectivity of the GI sheet, it was covered through aluminium foil adhesive tape (of about 0.1 mm thickness) on the inner surfaces. Figure 3.1 and Figure 3.2 show the schematic diagram and photograph of the box, respectively. Due to efficient design, it takes about 150 s for an empty box to achieve a temperature of 70 °C from an ambient temperature of 24 °C.

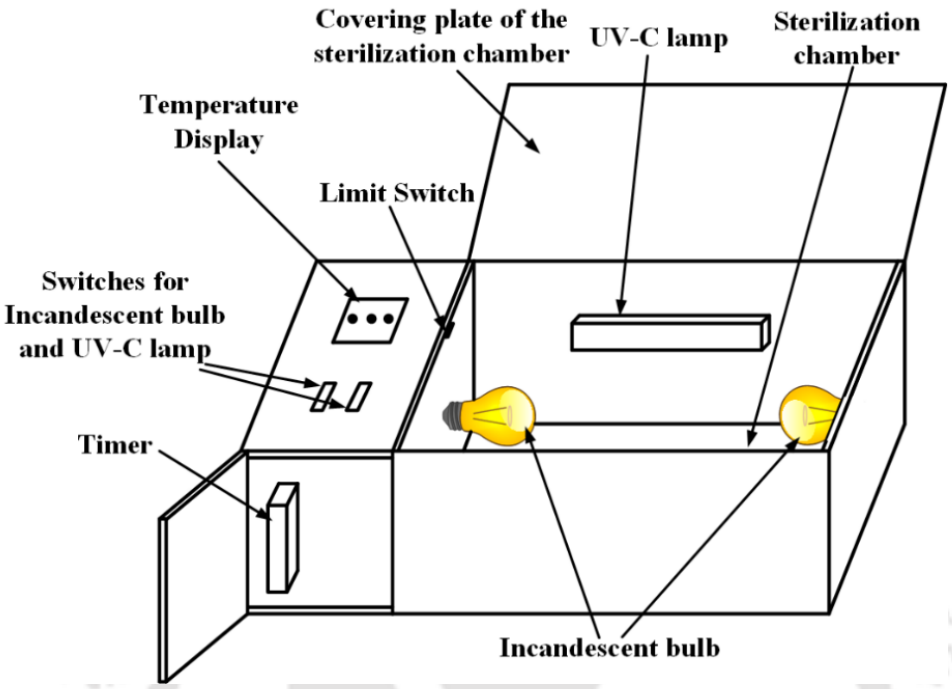

Figure 3.1 A schematic diagram of the sterilization box (fencing of bulbs removed)

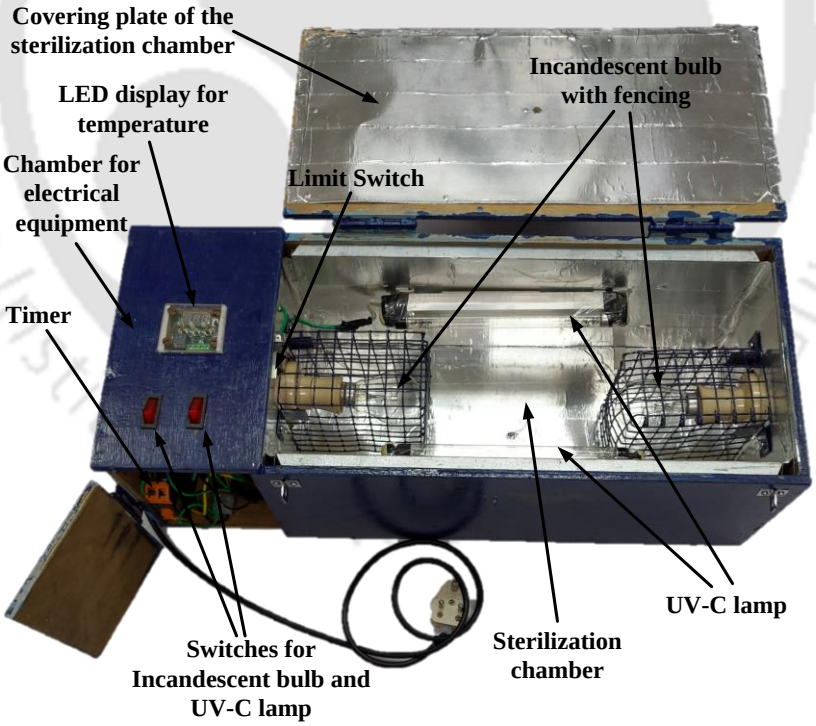

Figure 3.2 Photograph showing different parts of the sterilization box

3.3 Cost Estimation of the Designed Sterilization Box

Table 3.1 lists the items that were used in fabricating the sterilization box. A total amount of US $34.16 was spent on material for fabricating one unit of sterilization box. The labour cost for fabricating a sterilization box was estimated as $13.58. This was based on considering 8 man-hours for fabrication and assuming a monthly emolument of $339.38 for a skilled technician based on the average Indian scenario. Thus, the total fabrication cost was estimated as $47.74 per unit of sterilization box. In mass production and scale-up, the cost will further reduce. Online shopping portals provided a typical price of $176 for a UV based disinfection system of similar size. Compared to it, the proposed sterilization box is cost-effective. Moreover, it has both heat and UV-C radiation facilities.

Table 3.1 Material cost in the fabrication of a sterilization box

S. N.	Item	Quantity	Unit cost ($)	Total cost ($)
1	11-W UV-C Lamp	2	3.12	6.24
2	UV-C Lamp holder	2	2.99	5.98
3	100-W Incandescent bulb	2	0.20	0.4
4	Incandescent bulb holder	2	0.20	0.4
5	Electrical switches	2	0.14	0.28
6	Digital Temperature Controller (DTC)	1	2.72	2.72
7	Timer	1	9.37	9.37
8	Limit switch	1	0.41	0.41
9	8 mm thick plywood of surface area 6026.5 cm^2			3.99
10	0.8 mm thick GI sheet of surface area 4073.94 cm^2			2.33
11	Miscellaneous			2.04
	Total			**$34.16**

3.4 Performance Study of the Designed Sterilization Box

To carry out the performance study, synergistic effect of temperature and UV-C over sterilization was examined by two assessments. First, unfolding of glycoprotein IgG incubated under heat and UV-C was studied. Conformational changes in IgG was studied as the unfolding of this protein leads to inactivation of SARS-CoV-2. Hence, IgG was used as a model material in lieu of SARS-CoV-2. Furthermore, antibacterial efficiency of the sterilization box for clinically relevant *E. coli* bacteria as well as for bacteria collected from daily use items was carried out.

3.4.1 Materials and Methods

A low-cost UV-C and heat-based sterilization box was fabricated. Lyophilized IgG from bovine serum was procured from Sigma Aldrich (L5506). NaCl (GRM 853), NaOH (TC460), and HCl (AS003) were purchased from HiMedia India. KCl (104936), Na_2HPO_4 (137036), and KH_2PO_4 (104873) were procured from Merck India. Milli-Q water (resistivity: 18 MΩ.cm at 25 ºC) was utilized throughout the chapter.

3.4.2 Design of Experimental Conditions

The effect of temperature and the UV-C incubation with respect to time was analyzed on the glycoprotein IgG and the bacterial cells. First, the expected time and temperature were determined by the Response Surface Methodology with Central Composite Design (RSM-CCD) technique using the Design-Expert software as shown in Table 3.2. The temperature range was varied from 40–70 °C and the time ranged from 5–15 min based on the previous reports (Pandey, 2020a; Pandey 2020b). The software resulted in 13 different combinations of input variables (time and temperature).

3.4.3 Preparation of Protein Solution

To analyze the effect of heat on the IgG protein, the stock solution of IgG (1 mg/mL) was prepared in phosphate buffer saline (PBS) at pH 7.4. PBS (1X) solution was prepared by mixing the appropriate amount of NaCl (8 g), KCl (0.2 g), Na_2HPO_4 (1.44 g), and KH_2PO_4 (0.24 g) in Milli-Q (800 mL) water, followed by mixing until a transparent and clear solution was obtained (Hasan et al., 2018a). The final volume was made up to 1000 mL by adding Milli-Q water. The pH of the as-prepared PBS solution was maintained at 7.4 through 0.1 M of NaOH and HCl solution. The protein solution was then filtered using a 0.22 µm syringe filter.

To estimate the final concentration of the stock solution, the absorbance values were measured using a UV spectrophotometer (Thermo Scientific; Evolution 201) at 280 nm. The stock concentration was calculated using Beer Lambert's law with the extinction coefficient value of 210,000 $M^{-1}cm^{-1}$ (Reader et al., 2019). A final concentration of 0.1 mg/mL was prepared as a working solution for further usage.

Table 3.2 Experimental conditions obtained from RSM-CCD technique

Experimental conditions	Time (min)	Temperature (°C)
1	2.93	55
2	10	55
3	5	40
4	5	70
5	15	70
6	10	76.21
7	17.07	55
8	15	40
9	10	33.79
10	10	55
11	10	55
12	10	55
13	10	55

3.4.4 Analysis of Temperature and UV-C Incubation on the Stability of Protein

The protein samples were transferred to a 5 mL glass test tube, and the protein samples were incubated under heat and UV-C along with heat as listed in Table 3.2. After treatment, the samples were investigated via calculating the absorbance at 280 nm ($Absorbance_{280}$) wavelength for the protein estimation. Similarly, the hydrodynamic sizes of the treated protein under heat and combined (UV-C + heat) incubation were calculated through dynamic light scattering (DLS) analysis using Litesizer 500 (Anton Paar) at room temperature. Further, the intrinsic fluorescence of the protein was measured using a fluorimeter (Fluoromax 4). The

native protein at room temperature without any incubation was considered as the control sample. The hydrodynamic sizes, absorbance$_{280}$, and intrinsic fluorescence were evaluated, which reflect the unfolding of the protein (Sharma and Pandey, 2021a; Sharma and Pandey, 2021b).

3.4.5 Effect of Temperature and UV-C Incubation over Bacterial Inactivation

Similar to that of protein, the effect of temperature and UV-C incubation was analyzed over the bacterial cells. For this purpose, two separate experiments were performed– (1) experiments on clinically relevant bacteria and (2) experiments on real samples. The methodology is described in the sequel.

3.4.5.1 Effect of temperature and UV incubation over clinically relevant bacteria

To analyze the effect of temperature and UV-C incubation over bacterial cells, *E coli* (*Gram-negative*, MTCC 1610) was first incubated in autoclaved Luria Bertani (LB) Medium (GM1245; Himedia, India) for overnight. After incubation, the bacteria were subcultured for 6 hours to obtain the log phase. The bacterial cells were centrifuged at 8000 revolutions per minute (RPM) for 5 min, and the pallets were incubated into sterile Milli-Q water at pH 7.4. The optical density at 600 nm (OD_{600}) of the culture was adjusted to 0.1 corresponding to an approximate concentration of 10^7 CFU/mL (control cells). The bacterial cells were then treated at 70 °C, under UV-C incubation (1 mL bacterial suspension in 5 mL of a glass test tube) as well as under simultaneous heat and UV-C incubation up to 15 min and the OD_{600} values were measured after incubation. The 4th dilution of the control and undiluted treated samples were spread over LB agar plate overnight to confirm the bacterial inactivation. In addition, the death rate (k_d) of the *E. coli* was estimated under all the given incubations using $OD_{600}t_t = OD_{600}t_0\, e^{-k_d t}$. k_d values were calculated from the $\left(\frac{OD_{600}t_t}{OD_{600}t_0}\right)$ versus time graph, where, $OD_{600}t_t$ is the OD_{600} value at time *t*, and $OD_{600}t_0$ is OD_{600} value at time zero.

3.4.5.2 Effect of temperature and UV incubation over real samples

To estimate the effect of temperature and UV-C incubation over real samples, the bacterial cells were isolated from the 1×1 cm^2 area of the leather belt, leather wallet, and metallic wristwatch using a sterile cotton swab and incubated into 1 mL of the autoclaved Milli-Q water. Next, these samples (leather belt, leather wallet, and metallic wristwatch) were treated at 70 °C under UV-C incubation for 15 min. After the treatment, again samples were isolated from

the 1×1 cm^2 area using a sterile cotton swab and incubated into 1 mL of the autoclaved Milli-Q water. Similar to that of *E. coli*, the isolated bacteria from the given real samples before and after treatment were spread over the LB agar plate for overnight at 4^{th} dilution and undiluted, respectively. The bacterial growth (colony) after the incubation was examined. All the experiments were performed in triplicates. The results shown in the manuscript are the average values with their respective standard deviations.

3.5 Results and Discussion

In this chapter, a cost-effective sterilization box is developed and the synergistic effect of UV-C irradiation and temperature over sterilization was examined. For this purpose, the effect of UV-C and heat on glycoprotein viz., IgG as well as bacterial cells were observed. The detailed results are described in the sequel.

3.5.1 Effect of Heat and UV-C Treatment over IgG

The effects of temperature alone and UV incubation along with temperature were analyzed on IgG model protein. The hydrodynamic size of the native IgG was found to be ~5 nm, in agreement with the literature (Hawe et al., 2011). The absorbance of native IgG was 0.172, which corresponded to 0.1 mg/mL of IgG using Beer Lambert's law (Reader et al., 2019). The effects of varying temperature and combined UV and temperature with time were evaluated at the conditions suggested by Design-Expert software (Table 3.2). For this purpose, the absorbance values at 280 nm and hydrodynamic sizes were measured after treating the protein at different experimental conditions as discussed in Section 3.3.2. The responses (hydrodynamic size and absorbance) at these conditions are shown in Figure 3.3. In the Figure, unfilled symbols pertain to heat only and filled symbol correspond to heat with UV-C. The experimental data of responses are also listed in Table 3.3 for better representation.

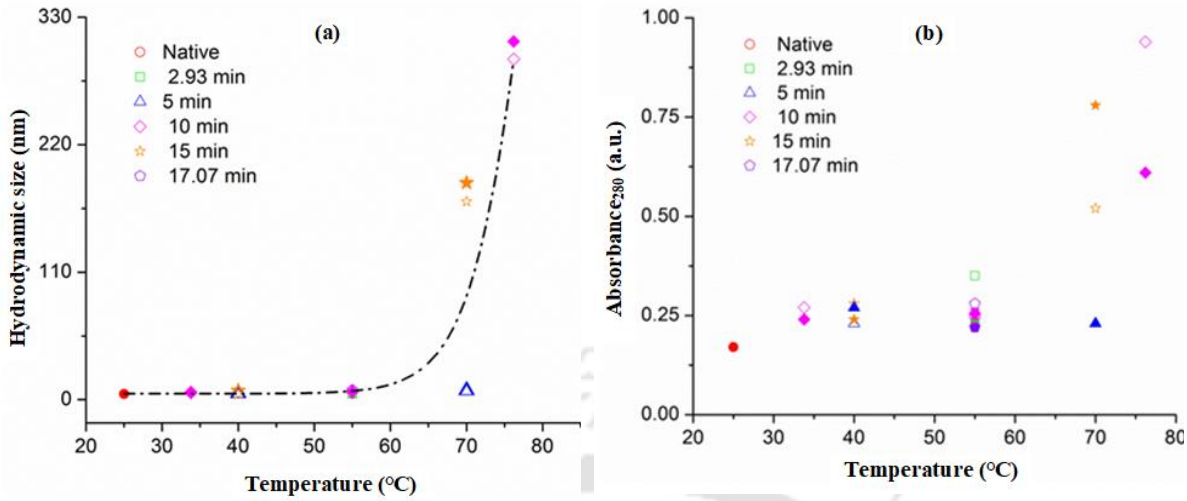

Figure 3.3 Effect of temperature and UV incubation over **(a)** hydrodynamic sizes and **(b)** absorbance$_{280}$ of IgG. (Empty symbols represent heat treated IgG, and filled symbols correspond to the heat and UV-C treated IgG)

Table 3.3 Hydrodynamic size and optical density in different experimental combinations

Input variables	**Responses**			
Experimental conditions	**Hydrodynamic size (nm)**		**OD_{280}**	
	Heat	**UV+ Heat**	**Heat**	**UV+ Heat**
1 (2.93 min, 55 °C)	6.38	4.99	0.35	0.23
2 (10 min, 55 °C)	8.44	6.78	0.24	0.25
3 (5 min, 40 °C)	5.81	5.59	0.23	0.27
4 (5 min, 70 °C)	7.36	8.08	0.23	0.23
5 (15 min, 70 °C)	171.03	187.06	0.52	0.78
6 (10 min, 76.21 °C)	293.93	309.02	0.94	0.61
7 (17.07 min, 55 °C)	8.49	7.65	0.28	0.22
8 (15 min, 40 °C)	4.812	7.87	0.28	0.24
9 (10 min, 33.79 °C)	6.00	6.50	0.27	0.24
10 (10 min, 55 °C)	7.76	7.52	0.23	0.24
11 (10 min, 55 °C)	7.74	7.93	0.26	0.26
12 (10 min, 55 °C)	6.82	5.48	0.25	0.25
13 (10 min, 55 °C)	6.92	7.57	0.25	0.27

The absorbance values at 280 nm were found to increase with the increase in temperature above 70 °C. Protein solution incubated at 76.21 °C exhibited the maximum absorbance value of 0.94 within 10 min followed by absorbance at 70 °C. The increase in absorbance is related to the exposure of aromatic amino acids present in IgG because of the conformational changes (Sharma and Pandey, 2021a). The denaturation temperatures of IgG are reported as 61 and 71 °C (Vermeer and Norde, 2000). Moreover, the melting point, T_m of the IgG was found to be 69 °C (Martin et al., 2014); hence, the observed increase in the absorbance values indicated the deformation in the IgG's native conformation. However, the effect of time was found not to be significant below the temperature of 70 °C.

Similar to the absorbance values at a higher temperature, the hydrodynamic sizes of the IgG protein were found to increase with the increase in temperature and time of exposure. The increase in the hydrodynamic size at a higher temperature indicated the unfolding (increase in the size) of IgG at elevated temperatures (Martin et al., 2014; Zhang and Topp, 2012). IgG incubated at 76.21 °C under UV-C incubation resulted in the maximum hydrodynamic size of 309.02 nm; at the same temperature without UV the hydrodynamic size was found to be lower i.e., 293.93 nm (Figure 3.3(a)). It indicates the significant role of UV-C incubation on the unfolding/denaturation of the IgG at elevated temperatures (Zhang and Topp, 2012). It has been observed that a 4 W UV-C lamp under 0.930–0.932 mW/cm^2 and 65 °C dry heat for 20 min was sufficient to inactivate the entire swine coronavirus from N95 mask surfaces (Chotiprasitsakul et al., 2020). In the present chapter, two 11 W UV-C lamps resulted in the unfolding of IgG protein.

The effect of temperature below a critical time was found not to be significant at the conditions selected in this study. Similarly, the effect of time up to 15 min was also ineffective below a critical temperature. Hence, model equations relating input variables with the responses as predicted by Design-Expert software were not significant. However, the experimental data were fitted to a sigmoidal expression as shown in Figure 3.3(a) (dotted line). The data fitted very well with R^2 value of 0.99. The critical point (lag time) was estimated from the sigmoidal expression and was found to be 70 ± 1 °C. This temperature also agreed to the denaturation temperatures of IgG (Vermeer et al., 1998). Therefore, a temperature of 70 °C appears to be optimal for the unfolding of this model glycoprotein. It has been reported that unfolding/conformation changes of the surface glycoprotein of a virus leads to its

disintegration and finally its inactivation (Hsu et al., 2011). The loss of viral surface protein due to external factors like a higher temperature and the strong surface-protein interactions disintegrates the virus assembly (Liu et al., 2015; Pandey, 2020b). It is also observed that UV-C light enhances the hydrodynamic size, but not drastically. Heat alone can perform well in the denaturation of IgG. Figure 3.3(b) shows $Absorbance_{280}$ of IgG at various conditions.

To examine the combined effect of heat and UV-C treatments on the conformational changes of IgG, the intrinsic fluorescence values were recorded by exciting the protein at 290 nm and the emission values were scanned from 300 nm to 450 nm. The intrinsic fluorescence is produced due to the presence of aromatic amino acids (monomers) of the protein. The native IgG exhibited the maxima at 327 nm, whereas a peak-shift was observed at 332 nm and 331 nm at 76.21 °C for 10 min and 70 °C for 15 min, respectively (Figure 3.4(a)). This indicates the unfolding and deformation in the native structure of the IgG at temperatures above a critical temperature of 70 °C (Arfat et al., 2014; Pandey, 2020b). Further, in the case of combined UV-C and heat exposure, the maximum fluorescence intensity was observed at 70 °C for 15 min (Figure 3.4(b)). This indicates the synergistic effective role of UV-C in the unfolding and conformational changes in the IgG structure (Arfat et al., 2014). All these results suggested that the incubation of heat and UV-C together at 70 °C for 15 min unfolds the glycoprotein to a required extent and can be useful for the inactivation of viruses for sanitization purposes.

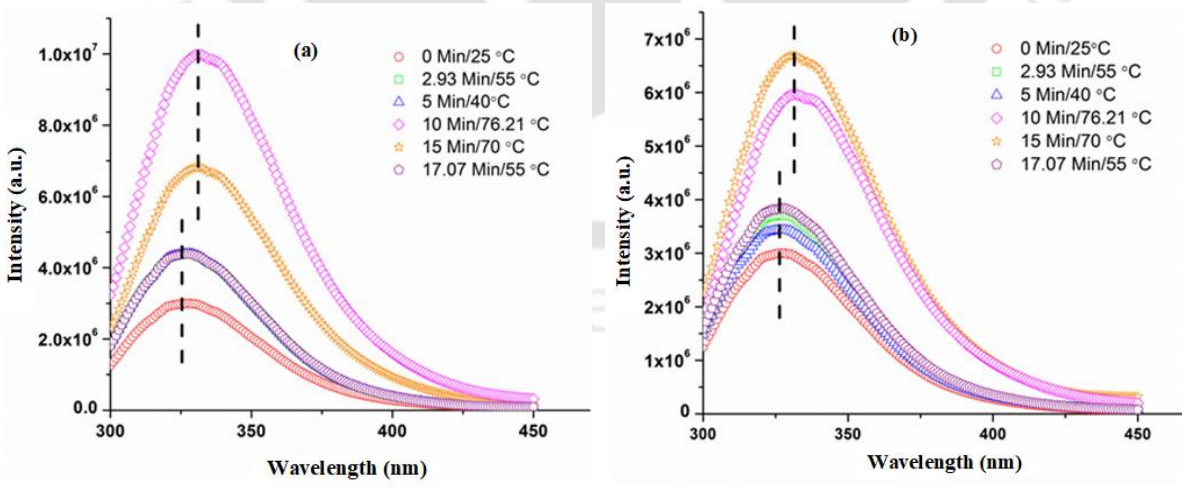

Figure 3.4 Intrinsic fluorescence of IgG protein at various time/temperature: **(a)** heat only and **(b)** combined UV and heat

Further, the conformation changes of the combined heat and UV treated IgG at the above optimized condition (70 °C for 15 min) were analyzed as compared to the native IgG using Fourier Transform Infrared Spectroscopy (FTIR) analysis. The FTIR spectra of native and heat-treated IgG are shown in Figure 3.5, which were de-convoluted and the area of de-convoluted peaks have been used to deduce the contents of the secondary structure (Sharma and Pandey, 2021a). The contents of α-helix, β-sheet, and β-turn in native IgG were found to be 32, 55, and 13%, respectively, which agreed to the reported data (Hasan et al., 2018a). In the case of heat-treated IgG, the contents of β-sheet increased to 70% and α-helix decreased to 22%. This complemented the DLS, absorbance, and fluorescence data.

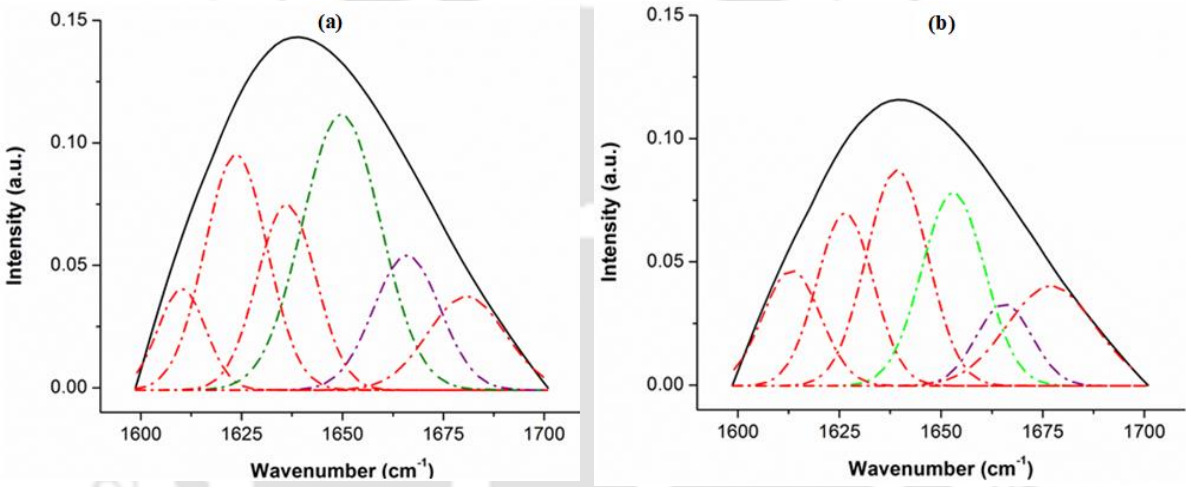

Figure 3.5 FTIR spectra of **(a)** native and **(b)** heat and UV treated IgG at 70 °C for 15 min. Dotted lines refer to the deconvoluted spectra. The areas of deconvoluted peaks have been used to deduce the contents of the secondary structure. The dotted lines indicate the following secondary structures viz., Green line: α-helix, Purple line: β-turn, and Red lines: β-sheet

3.5.2 Effect of Temperature and UV Incubation over Bacterial Inactivation

The effect of temperature and UV incubation was scrutinized over clinically relevant Gram-negative bacteria, *E. coli* as discussed in Section 3.3.5.1. OD_{600} values were found to decrease with an increase in time (Figure 3.6). At 15 min of incubation, the OD_{600} values followed the order of 0.09 ± 0.01 (UV-C only) > heat only at 70 °C (0.082 ± 0.007) > 0.077 ± 0.007 (combined UV-C and heat). The result indicated that UV-C incubation along with heat treatment is more effective in bacterial destruction than that of either heat or UV-C treatment. The death rate (k_d) of the *E. coli* samples were calculated from the exponential fitting of $\frac{OD_{600}t_t}{OD_{600}t_0}$

versus time graph. The k_d values were found to be 0.008, 0.014, and 0.019 min^{-1} for UV-C, heat, and simultaneous heat and UV-C incubation treatments, respectively. The highest death rate during the simultaneous heat and UV-C incubation reflected the effectiveness of the designed box for bacterial sterilization purposes.

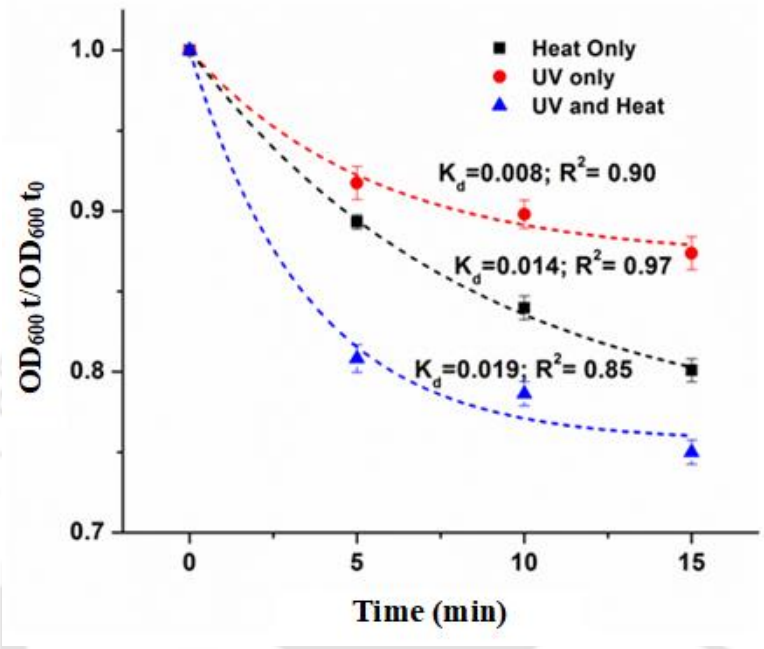

Figure 3.6 Reduction in the OD_{600} values of *E. coli* treated by heat (70 °C), UV-C, and combined UV-C and heat for different time intervals. The dotted lines are filled data to determine the value of k_d

The incubation time of 15 min is not adequate to observe the actual decrease in cell numbers through the measurement of optical density. Thus, in order to confirm the bacterial destruction, the treated and non-treated *E. coli* cells were spread over LB agar plate to determine the live and dead cells. Untreated bacterial cells were used as control samples as discussed in Section 3.3.5.1. As expected, the *E. coli* control samples reflected colonies of live cells and concentration was calculated to be 10^7 CFU/mL (10^{-4} dilutions), which agrees with literature (Shivaprasad et al., 2021; Singh et al., 2021c). As compared to the control samples, a significant decrease in the bacterial colonies was observed after the incubation as depicted in Figure 3.7. No colony could be seen in the treated sample spread over the agar plate without any dilution. This indicates the efficacy of the heat and UV-C treatment for the complete and effective disinfection of bacterial pathogens.

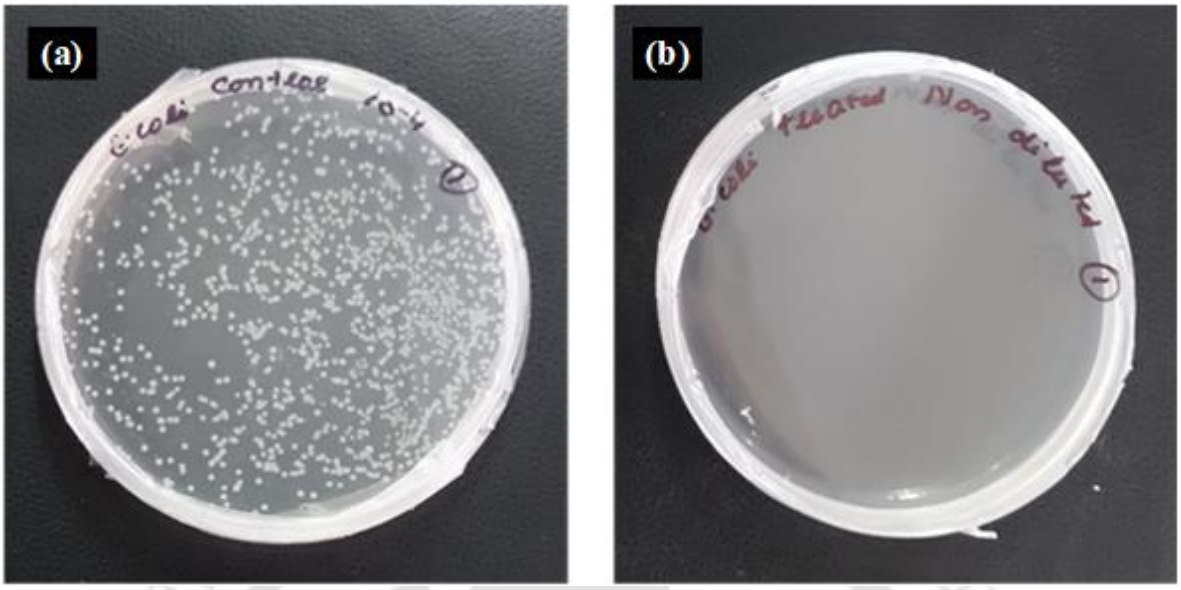

Figure 3.7 The number of *E. coli* bacteria colonies in case of **(a)** control (OD_{600} = 0.1) spread at 10^{-4} dilutions and **(b)** treated at 70 °C under UV-C incubation for 15 min spread at 10^{0} dilution (undiluted). No colonies are observed after the treatment as compared to the control cells

Heat treatment is the most basic method for reducing the populations of pathogenic microorganisms. It has been reported that the heat treatment alone at 60 °C did not show a required sterilization effect, but was found to be effective at simultaneous UV-C and heat treatment of *Salmonella* and *Escherichia sp*ecies (Park et al., 2019). Moreover, a single treatment with either heat or UV radiation may not kill or inactivate the pathogenic microorganisms, but can injure the cells. However, these injured cells may exhibit a revival and hence, can be quite harmful (Back et al., 2012). This effect stems from the fact that heat increases the fluidity of the cell membrane making the affected cells more sensitive to UV exposure (Gayán et al., 2013; Zhang et al., 2015). Thus, it can be concluded that the combination of both UV-C and heat treatments is much more effective than the individual use of either of these. It has been reported that UV-C light was found to be effective for decontamination up to a distance of 1 meter (González, 2021). In another study, *Candida auris* were effectively killed by the UV-C light in 30 min up to a distance of 2 meters (de Groot et al., 2019). In this study, the dimensions of the sterilization chamber are 0.17 × 0.43 × 0.20 m (H × L × W), which are adequate for the UV-C sterilization. To further analyze the synergistic effect of UV-C and heat over real samples, the bacterial cells were collected from various

sources as given in Section 3.3.5.2. Samples collected from given surfaces reflected > 10^2 colonies from belt, watch, and wallet surfaces at 10^{-4} dilutions as shown in Figure 3.8. Interesting results are obtained after the treatment. After treatment, no colonies were observed in all the samples without any dilution as shown in Figure 3.8(d–f). This reflects the effective sterilization of real samples in the designed chamber. These results suggest that UV-C irradiation combined with mild heating can be utilized for sterilization of personal accessories. Hence, combined UV-C and heat treatment can be utilized for sanitzing the bacteria and viruses from various day-to-day surfaces.

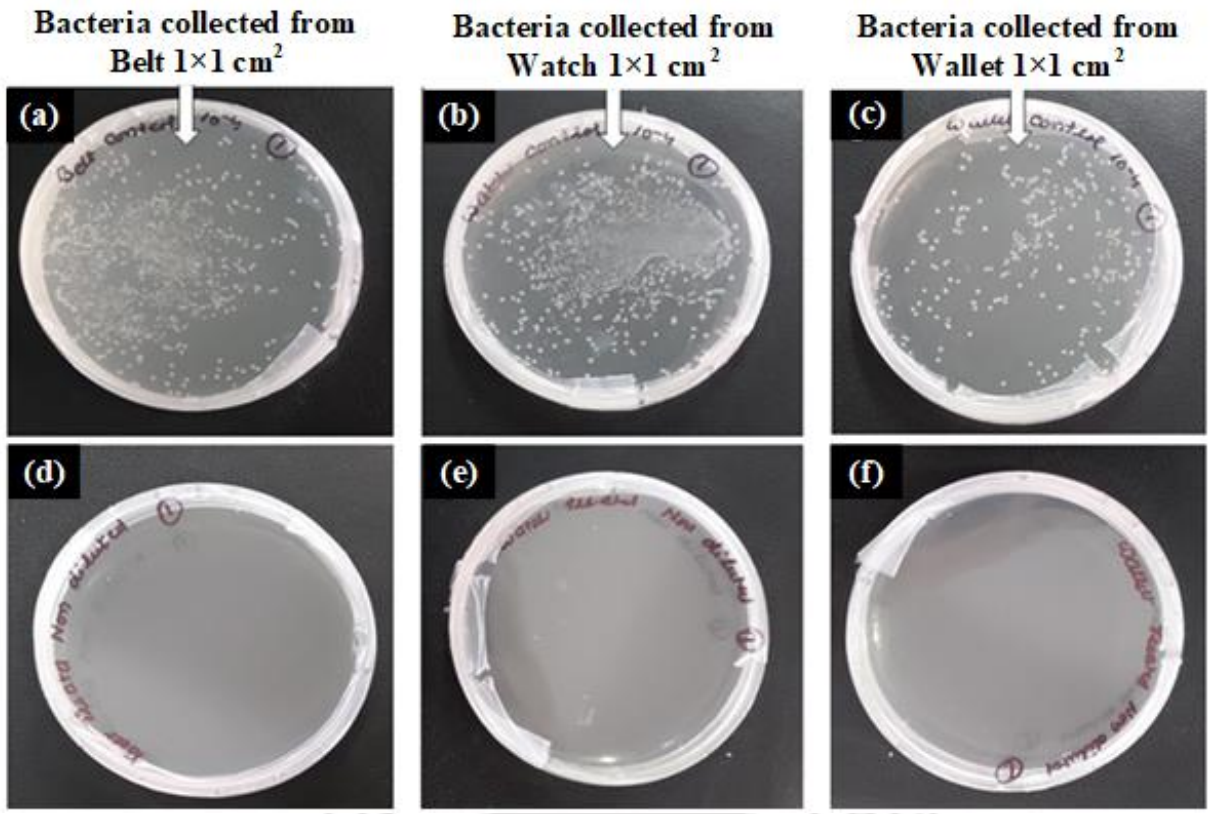

Figure 3.8 Bacterial inactivation at UV and heat treatment. The samples were taken from **(a)** belt, **(b)** watch, and **(c)** wallet and at spread at 10^{-4} dilutions. (**d**–**f**) are treated samples spread at 10^0 dilution (undiluted). No colonies as compared to control samples were observed after treatment at 70 °C under UV-C incubation for 15 min

3.6 Conclusions

Considering the crisis created by COVID-19 pandemic, a sterilization box (prototype) was designed and fabricated for disinfecting the items of daily use such as face masks, wallets, belt, and wristwatch. The box comprised two 100 W incandescent bulbs and two 11 W UV-C lamps

along with some electronic accessories. The cost of fabricating the prototype was less than $50. A study was conducted to study the effectiveness of the box chamber for sanitizing the items from bacteria and viruses. The salient findings are as follows:

1. The hydrodynamic size of IgG protein (used as a model material) during simultaneous UV-C and heat incubation was found to be much higher than that of only heat treatment, demonstrating the significant role of UV-C in the unfolding of IgG protein. However, heat alone was also found to be effective to some extent.
2. The results suggested that the incubation of heat and UV-C together at 70 °C for 15 min unfolds the glycoprotein to a required extent and can be useful for the deformation of several bacteria and viruses for sanitizing purposes.
3. Dry heat at 70 °C along with the UV-C incubation was found to be a suitable condition to sanitize items of daily use with 100% antiviral and antibacterial efficiency.
4. The present study also demonstrated the experimental protocols to test the efficacy of sterilization boxes or chambers.
5. The designed prototype can be scaled-up for handling a large number of samples for sterilization before their disposal to the environment.

Chapter 4

Design of a Sterilization Box having Both IR Radiation Heating and UV-C Irradiation Facilities and its Performance Assessment

4.1 Introduction

Coronavirus disease 2019 (COVID-19) pandemic underlined the performance assessment of sterilizing box equipped with an appropriate technique. The severe acute respiratory syndrome coronavirus 2 (SARS-CoV-2) comprises surface spike glycoprotein and Ribonucleic acid (RNA) (Zeng et al., 2020). The inactivation of the coronavirus is achieved through two approaches— (1) interfering with RNA or synthesized protein viz., antigen and (2) unfolding/denaturation of the spike protein (Pandey, 2020b). The unfolding of the protein disables its binding with surface receptors, e.g., angiotensin converting enzyme 2 (ACE2) and entry into the host cells (Li and Hirst, 2020; Lokman et al., 2020). Approach 2 is mostly recommended as a preventive measure.

In this chapter, a sterilization box is designed and tested its effectiveness for killing bacteria pathogens along with the unfolding of proteins. Broad-spectrum of antibacterial activities are also presented to enable the multipurpose usage of the box in healthcare. Infrared (IR) radiation is set up in the disinfection box along with ultraviolet type C (UV-C). Optimization of UV-IR disinfection time and temperature are presented for the inactivation of bacterial growth on both a Gram-positive, viz., *Staphylococcus aureus* (*S. aureus*) and a Gram-negative, namely, *Salmonella typhi* (*S. typhi*) using a statistical tool Response Surface Methodology with Central Composite Design (RSM-CCD). Based on the obtained optimized conditions, the effect of treatment on the secondary structures of SARS-CoV-2 spike protein and another model protein RNase is studied. The main focus of the present chapter is to provide an inexpensive and efficient sterilization method by combining IR and UV-C irradiations to fight against contagious infections by viruses and bacterial pathogens.

4.2 Design of a Sterilization Box with UV-C and IR Radiation Facility

The sterilization box consisted of a wooden box of size 53 cm × 24 cm × 21 cm, a 250 W IR lamp, two 11 W UV-C lamps, a Digital Temperature Controller (DTC), a limit switch, and a timer. A minor modification is implemented in the newly designed sterilization box.

Incandescent bulb heating is replaced by the effective IR radiation heating. Except the heating method, the rest of the design procedure is same as the previously designed sterilization box as discussed in chapter 3. Figure 4.1 and Figure 4.2 show the schematic diagram and a photograph of the box, respectively. The sterilization box was designed in such an effective way that it took only 70 s for an empty box to achieve a temperature of 70 °C from an ambient temperature of 25 °C. DTC maintained the temperature at T ±1 °C inside the box for a given period of the experiment. The temperature at the center of the sterilization box (where items to be sterilized were kept) was also measured using a thermometer and no difference was found compared to the temperature measured by DTC.

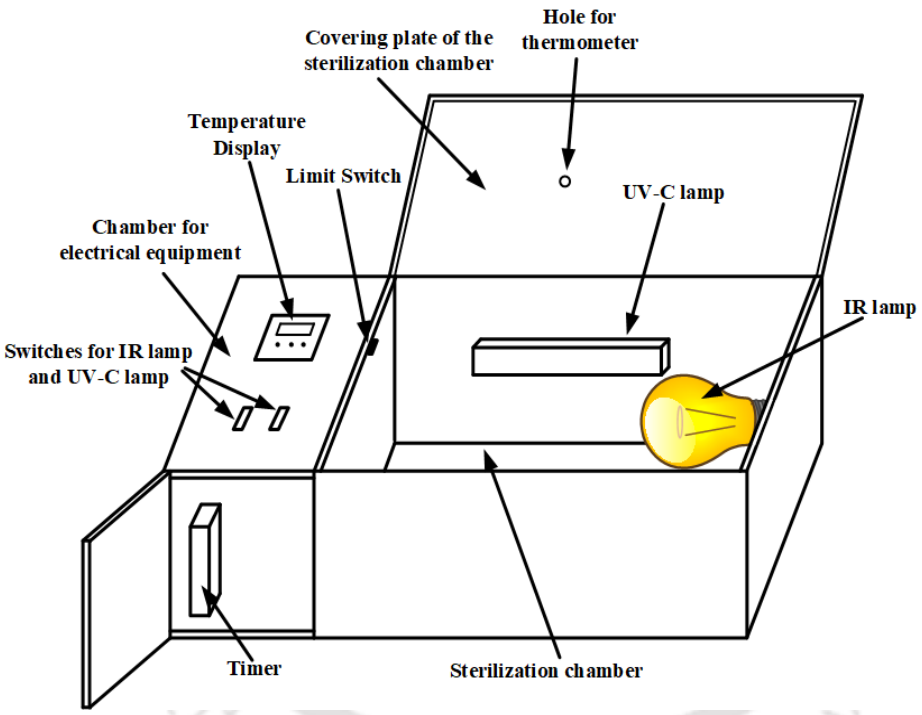

Figure 4.1 A schematic diagram of the sterilization box

UV-C radiation required to inactivate SARS-CoV was suggested to be above ~3.6 J/cm^2 (Liao et al., 2020). In the designed box, UV-C dose can be calculated using (Yujie et al., 2020)

$$D \propto \frac{Pt}{4\pi d^2} \tag{4.1}$$

where D is UV-C dose, P is UV bulb power, t is exposure time, and d is distance of bulb from the surface to be sterilized. Using Eq. 4.1, UV-C dose provided to the items to be disinfected

in this sterilization box was calculated as 11.11 J/cm^2 (assuming a proportionality factor of 1 in Eq. 4.1), which was found to be more than the dose suggested (Liao et al., 2020).

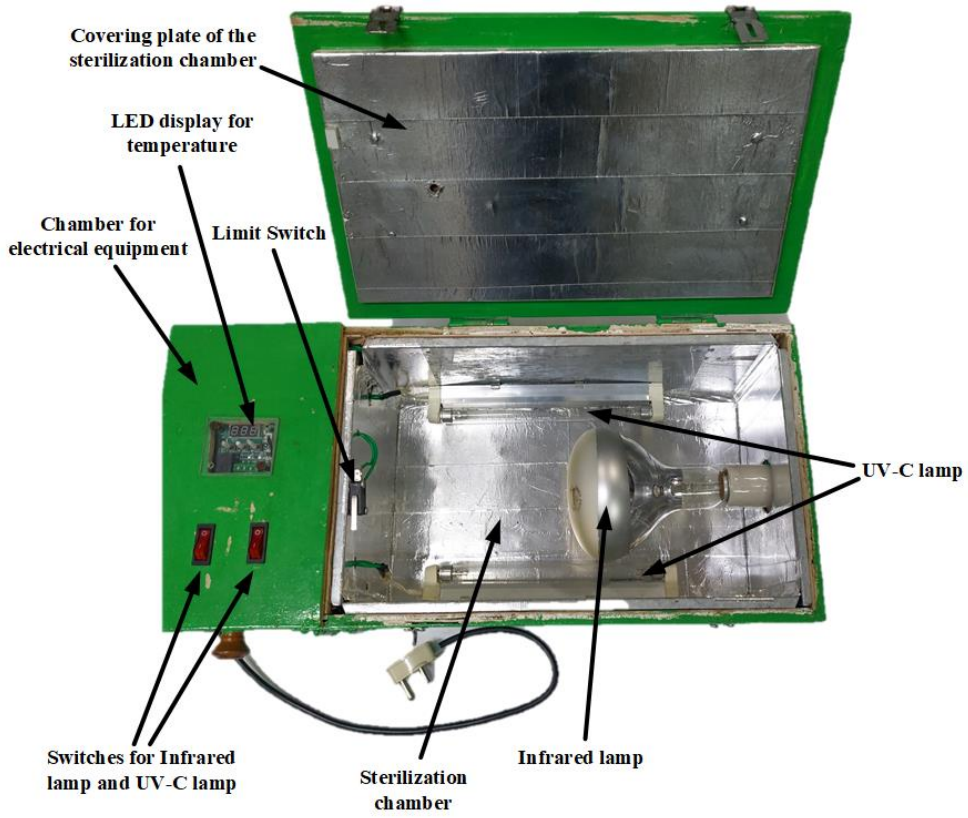

Figure 4.2 Photograph showing different parts of the sterilization box

4.3 Cost Estimation of the Designed Sterilization Box

Items used in fabricating the sterilization box are listed in Table 4.1. An amount of US $40.86 was the material cost for fabricating one unit of sterilization box. Considering the present Indian scenario, the labour cost for fabricating one unit of sterilization box was estimated as $13.13. Thus, the total cost was calculated as $53.99 for fabricating one unit of sterilization box. This cost will further reduce in mass production. Online shopping portals delivered UV-C based sterilization systems of similar size at a price range of $98–183. Thus, the proposed sterilization box is economical compared to those available in online shopping portals. In addition, the proposed sterilization box has IR radiation heating facility along with UV-C radiation facility.

Table 4.1 Material cost in the fabrication of a sterilization box

S. N.	Item	Quantity	Unit cost ($)	Total cost ($)
1	11-W UV-C Lamp	2	3.28	6.56
2	UV-C Lamp holder	2	2.76	5.52
3	250-W IR Lamp	1	6.57	6.57
4	IR Lamp holder	1	0.66	0.66
5	Electrical switches	2	0.20	0.40
6	Digital Temperature Controller (DTC)	1	2.76	2.76
7	Timer	1	9.85	9.85
8	Limit switch	1	0.46	0.46
9	8 mm thick plywood of surface area 6026.5 cm^2			3.86
10	0.8 mm thick GI sheet of surface area 4073.94 cm^2			2.25
11	Miscellaneous			1.97
	Total			**$40.86**

4.4 Performance Study of the Designed Sterilization Box

To carry out the performance study, synergistic effect of IR radiation heating and UV-C over sterilization was examined by two assessments. First, inactivation of both Gram-positive viz., *S. aureus* as well as Gram-negative viz., *S. typhi* bacteria is studied. Furthermore, unfolding of SARS-CoV-2 spike protein and a model protein RNase A is investigated experimentally.

4.4.1 Materials and Methods

A cost-effective IR radiation heating and UV-C based sterilization box was designed and fabricated. Recombinant spike SARS-CoV-2 (catalogue # NR-52397) was procured from Biodefense and Emerging Infections Research Resources Repository (BEI Resource) free of cost for supporting research in COVID-19 disease and Bovine Pancreatic Ribonuclease A (RNase A, catalogue # R6513) was purchased from Sigma Aldrich. Milli-Q water of resistivity 18 MΩ-cm at 25 °C was used for all the experimental studies.

4.4.2 Design of Experimental Conditions

The experimental design to explore the effect of UV-IR treatment on bacterial growth was performed using RSM-CCD tool in Design-Expert (ver 7.0). A range of UV sterilization time (5 to 15 min) and IR mediated temperature (40 to 70 °C) were selected as input parameters for the RSM-CCD model to analyze the interaction effects on antibacterial activity as discussed in chapter 3. The RSM-CCD model suggested a set of 13 experimental conditions to predict the optimum time and temperature responsible for significant antibacterial action as shown in Table 4.2. Among these five experiments were replicate experiments. To examine the bacterial growth inhibition, the bacterial cells were subjected to tabulated UV-IR irradiation time and temperatures.

Table 4.2 Experimental conditions designed by RSM-CCD technique

Experimental conditions	Time (min)	Temperature (°C)
1	10	40
2	6.46	44.39
3	13.54	44.39
4	10	55
5	10	55
6	10	55
7	10	55
8	15	55
9	5	55
10	10	55
11	13.54	65.61
12	6.46	65.61
13	10	70

4.4.3 Antibacterial Effect of UV-IR Treatment

The antibacterial effect of UV and IR heat was investigated on Gram-positive bacteria, *S. aureus* and Gram-negative bacteria, *S. typhi*. The bacteria were initially enriched overnight in

Nutrient broth (N.B., M002) using a shaker incubator maintained at 180 revolutions per minute (RPM) and 25 °C and further sub-cultured in the same medium for 6 h to obtain cells in the early log phase. The culture was centrifuged at 5000 RPM for 5 min and bacteria were resuspended in sterile water to obtain the optical density (OD) value of 0.1 corresponding to bacterial concentration of 10^7 CFU/mL. Thus, obtained bacterial suspension was aliquoted to a 5 mL glass test tube and subjected to UV-IR treatment. After treatment, the viability of cells was determined using the colourimetric, agar spread plate and microscopy.

4.4.3.1 Colourimetric assay

For the colourimetric bacterial cell viability determination, a resazurin dye assay was performed. The assay uses colourimetric redox dye, which changes the color from blue (A_{600} absorbance) in the oxidized form to pink color when reduced (A_{570} absorbance) due to the formation of resorufin (Zrimsek et al., 2004; Zare et al., 2015; Costa et al., 2021). For the assay, an equal volume of resazurin dye (67.5 mg/L) was mixed with treated bacterial suspension and incubated statically at 37 °C under dark for 4 h. After incubation, the samples were spectrophotometrically measured at 570 nm and 600 nm. A similar experiment was performed using untreated bacterial suspension as a positive control. The bacterial growth inhibition was calculated using (Lancaster and Fields, 1996)

$$G_i = \left\{ \frac{\left(A_{570} - A_{600}R_0\right)_{untreated} - \left(A_{570} - A_{600}R_0\right)_{treated}}{\left(A_{570} - A_{600}R_0\right)_{untreated}} \right\} \times 100 \qquad (4.2)$$

where G_i is percentage growth inhibition. R_0 was calculated as a correction factor (A_{570}/A_{600}) using only dye in water as a sample.

4.4.3.2 Agar spread plate assay

In addition, the spread plate technique was performed using treated bacterial suspension to evaluate the bacterial viability after sterilization treatment. For this, the treated bacterial suspension was serially diluted five times in sterile water and 50 µL of 10^{-5} dilution was spread plated on nutrient agar, and incubated overnight at 37 °C. The concentration (CFU/mL) of viable bacteria was determined using

$$CFU / mL = \frac{ND_i}{V} \qquad (4.3)$$

where N is number of bacterial colonies, D_i is dilution factor, and V is volume plated (in mL). An untreated bacterial suspension was also serially diluted and spread plated as a positive control. The percentage growth inhibition was calculated from

$$G_i = \frac{CFU/mL_{untreated} - CFU/mL_{treated}}{CFU/mL_{untreated}} \times 100 \quad (4.4)$$

4.4.3.3 Surface morphology of treated bacteria

The effect of UV-IR treatment on bacterial viability was further evaluated using Field emission scanning electron microscopy (FESEM) (model Sigma, make Zeiss). The bacteria were treated under optimized temperature and sterilization time and later drop casted on C tape (Saxena et al., 2018). Krishnamurthy et al. (2010) carried out microscopic and spectroscopic analyses to explore the damage of *S. aureus* treated with pulsed UV light and IR heating. Cell wall damage and cellular content leakage confirmed the inactivation of bacteria. In this work, microscopic evaluation was carried out to analyze the change in the bacterial morphology due to the inactivation using UV-C and IR heat.

4.4.4 Effect of UV-IR Heat Treatment on Proteins

Aqueous solutions of spike and RNase A proteins were exposed in the IR and UV-C treatment box. The samples were collected and the secondary structure determination was performed through intrinsic fluorescence, Fourier Transform Infrared Spectroscopy (FTIR), and Circular Dichroism (CD) spectroscopy.

4.4.4.1 Protein sample preparation

An amount of 0.45 µM Recombinant SARS-CoV-2 spike protein was prepared from the stock solution of 0.57 µM in Trish HCl buffer. The recombinant SARS-CoV-2 spike protein was packed in vials and it is used as it is from the stock. 72 µM stock solution of RNase A was prepared in 10 mM phosphate buffer saline (PBS) and checked its concentration under UV absorbance at 280 nm (Fowler et al., 2011). Its concentration was determined from Beer-Lambert's law using an extinction coefficient of ~9727 $M^{-1}cm^{-1}$. For the IR treatment studies, (36 µM) 0.5 mg/mL working solution was prepared.

4.4.4.2 Secondary structure analysis of proteins

4.4.4.2.1 FTIR spectroscopy

FTIR spectroscopy was performed using the FTIR instrument from (Shimadzu IR Affinity S1). A sample solution of 2 µL was added on top of the ZnSe crystal. For the entire investigation, a minimum of 64 scans and a resolution of 4 cm^{-1} were preset and spectra were recorded in the full range of 400–4000 cm^{-1}. The protein sample was prepared in a buffer solution. Thus, the buffer was recorded as the background spectra which was automatically subtracted from the sample spectra. The CO_2 and moisture corrections were also performed by the instrument. Further, the amide-I region (1600–1700 cm^{-1}) of the spectrum was resolved, deconvoluted, and fitted with Gaussian curves using Origin 8.5 software (Sharma and Pandey, 2021b; Hasan et al., 2018b; Yang et al., 2022).

4.4.4.2.2 CD spectroscopy

Far UV-CD spectroscopic measurement was performed using a CD spectrophotometer (JASCO, J-1500) to investigate the change in the secondary structure of UV-IR treated protein sample. A quartz cuvette of 0.1 cm path length was used for this study. The spectra were collected in the range of 260–190 nm (Iannazzo et al., 2018; Zhang et al., 2008; Militello et al., 2003; Sharma and Pandey, 2021a). Samples were scanned as an average of 5 accumulations with a scan speed of 100 nm/min and at 0.1 nm bandwidth. The spectrum of the buffer was used for the baseline correction prior to the measurement of the samples. A sample of 0.2 mg/mL concentration was prepared for the reading. The machine CD signal value θ in millidegree (mdeg) has been converted to mean residue ellipticity value (MRE) in deg cm^2 $dmol^{-1}$ $residue^{-1}$.

4.4.4.2.3 Tryptophan Intrinsic fluorescence

The alternation in the secondary structure was also correlated with the intrinsic fluorescence of aromatic amino acids. The native and treated samples of spike protein were diluted in Tris buffer to prepare 1 ml of 0.01 µM solution. The native and the treated spike protein solutions were then loaded in a quartz crystal cuvette to check the change in intrinsic fluorescence using a Fluoromax 4 spectrofluorometer (Horiba Scientific). The excitation wavelength was set at 290 nm. A 5 nm excitation and emission slit width was fixed and an average of five scans was accumulated for all the readings.

4.5 Results and Discussion

In this study, a simple, easy to handle, and low-cost sterilization box is fabricated and the synergistic effect of UV-C and IR heat over sanitization was investigated. For this purpose, the effect of UV-C and IR heat sanitization was performed, and its effect on the bacterial cells viz., *S. aureus* and *S. typhi* were observed and also on two proteins viz., whole spike protein and RNase A were checked. The detailed results are described in the sequel.

4.5.1 Effect of IR Heat and UV Treatment on Bacterial Cells

Temperature and UV-C irradiation time have shown significant inhibitory effects on bacterial growth, as previously established in chapter 3. It was reported that only heat or only UV may injure the cell but may not kill them, increasing the chance of their revival and hence pathogenicity. Thus, simultaneous UV-heat treatment using IR irradiation was explored for sterilization in this chapter. Colourimetric technique (Lancaster and Fields, 1996) and spread plate technique (as discussed in chapter 3) were used to study antibacterial activities against both *S. aureus* and *S. typhi.* Temperature and sterilization time were considered as input variables as well as experimental conditions (suggested by the RSM-CCD optimization design) and were investigated to achieve maximum growth inhibition of bacteria (response). The response was evaluated as the percentage of bacterial growth inhibition after sterilization treatment in comparison to the untreated (positive control) condition. The multiple regression analysis provided optimized and statistically significant solutions using two-way analysis of variance (ANOVA). Table 4.3 lists the 13 sets of experimental conditions and their respective experimental and predicted responses. For 5 replicate experiments, coefficient of variation in cell viability was 1% and 2.5% for *S. aureus* and *S. typhi*, respectively.

In the case of the colourimetric assay, the viable bacteria utilize the available oxygen resulting in the reduction of the dye (Resazurin). This leads to a change in the colour of the dye from blue to pink. Figure 4.3 shows the colourimetric change in the dye due to the occurrence of reduced culture conditions in the presence of live bacterial cells treated under various conditions as listed in Table 4.2. The experiments were performed in triplicates and SA represents *S. aureus* while ST refers *S. typhi*. The presence of blue colour in the microplate well numbers 11 and 13 suggested the inactivation of bacteria under treatment conditions of

Table 4.3 The experimental conditions designed by RSM-CCD with predicted and obtained responses for *S. aureus* and *S. typhi* antibacterial study

Input variables (Experimental conditions)	**Responses**							
	S. aureus				*S. typhi*			
	Growth inhibition in dye (%)		Cell viability (log CFU/mL)		Growth inhibition in dye (%)		Cell viability (log CFU/mL)	
	Expt.	Pred.	Expt.	Pred.	Expt.	Pred.	Expt.	Pred.
1 (10 min, 40 °C)	0.59	2.33	4.31	4.21	20.54	19.90	4.63	4.45
2 (6.46 min, 44.39 °C)	6.11	7.36	4.26	4.37	14.37	18.06	4.48	4.57
3 (13.54 min, 44.39 °C)	9.47	6.64	4.18	4.28	24.84	23.23	4.07	4.27
4 (10 min, 55 °C)	8.75	9.71	4.18	4.18	27.31	26.89	3.97	3.96
5 (10 min, 55 °C)	11.07	9.71	4.18	4.18	24.70	26.89	3.95	3.96
6 (10 min, 55 °C)	9.60	9.71	4.19	4.18	27.18	26.89	3.94	3.96
7 (10 min, 55 °C)	8.93	9.71	4.18	4.18	29.50	26.89	3.95	3.96
8 (15 min, 55 °C)	31.81	33.21	3.94	3.81	43.55	45.30	3.90	3.75
9 (5 min, 55 °C)	14.23	9.85	4.24	4.09	23.77	18.03	4.02	4.02
10 (10 min, 55 °C)	10.18	9.71	4.18	4.18	25.73	26.89	3.95	3.96
11 (13.54 min, 65.61 °C)	55.94	57.66	2.30	2.47	72.21	72.49	2.60	2.66
12 (6.46 min, 65.61 °C)	18.06	23.87	2.60	2.78	33.48	39.05	2.78	2.74
13 (10 min, 70 °C)	54.78	50.07	2.00	1.81	72.88	69.56	2.00	2.02

Note: Expt. → Experimental, Pred. → Predicted, Temp. → Temperature

13.54 min at 65.61 ℃ and 10 min at 70 ℃, respectively, leading to an insignificant change in dye colour than the control. The positive control (wells 15) represented untreated bacterial viability showing a complete pink colour whereas the negative control indicated the original blue colour of dye in sterile water. Thus, lesser pink colouration suggested a decrease in cell

viability and an increase in growth inhibition due to sterilization treatment. In addition, well number 14 represented sterilization at the previously optimized treatment conditions (UV-C and dry heat) of 15 min at 70 °C from chapter 3. This suggested that the present IR heating and UV treatment are more effective in achieving growth inhibition within 13.54 min at a comparatively lesser temperature of 65.61 °C. The better sterilization by IR irradiation is due to its larger penetration depth. The IR waves can penetrate up to subcutaneous tissues (1–4 mm), while UV and visible lights penetrate up to epidermis (≤ 200 µm) and dermis (200-1500 µm) layers, respectively (Tanaka et al., 2013). Further, the power density of IR irradiation was estimated as 3.18×10^4 W/m^2, which effectively inactivated bacterial pathogens. Damit et al. (2011) reported the inactivation of *Escherichia coli* and *B. subtilis* spores with IR irradiation of a power density of 2.0×10^4 W/m^2.

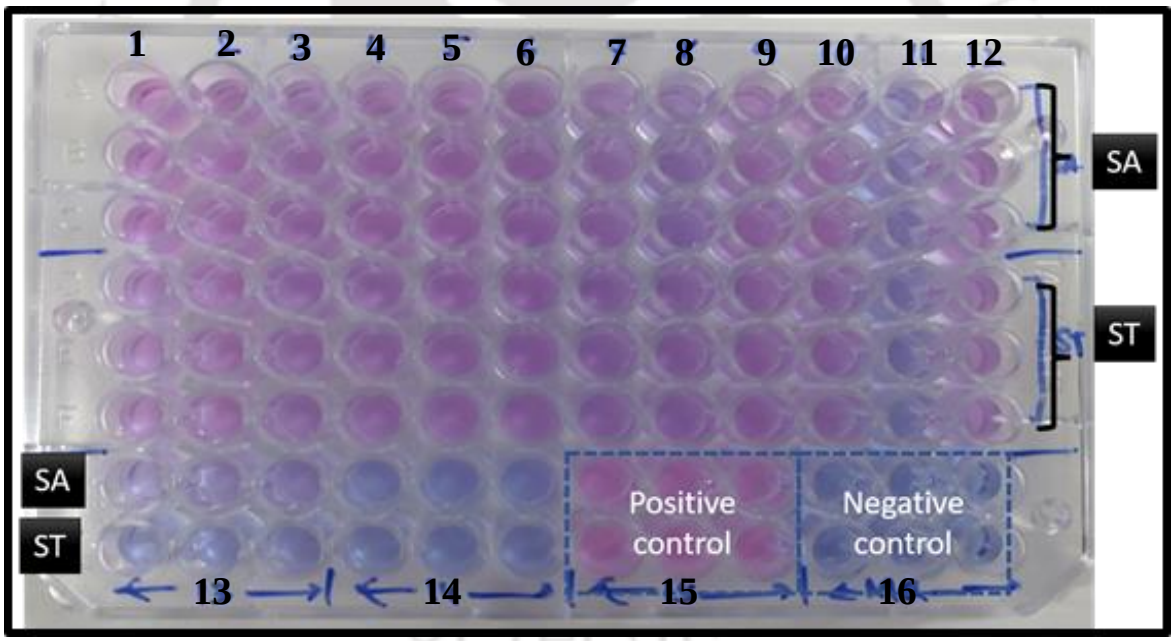

Figure 4.3 Colourimetric assay of bacterial growth inhibition in the presence of UV-IR treatment at RSM-CCD suggested experimental conditions (1 to 13) using Resazurin dye [SA: *S. aureus*; ST: *S typhi*; well no. 14: previously optimized treatment conditions of UV-C and dry heat at 70 ℃ for 15 min; well no. 15: positive control (untreated bacterial suspension in dye) and well no. 16: negative control (only dye in sterile water)

In addition, the inhibition of bacterial growth was monitored by spread plate techniques. The treated bacterial suspension was serially diluted five times and plated on nutrient agar (NA) plates, and visible colonies were counted after 12 h of incubation. The untreated bacterial suspension was also plated under 5 times dilution, and colonies were counted as a positive control. The cell viability for control (untreated) was obtained as 2.5×10^4 and 6.5×10^4 CFU/mL for SA and ST, respectively. Figure 4.4 shows the cell viability for various treatment conditions. The decrease in the number of colonies indicated the effectiveness of sterilization. More than 95% of bacterial growth inhibition was obtained for the combined IR and UV irradiation at temperature ≥ 65.61 °C and time ≥ 10 min for both the SA (≤ 2×10^2 CFU/mL) and ST (≤4×10^2 CFU/mL) bacteria. These results are in concordance to the sterilization effects observed from colourimetric assay.

Figure 4.5 and Figure 4.6 show 3D contour response surface plots describing the percentage of bacterial growth inhibition in the range of sterilization temperature and time chosen for this study. The obtained responses were fitted to quadratic polynomial equations as mentioned in Table 4.4. Both response factors fitted well to quadratic model equations and predicted responses are also listed in Table 4.3. The ANOVA analysis was performed for the statistical analysis. The coefficient of determination (R^2) values of experimental and predicted data were found to be ≥ 0.94. The *p*-value of ≤ 0.001 indicated the fitness of the quadratic model equations. Both the time and temperature of UV-IR irradiation were found to be significant for bacterial growth inhibition. The optimized condition for the maximum inhibition of bacterial growth in the given range of input variables was predicted to be 65.61 °C of temperature for 13.54 min.

Table 4.4 RSM-CCD Quadratic model fitting to the experimental parameters with ANOVA analysis

Bacteria pathogen	**Quadratic polynomial equation (*A*: Time; *B*: Temperature)**	**ANOVA analysis**
S. aureus	$9.71 + 8.26A + 16.88B + 8.62AB + 5.91A^2 + 8.24B^2$	*A, B, AB,* A^2, B^2 are significant model terms. (R^2 = 0.97)
S. typhi	$26.89 + 9.64A + 17.56B + 7.05AB + 2.39A^2 + 8.92B^2$	*A, B, AB,* B^2 are significant model terms. (R^2= 0.97)

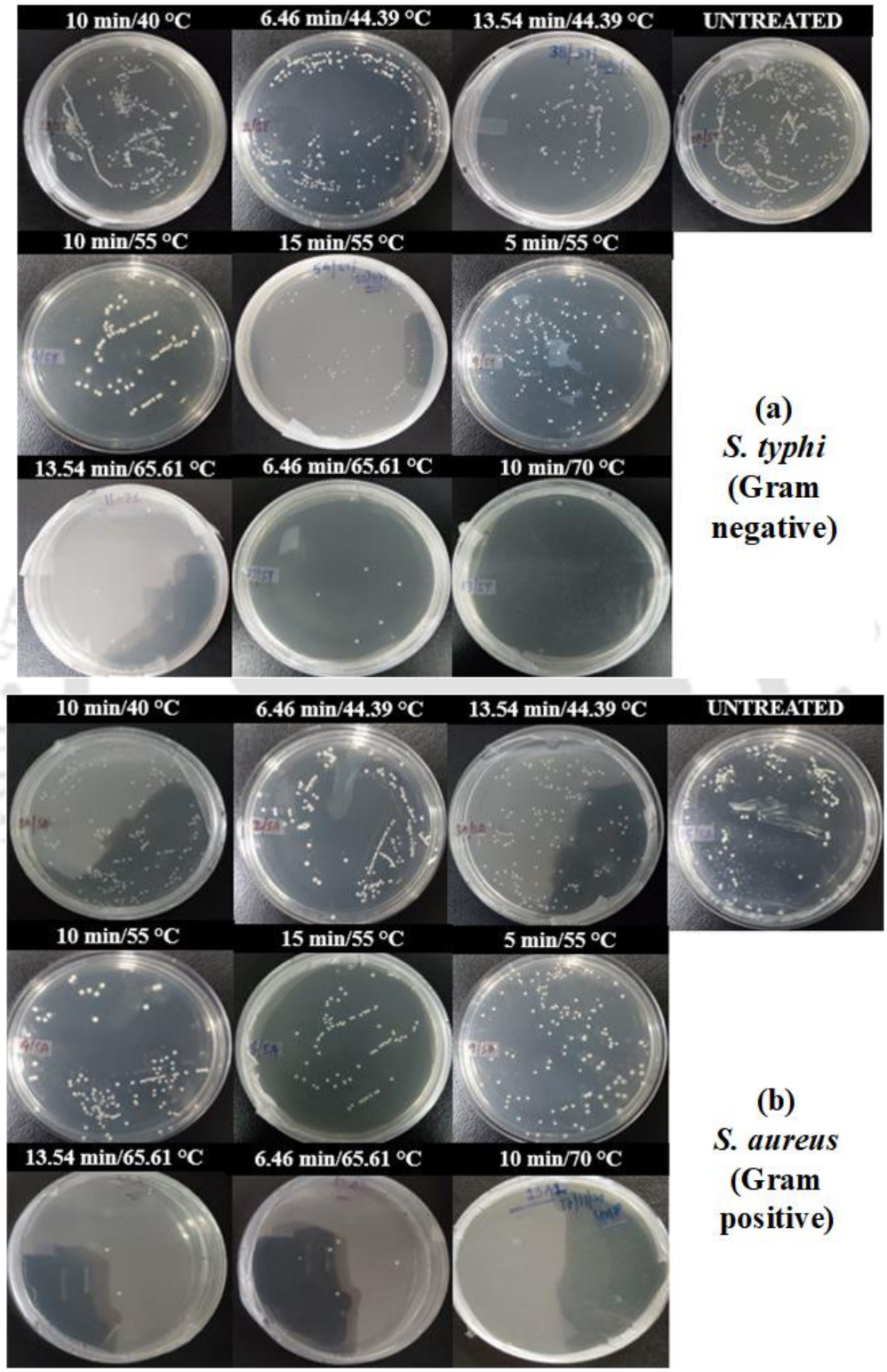

Figure 4.4 Bacterial growth inhibition study using serial dilution (5 times) and agar spread plate technique at various RSM-CCD experimental conditions against **(a)** Gram-negative (*S. typhi*) and **(b)** Gram-positive (*S. aureus*)

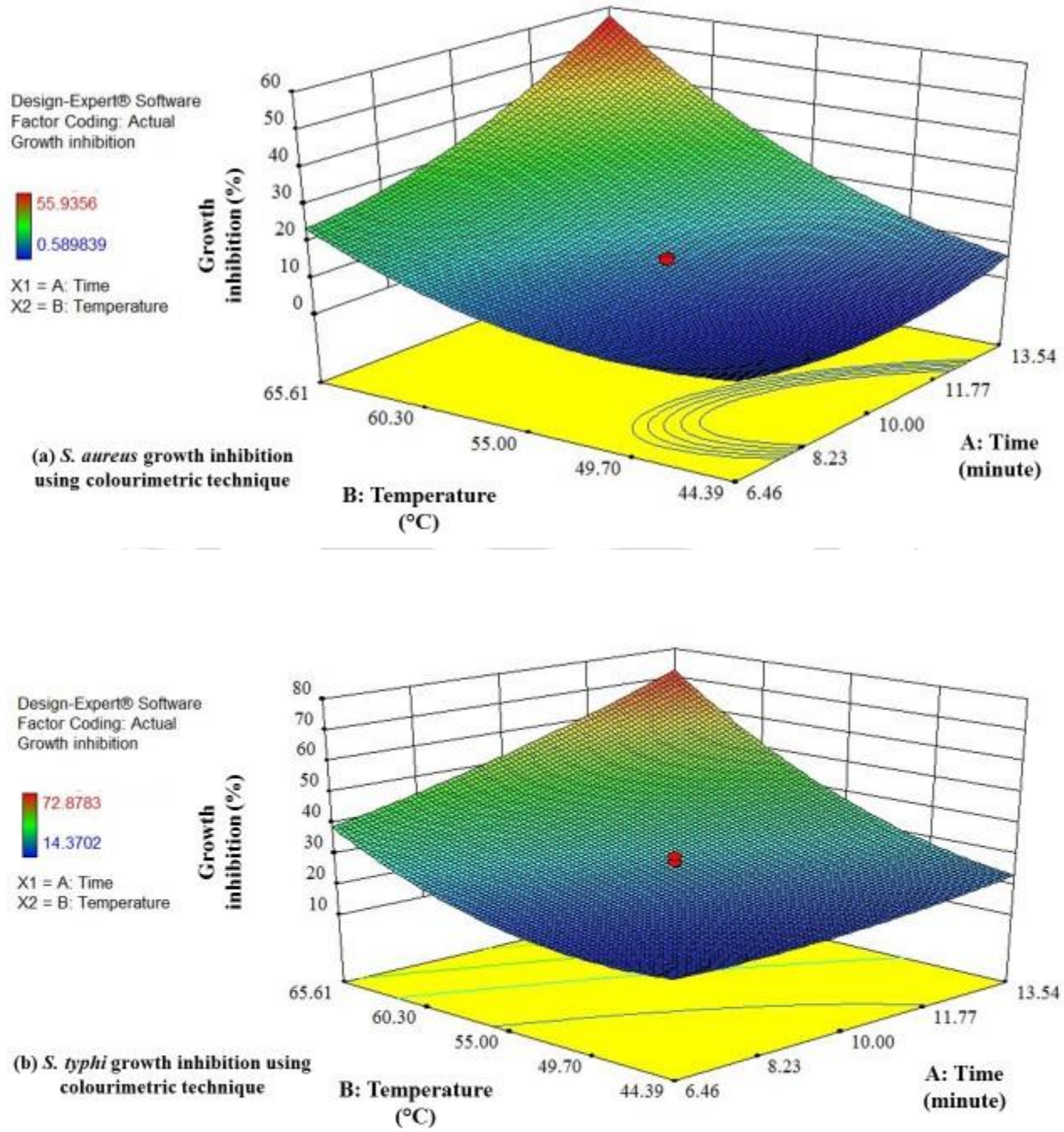

Figure 4.5 Contour 3D response surface plots showing bacterial growth inhibition using colourimetric technique in **(a)** *S. aureus* and **(b)** *S. typhi* considering Temperature and UV irradiation time as the variable input parameters

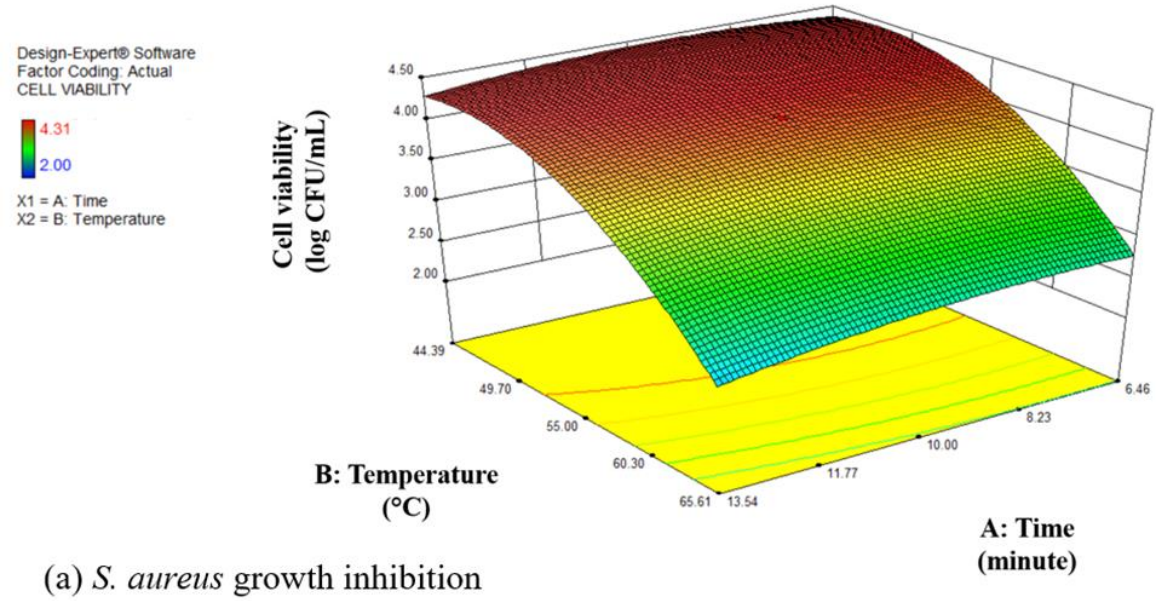

(a) *S. aureus* growth inhibition using serial dilution spread plate technique

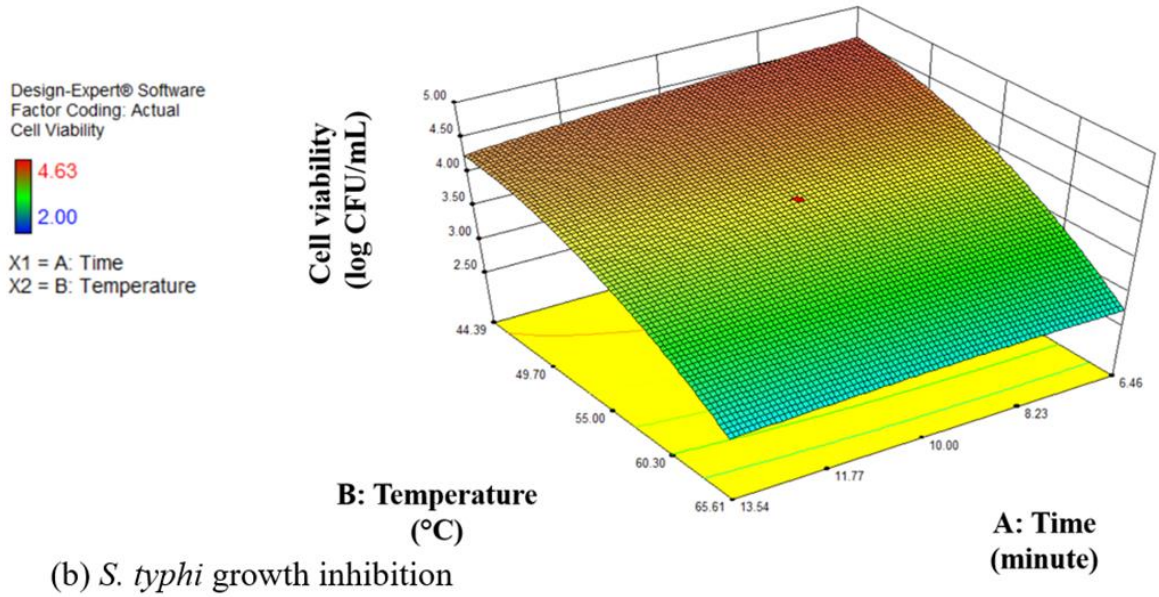

(b) *S. typhi* growth inhibition using serial dilution spread plate technique

Figure 4.6 Contour 3D response surface plots showing bacterial growth inhibition using serial dilution spread plate technique in **(a)** *S. aureus* and **(b)** *S. typhi* considering; Temperature and UV irradiation time as the variable input parameters

4.5.2 Microscopic Evaluation of Bacterial Cell using FESEM

The killing of bacterial pathogen occurs via multiple routes like rupture of cell membrane, inactivation of genetic materials/proteins and interfering with cell division. Calderon-Miranda et al. (1999) reported that pulsed electric field inactivated the microorganisms by affecting the cells physiology and morphology namely, dielectric damage of the cell wall, leakage of cellular material, cytoplasmic clumping, increase in cell wall roughness, and fracture of the cell walls and cell membranes. Liu et al. (2004) reported that chitosan treated *S. aureus* were inactivated by disrupting the membrane of dividing cells along with leakage of cell contents. In this work, the synergistic effects of UV-C and IR heat treatment on *S. aureus* and *S. typhi* were analyzed on cellular morphology. The microscopic evaluation of the combined UV-C and IR heat treated *S. aureus* and *S. typhi* was carried out using FESEM. The morphologies (images) of untreated and treated *S. aureus* and *S. typhi* are shown in Figure 4.7. Sample of 1 mL from each bacterium was treated at 65.61 ℃ for 13.54 min in the designed sterilization box. Microscopic analyses of *S. aureus* and *S. typhi* cells indicated that damage of cell wall integrity (rupture of cell wall) due to the combined UV-C and IR heat treatment. In control samples, cell walls have definite boundaries as shown in Figure 4.7(a) and Figure 4.7(c). However, treated samples have broken boundaries as the cell walls were destroyed (Figure 4.7(b) and Figure 4.7(d)). These observations indicated the effectiveness of the designed chamber for the killing of bacterial pathogens by disrupting the cell walls.

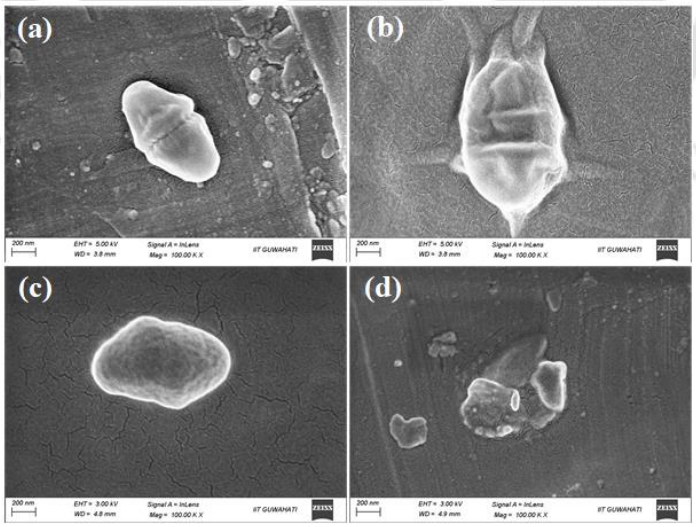

Figure 4.7 Microscopic evaluation ($X10^5$) of **(a)** *S. aureus* control sample, **(b)** *S. aureus* sample treated to combined UV-C and IR heat showing cell wall breakage, **(c)** *S. typhi* control sample, and **(d)** *S. typhi* sample treated to combined UV-C and IR heat showing cell wall breakage (1 mL sample was treated at 65.61 ℃ for 13.54 min)

4.5.3 Effect of IR Heat and UV Treatment on the Unfolding of Spike Protein and RNase A

The sterilization process is frequently being followed to inactivate the novel coronavirus. Unfolding or change in conformation of the surface glycoprotein of a virus can lead to its disintegration and inactivation (Pandey, 2020b). Thus, heating is one of the sterilization methods, which unfolds/denatures the virus spike protein and thus inactivates the virus. It has been reported that a high temperature of 70 °C leads to the loss of viral surface protein, disintegrating the viral assembly (Pandey, 2020b; Liu et al., 2015). In this work, the effect of UV-C and IR heating has been tested on two important proteins: SARS-CoV-2 spike protein and RNase A. The virus spike protein mainly aids in the attachment and entry of the coronaviruses inside the host cells. It is a homotrimer where the S1 part is partly exposed to the outer environment and the S2 domain is partly immersed inside the lipid bilayer of the viral envelope (Rath and Kumar, 2020). RNase A is a very stable protein and is used as a model protein for studying the unfolding-refolding process (Pecher and Arnold, 2009). The proteins in an aqueous solution were exposed inside the designed IR treatment box at the optimized conditions of 65.61 °C for 13.54 min as discussed in the earlier Sections. The unfolding of proteins was analyzed by measuring the changes in the secondary structure and intrinsic fluorescence.

Figure 4.8(a) and Figure 4.8(b) show the FTIR spectra in the amide I region of native and treated spike protein. The spectra were deconvoluted and respective peak area were used to determine the contents of the secondary structure. The major peaks in the range of 1620–1635, 1642–1645, 1651–1655, and 1665–1685 cm^{-1} correspond to β-sheet, random coil, α-helix, and β-turn, respectively (Kong and Yu, 2007). The native spike protein contained 16.4 ± 0.5% of α-helix, 34.7 ± 0.8% of β-sheet, 28.9 ± 0.9% of β-turn, and 14.0 ± 2.0% of random coil. These data correlate well with the literature reported by others (Li and Hirst, 2020; Singh et al., 2020; Kumar et al., 2022). However, post heat treatment, the contents of β-sheet increased to 43.7 ± 1.1%, while α-helix decreased to 11.9 ± 1.5%. This indicated the unfolding of spike protein after the heat treatment at 65.61 ℃ for 13.54 min in the designed chamber. Rath and Kumar (2020) studied the effects of different temperatures on the spike glycoprotein by molecular dynamics simulation. It was reported that at temperatures ≥ 50 ℃ (particularly

at 70 ℃), the receptor-binding domain (RBD) was found to get closed. The RBD is a part of S1 unit of spike protein and binds to the ACE2 receptor of the host protein. The unfolding of RBD stops the attachment of the spike protein to the host and thus inhibits the transmission of the virus (Rath and Kumar, 2020; Lan et al., 2020).

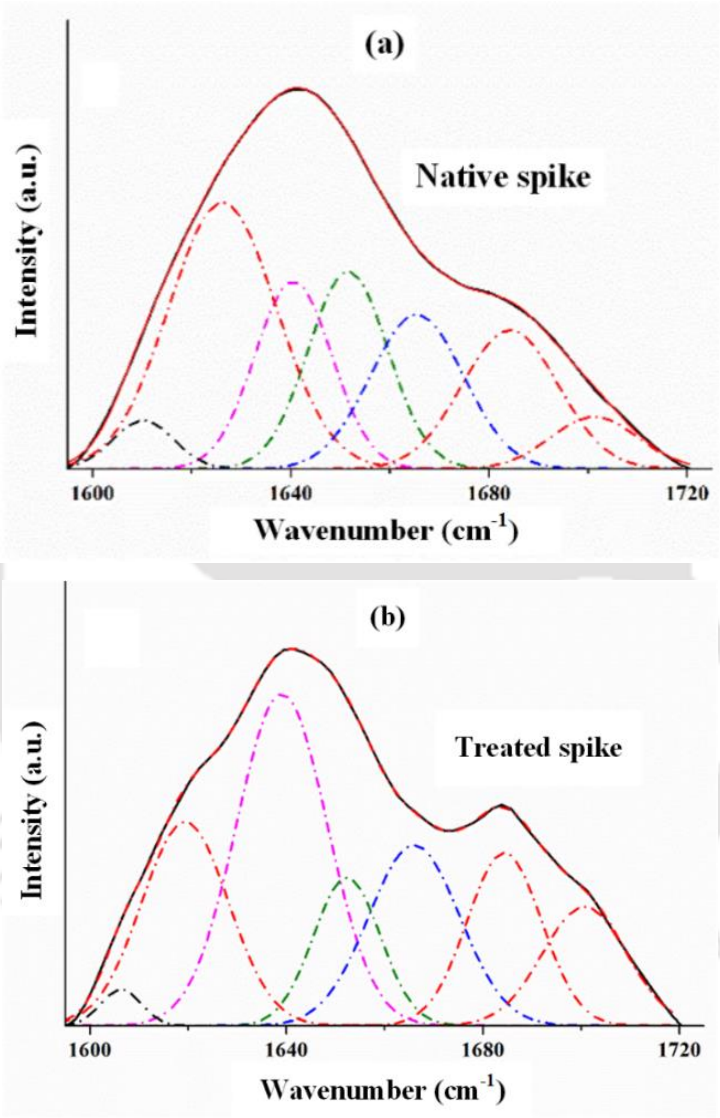

Figure 4.8 Deconvulated second derivative spectra of **(a)** native spike and **(b)** IR and UV-C treated spike

In Figure 4.9, FTIR data were correlated with the intrinsic fluorescence of the spike proteins. The intrinsic fluorescence is contributed by the presence of aromatic amino acids. Any alternation in the secondary structure of a protein interferes with the fluorescence intensity due to the reorganization of aromatic amino acids which results in the change of the microenvironment of the protein (Ghisaidoobe and Chung, 2014). A decrease in the fluorescence intensity was observed for the treated spike protein as compared to the native protein (Figure 4.9). A decrease in tryptophan fluorescence indicated that there is an exposure of some of the tryptophan residues because of IR and UV-C radiations (Lakowicz, 2006). This resulted in an early quenching of the fluorescence as compared to the native spike protein.

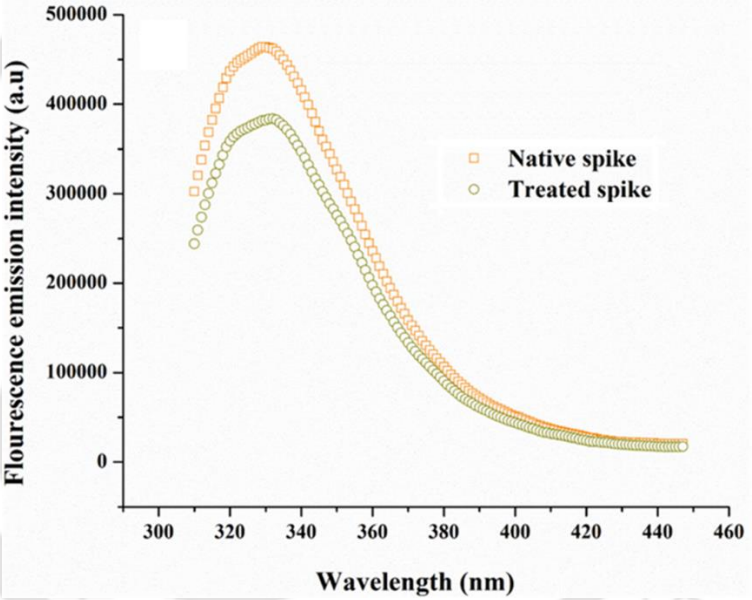

Figure 4.9 Intrinsic tryptophan fluorescence for native spike and IR and UV-C treated spike protein

Figure 4.10(a) and Figure 4.10(b) show the deconvoluted second derivative FTIR spectra in the amide 1 region of the native and treated samples of RNase A, respectively. RNase A contained 19.8 ± 1.0% of α-helix, 37.5 ± 1.5% of β-sheet, 14.3 ± 1.0% of β-turn, and 23.5 ± 0.9% of random coil. Similar to the spike protein, the heat treatment using IR and UV-C irradiations resulted in the unfolding. The contents of α-helix decreased to 16.2 ± 1.3% and in turn β-sheet increased to 42.5 ± 1.0% after the treatment. Stelea et al. (2001) reported the distinct changes in the FTIR spectra of RNase A in the temperature range of 50 to 70 °C. Also,

the unfolding of RNase A protein was analyzed using CD spectroscopy. Figure 4.10(c) shows the CD spectra of native and treated RNase A protein. A decrease in the negative dip at 208 nm indicated the reduction in the contents of α-helix (Stelea et al., 2001). Therefore, the combined UV-C and IR radiations have shown the ability to kill the bacteria and also effectively denature the glycoproteins. The IR radiation is found to lower the polarization of C=O bonds (carboxylic groups) and thus weaken the hydrogen bonds (Kowacz and Warszynski, 2018). The breaking and making of hydrogen and other intermolecular interactions leads to the unfolding of proteins (Pandey, 2022; Hubbard and Haider, 2010).

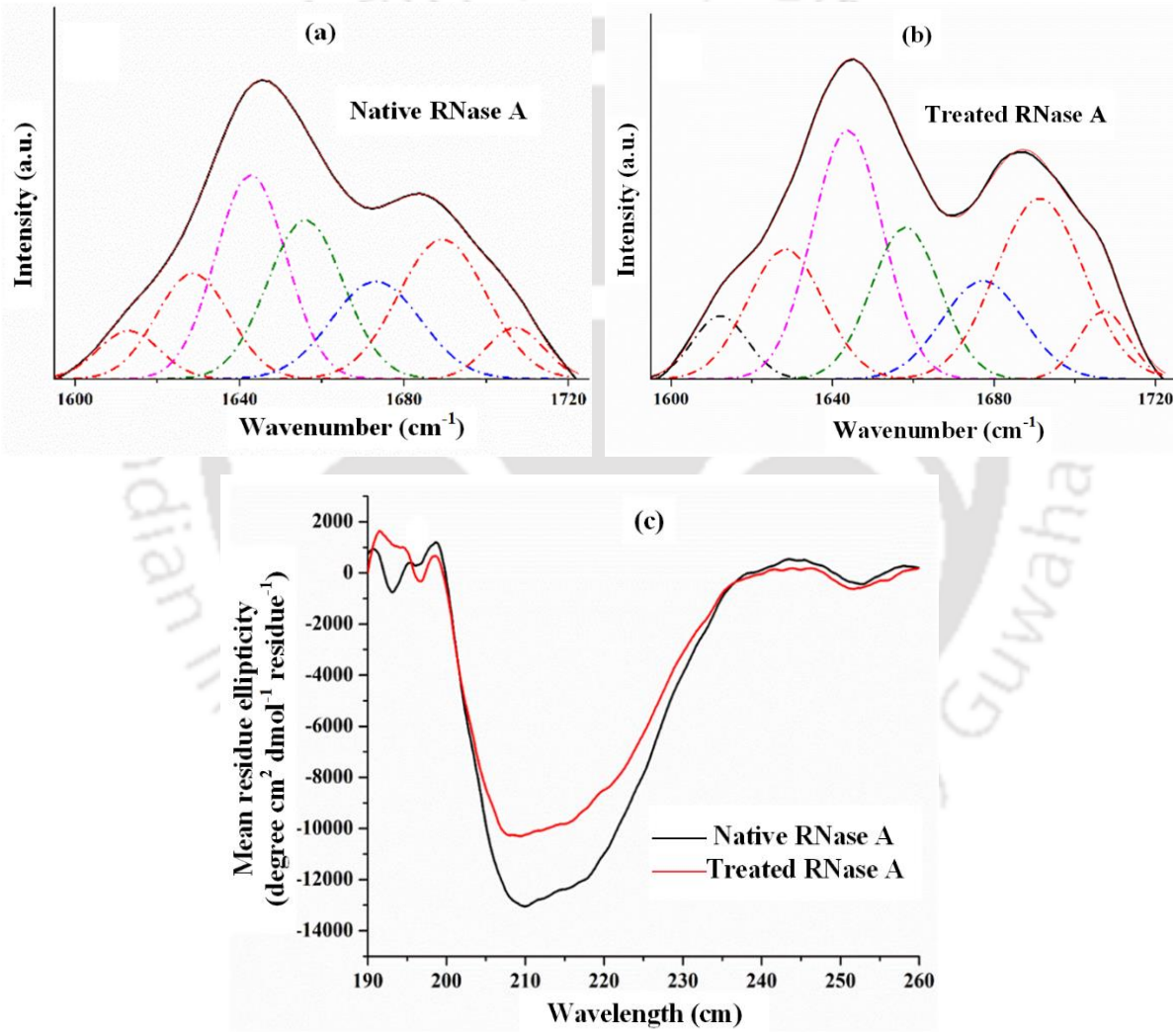

Figure 4.10 Deconvulated second derivative spectra of **(a)** native RNase A, **(b)** treated RNase A, and **(c)** Far-UV CD spectra of the native and IR-UVC treated RNase A enzyme

4.6 Conclusion

Considering the global pandemic caused by COVID-19, a sterilization box equipped with both UV-C radiation and IR heating facility was designed and tested for antibacterial and antiviral activities. An IR lamp of 250 W and two 11 W UV-C lamps were the most important parts of the box for sterilization purposes. The broad-spectrum antibacterial activity was tested against Gram-positive viz., *S. aureus* and Gram-negative viz., *S. typhi* and antiviral ability was accessed through the unfolding of SARS-CoV-2 spike glycoprotein. Experiments were carried out to optimize the time and temperature for the effective sterilization against the above-mentioned bacteria and virus. Small day-to-day life items namely belt, wallet, wrist watch, and mask can be disinfected in the optimized conditions. The designed box can be used for the sterilization of contagious hospital wastes before their disposal. The salient observations and recommendations are as follows:

1. The overall observations suggested that combined IR and UV-C irradiations together at 65.61 °C for 13.54 min was sufficient to kill both Gram-positive (*S. aureus*) and Gram-negative (*S. typhi*) bacteria along with inactivation of spike and RNase proteins. This temperature is lower than 70 °C used in visible light and UV-C radiation due to larger penetration depth of IR irradiation up to subcutaneous tissues (1–4 mm).
2. The microscopic evaluation confirmed the cell wall damage that further led to the killing of treated bacteria.
3. Change in secondary structures in spike protein was investigated by FTIR and intrinsic fluorescence, which confirmed the decrease in helicity and increase in β-sheets. In the case of RNase A, FTIR and CD confirmed the unfolding.
4. The present study confirmed the suitability of the designed low-cost sterilization box based on UV-C and IR radiations for effective sterilization.

Chapter 5

A Study on Degradation of N95 Respirator After Disinfecting it by Various Techniques

5.1 Introduction

Rapid spreading of coronavirus disease 2019 (COVID-19), caused by severe acute respiratory syndrome coronavirus 2 (SARS-CoV-2), has affected the healthcare systems all over the world. United States Centers for Disease Control and Prevention (CDC) recommended the usage of N95 filtering face-piece respirators (FFRs) to prevent the transmission of the virus from aerosols and contacting surfaces. CDC defined the N95 grade FFR as a minimum filtration efficiency of 95% for 0.3 μm size NaCl particle. N99 and N100 grades of FFR represent 99% and 99.97% filtration efficiency, respectively. CDC advised the healthcare workers to use the N95 FFR as a personal protective equipment (PPE) (Liao et al., 2020). Disposal of the used and possibly infected FFRs to the environment can cause contagious pollution in the water, air, and soil. A good practice is to reuse FFRs after disinfecting them till their filtration efficiency reduces significantly.

An N95 face mask contains multiple filtration layers; its inner filtration layer is the main component. Melt-blown fabric is used to make the inner layer of polypropylene, which has a melting point around 160 °C. Researchers have studied different methods to disinfect the FFRs and their effects on FFRs. Campos et al. (2020) heated N95 level polypropylene fabric and noted that with 100% relative humidity, the filtration efficiency is preserved up to 5 cycles for 95 °C temperature and up to 20 cycles for 85 °C. Saini et al. (2020) investigated the effect of different concentrations of vaporized hydrogen peroxide (VHP) on fabric integrity, permeability, and physical feature of the N95 masks. They concluded that repeated cycle of VHP decontamination did not make any remarkable change in deformity or physical tear in N95 masks. However, residues left in N95 mask due to VHP decontamination can cause serious skin and respiratory hazard (Banerjee et al., 2021). Viscusi et al. (2007) studied various disinfection methods on two FFR types— N95 and P100. They observed that dry heat at 160 °C, soap and water (dipping for 20 min), autoclaving, and immersion in 70% isopropyl alcohol resulted in significant degradation of filter in both the FFRs. Cramer et al. (2020) listed

advantages and concerns of various N95 sterilization techniques, viz., gamma radiation, electron beam radiation, ultraviolet (UV) exposure, dry heating, steam heating, VHP, C_2H_4O, and microwave oven. Molin and Östlund (1975) developed an equipment for the study of inactivation kinetics of *Bacillus subtilis* spores in dry heat using IR radiation. A sterilization box equipped with both incandescent bulb heating and UV-C irradiation facility was tested against virus, *Escherichia coli* bacteria as well as other bacteria collected from daily-use items such as belt, wrist watch, and wallet, as discussed in chapter 3. Yujie et al. (2020) studied the effects of different doses in UV-C treatment of N95 FFR on the topographical and nano-mechanical properties; they noticed the reduction of hardness, fiber width, and Young's modulus after UV-C exposure. Hence, it is essential to understand the degradation behavior of FFRs after disinfection.

In this chapter, mechanical properties of the N95 filtration fiber, disinfected by five well-established methods were presented. N95 face masks were disinfected using the sterilization box designed in chapter 3. Five disinfection methods were incandescent bulb heating, UV-C irradiation, alcohol immersion, steam exposure, and incandescent bulb heating with UV-C irradiation treatment. Fiber diameter, surface roughness (R_a), ultimate tensile strength (UTS), and scratch resistance of the fibers were studied using Field emission scanning electron microscopy (FESEM), atomic force microscope (AFM), universal testing machine (UTM), and scratch tester, respectively. X-ray diffraction (XRD) study was also carried out to check the chemical changes in the surface of the disinfected polypropylene fiber.

5.2 Materials and Methods

The N95 FFRs were disinfected using the designed box as discussed in chapter 3. Single N95 FFR (Brand: MASKWELL, make: Sanmati Packaging, India) comprising five filtration layers (2 layers of melt-blown polypropylene fabric, 2 layers of spun-melt polypropylene and 1 layer of hot air cotton) were procured. Polypropylene is one of the most widely used materials for the masks (Yujie et al., 2020). Considering that inner filtration layer (made of melt-blown polypropylene fabric) as the principal functioning part of an N95 FFR, sample of size 5 cm × 6 cm were cut from it. Samples were grouped as per five disinfection methods, which are described in sequel.

5.2.1 Alcohol Immersion

Samples were immersed into a 75% ethanol solution and air-dried in each cycle. Disinfection was carried out for total 5 cycles. It is reported that after this treatment filtration efficiency of N95 FFR reduces significantly (Liao et al., 2020).

5.2.2 Incandescent Bulb Heating

Samples were treated in an UV and heat-based sterilization box, as discussed in chapter 3. Only heating was carried out using two 100 W incandescent bulb without UV exposure. Campos et al. (2020) reported that heating at 85 °C for 20 min was sufficient to disinfect N95 level polypropylene fabric from SARS-CoV-2 without any significant reduction in filtration efficiency up to 20 cycles. Hence, in this work, samples were heated to 85 °C for 20 min. Total 20 cycles were carried out by keeping a gap of 10 min between the cycles.

5.2.3 Steam Exposure

Samples were placed approximately 4 cm above the boiling water inside an electric kettle. Samples were steamed for 10 min and afterwards kept in ambient to dry completely. Samples were disinfected for 10 cycles as significant drop in filtration efficiency was reported after 10 cycles (Liao et al., 2020).

5.2.4 UV-C Irradiation

Samples were treated in the same sterilization box as used for incandescent bulb heating. Only UV-C radiation facility was used without any dry heating. UV-C dose by two 11 W UV-C lamps was calculated as 24.62 J/cm^2 using Eq. 4.1. Calculated UV-C dose was more than the UV-C dose required to inactivate SARS-CoV, which should be above 3.6 J/cm^2 (Liao et al., 2020). In one cycle, samples were irradiated for 30 min and left at ambient condition for 10 min. Total 20 cycles were carried out, as filtration efficiency of N95 FFR reduces to 93% at 20 cycle of UVGI disinfection (Liao et al., 2020).

5.2.5 Combined Incandescent Bulb Heating with UV-C Irradiation

Samples were treated with simultaneous heat and UV-C radiation in the designed sterilization box, discussed in chapter 3. In chapter 3, incubation at 70 °C for 15 min under the both heat and UV-C irradiation was reported to be effective for inactivating SARS-CoV-2. Thus,

samples were treated at 70 °C for 15 min in one cycle and total 20 cycles were carried out with a gap of 10 min between the cycles.

5.3 Results and Discussion

In this chapter, effect of five disinfection methods on properties of N95 FFR was investigated. Properties of interest were R_a, UTS, and scratch resistance of inner filtration layer; diameter of individual fiber was also measured. XRD analysis of both untreated and disinfected fibers were also carried out to check the chemical changes occurring in the surface of the disinfected polypropylene fiber. The results are described in detail.

5.3.1 Study of Fiber Diameter Using FESEM

Polypropylene fibers get affected by UV exposure (Yujie et al., 2020). Figure 5.1 shows the images of fiber diameters in both untreated and all the disinfected fiber samples. Images were captured by FESEM (model: Sigma, make: Zeiss). In each sample, fiber diameter was measured at 8 different places. Average values along with standard deviation of fiber diameter measured at 8 different places are shown in Table 5.1. Alcohol treated and UV-C treated fibers became wider than the untreated fiber sample. Increase in fiber diameter and R_a in polypropylene fiber due to chemical treatment was reported (Hu and Ma, 2021). UV irradiation created some cracks on the surface of the polypropylene fiber causing rougher surface with increase in fiber diameter (Hu and Ma, 2021; Karami et al., 2013). In these cases, there is no significant increase in the temperature of the fiber; hence, any surface damage redistributes the material causing an increase in the peaks. However, fibers treated with incandescent bulb heat, steam as well as combined incandescent bulb heat and UV-C became thinner than the fibers of the untreated sample. In case of alcohol and UV-C treated fiber, average fiber diameter changed from 16.56 μm to 16.72 μm and 16.82 μm, respectively. Furthermore, average fiber diameter in incandescent bulb heat, steam, and combined incandescent bulb heat and UV-C treated sample reduced to 14.96 μm, 15.19 μm and 16.12 μm, respectively. It is evident that with heat the polymer shrinks (Tanaka et al., 1972). However, in all the cases shrinkage is less than 10%.

A hypothesis testing was conducted to understand the significance of change in diameter. For this a purpose a one-tailed Student's t-test was conducted (Dixit and Dixit, 2008; Mendenhall et al., 2009). The hypotheses to be tested are

H_0: No change in diameter versus H_a: Diameter increases (or reduces) (5.1)

where H_0 is null hypothesis and H_a is alternative hypothesis. For each treatment, the t-value was calculated as

$$t = \frac{\text{absolute difference in mean diameters}}{\sqrt{\left(s_1^2 + s_2^2\right)/n}}, \quad (5.2)$$

where s_1 and s_2 are the standard deviations of untreated and treated samples, respectively. Eq. 5.2 is for the case of equal sample sizes (n=8 in this case). This t-value is compared with critical value $t_{\alpha,\mathrm{df}}$, where α is the level of significance (taken 0.05 and 0.1 in this study) and df is the degree of freedom ($2n-2$=14). The critical values at degree of freedom of 14 for level of significance of 0.05 (5%) and 0.1 (10%) were obtained from standard t-table for one-tailed test (Mendenhall et al., 2009). For any difference between parameters to be significant, t-value should be greater than critical value. Table 5.2 summarizes the results of hypothesis testing. Alcohol immersion test does not change diameter significantly even at 10% significance level. However, in all other cases, diameter changes significantly as ascertained at 5% significance level. In some cases, the difference is significant at much lower significance level. However, for most of the engineering problems 5% significance level is considered appropriate. It indicates that probability of inference being wrong is less than 0.05.

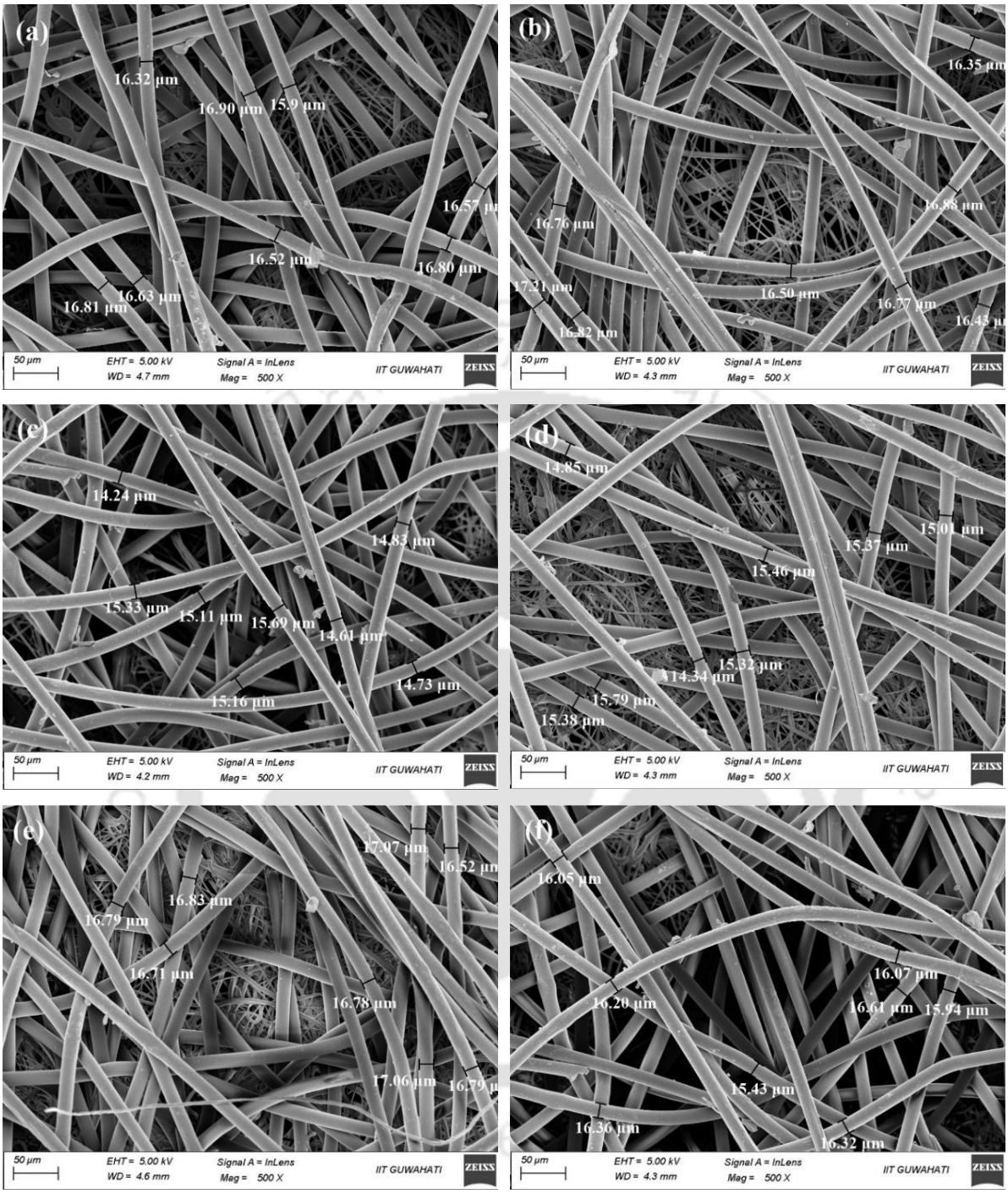

Figure 5.1 FESEM images (X500) showing fiber diameter of **(a)** untreated sample, **(b)** alcohol immersion sample, **(c)** incandescent bulb heating sample, **(d)** steam exposure sample, **(e)** UV-C irradiation sample, and **(f)** combined incandescent bulb heating and UV-C irradiation sample

5.3.2 Study of Surface Roughness (R_a) Using AFM

Figure 5.2 depicts the images showing R_a of each sample— untreated as well as disinfected. Images were captured by AFM (model: MFP 3D Infinity Bio, make: Asylum Research). In each sample, R_a was measured at 5 different places. Average values along with standard deviation of R_a are shown in Table 5.1. To understand the statistical significance of change in R_a, hypothesis testing was carried out as explained in Section 5.3.1. The results are presented in Table 5.2.

Table 5.1 Average values of fiber diameter and R_a in untreated and differently disinfected sample

S. N.	Sample	Average fiber diameter (with standard deviation in bracket) (μm)	Average R_a (with standard deviation in bracket) (nm)
1.	Untreated	16.56 (0.32)	7.37 (0.99)
2.	Alcohol immersion	16.72 (0.28)	8.03 (0.83)
3.	Incandescent bulb heating	14.96 (0.45)	4.86 (1.13)
4.	Steam exposure	15.19 (0.45)	5.32 (1.08)
5.	UV-C irradiation	16.82 (0.18)	8.23 (0.72)
6.	Incandescent bulb heating with UV-C irradiation	16.12 (0.35)	6.54 (0.91)

Average R_a value for untreated fiber sample was found to be 7.37 nm within a sampling area of 1 μm × 1 μm. Average R_a value got increased to 8.03 nm after alcohol treatment; however, the difference is insignificant even at 10% significance level. In UV-C treated fiber, increase in R_a value (average value of 8.23 nm) is significant at 10% significance level but not significant at 5% significance level. An increase in R_a of fiber with UV irradiation and chemical treatment was already reported (Hu and Ma, 2021; Li et al., 2013), but in the present case; the increase cannot be called significant. However, average R_a value reduced in incandescent bulb heating, steam exposure, and combined incandescent bulb heating and UV-C irradiation. The average R_a value reduced to 4.86 nm, 5.32 nm, and 6.54 nm in incandescent bulb heat, steam, and combined incandescent bulb heat and UV-C treated sample, respectively. In incandescent bulb heating and steam exposure of fiber, reduction in R_a value is significant based on

hypothesis testing at 5% significance level. In case of combined incandescent bulb heating and UV-C irradiation, reduction in R_a value is significant at 10% significance level but not significant at 5% significance level. Reduction in R_a with thermal-treatment time and temperature was reported in wood fiber (Ayrilmis et al., 2011), similar to this work. Less change in average R_a value was observed in combined incandescent bulb heat and UV-C treated sample as compared to incandescent bulb heat and UV-C treatment alone. The smoother surfaces resist adhesion to small particles. Moreover, it is easier to disinfect them further by radiation treatment, as microorganisms get less opportunity to hide in valleys.

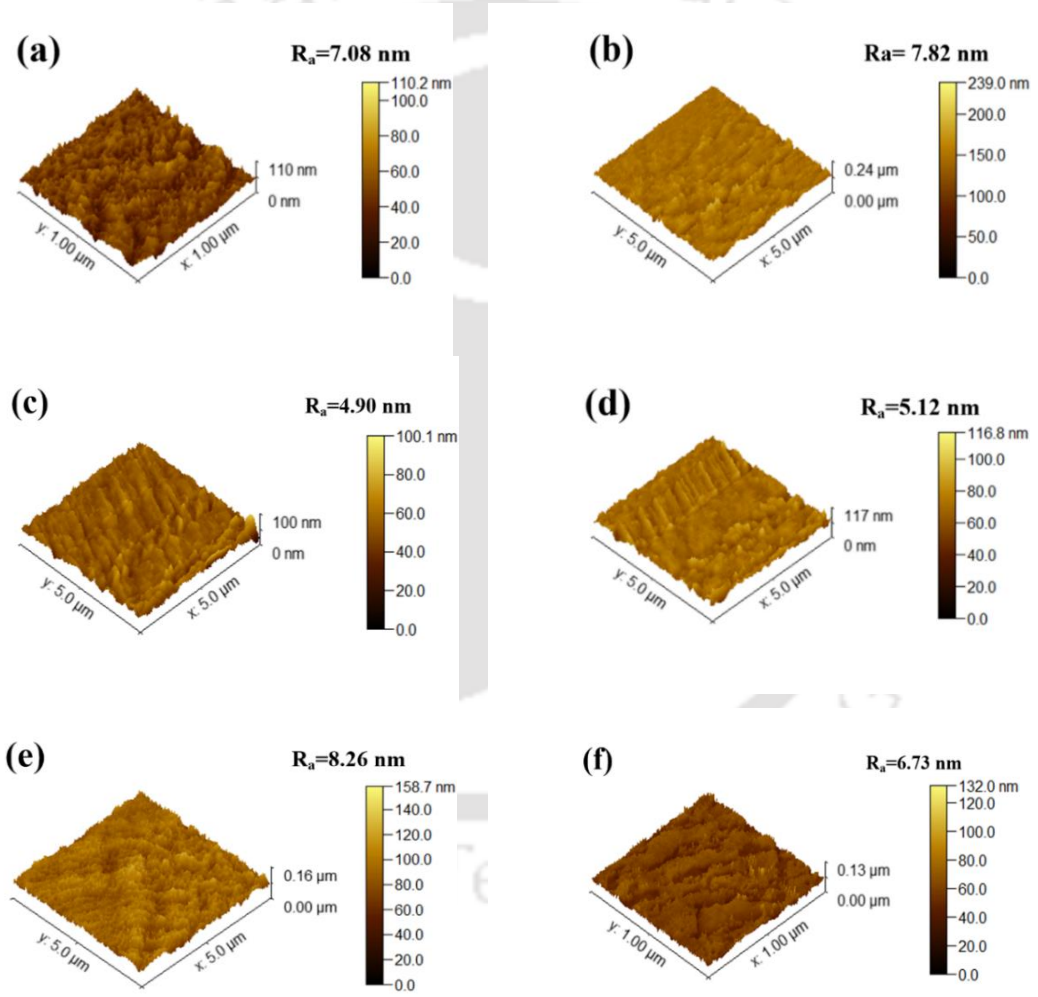

Figure 5.2 AFM images of showing surface roughness (R_a) in fiber of **(a)** untreated sample, **(b)** alcohol immersion sample, **(c)** incandescent bulb heating sample, **(d)** steam exposure sample, **(e)** UV-C irradiation sample, and **(f)** combined incandescent bulb heating and UV-C irradiation sample

Table 5.2 Inferences regarding change in diameter and R_a of fiber from hypothesis testing

Effect	*t*-value	Inference based on one-tailed test ($t_{0.1,14}$= 1.345, $t_{0.05,14}$=1.761)
Increase in fiber diameter after alcohol immersion	1.064	Insignificant increase at 5% as well as 10% significance level
Increase in R_a after alcohol immersion	1.142	Insignificant increase at 5% as well as 10% significance level
Reduction in fiber diameter after incandescent bulb heating	8.196	Significant reduction at 5% as well as 10% significance level
Reduction in R_a after incandescent bulb heating	3.736	Significant reduction at 5% as well as 10% significance level
Reduction in fiber diameter after steam exposure	7.018	Significant reduction at 5% as well as 10% significance level
Reduction in R_a after steam exposure	3.129	Significant reduction at 5% as well as 10% significance level
Increase in fiber diameter after UV-C irradiation	2.003	Significant increase at 5% as well as 10% significance level
Increase in R_a after UV-C irradiation	1.571	Insignificant increase at 5% but significant increase at 10% significance level
Reduction in fiber diameter after incandescent bulb heating with UV-C irradiation	2.624	Significant reduction at 5% as well as 10% significance level
Reduction in R_a after incandescent bulb heating with UV-C irradiation	1.380	Insignificant reduction at 5% but significant reduction at 10% significance level

5.3.3 Study of Ultimate Tensile Strength (UTS)

In this section, UTS tests of untreated as well as disinfected polypropylene fiber samples were carried out in a 5 kN UTM (model: Z005, make: Zwick Roell) at a test speed of 8 mm/min. This corresponds to a strain rate of about 3.3×10^{-3} s^{-1}, which can be treated as quasi-static loading. Samples for UTM were cut into 60 mm × 5 mm from the 5 cm × 6 cm fiber sample as shown in Figure 5.3, keeping 40 mm gauge length for all the fiber samples. For tensile testing in polymer and composite material, rectangular shaped tensile test specimens were used by many researchers (Miller et al., 2019; Deepa et al., 2020; Alarifi, 2021; Aknyede et al., 2010) as per ASTM D3039 or D638. The samples used by them were larger than samples used in

present work and aspect ratio (ratio of gauge length to width) varied approximately from 7 to 9. Hence, here the ratio of gauge length to width was fixed as 8. Five samples from each disinfected fiber were tested. Figure 5.4 shows the stress-strain graph of untreated and all disinfected polypropylene fiber sample. Average values along with standard deviation of UTS are shown in Table 5.3. UTSs of all the disinfected fiber samples reduced as compared to untreated sample. Reduction in fiber strength due to chemical treatment has been reported (Hu and Ma, 2021). Reduction in tensile strength with heat treatment and UV irradiation was also reported for various fibers (Karami et al., 2013; Yue et al., 2000; Ochi et al., 2002), similar to this work. Heat treatment caused thermal degradation of the fiber, which resulted in loss of fiber strength (Ochi et al., 2002). UV irradiation of polypropylene fiber increased carbonyl and hydroperoxide that resulted in reduction of tensile strength (Karami et al., 2013). Moreover, some surface cracks normal to the fiber axis were observed in UV treated fiber (Karami et al., 2013). In case of incandescent bulb heat treated and UV-C treated fiber sample, UTSs were found to be lesser than the combined incandescent bulb heat and UV-C treated fiber sample. Reduction in UTSs for incandescent bulb heat, UV-C irradiated and combined incandescent bulb heat and UV-C irradiated fiber sample was found to be 34.8%, 30.6%, and 21.5%, respectively. Thus, combined incandescent bulb heat and UV-C treatment caused less reduction in UTS than both incandescent bulb heat and UV-C treatment alone.

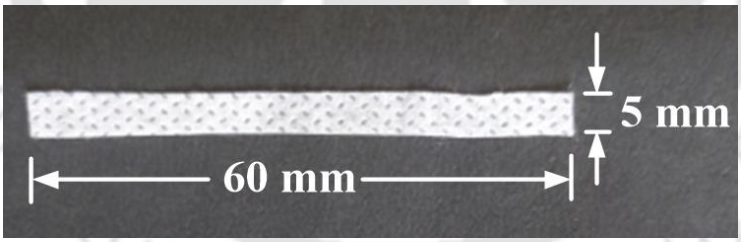

Figure 5.3 Prepared polypropylene fiber sample for ultimate tensile strength testing

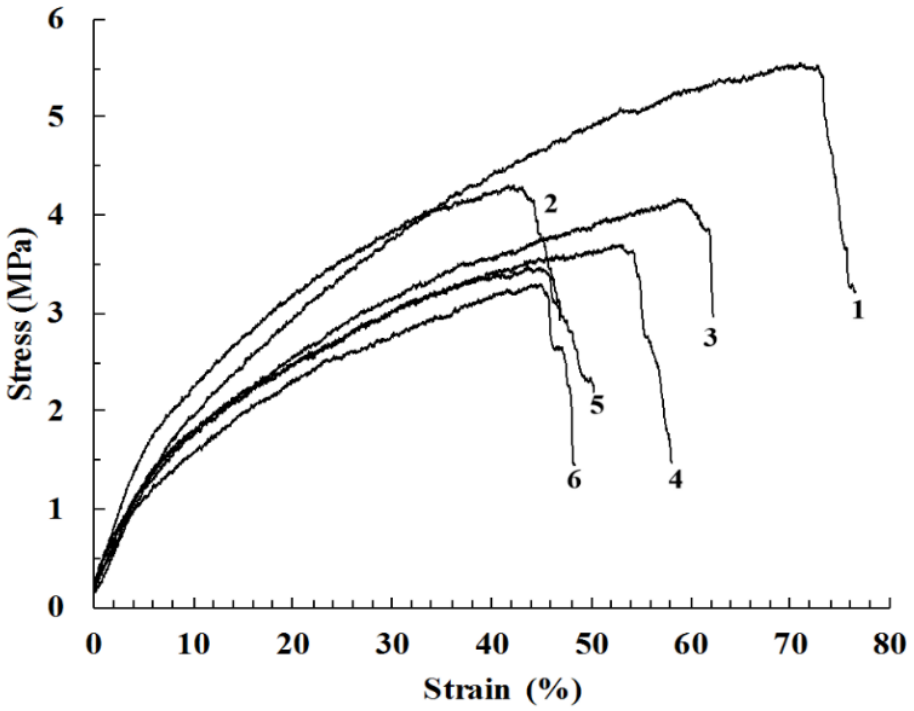

Figure 5.4 Stress-strain graph of **(1)** untreated, **(2)** alcohol immersion, **(3)** combined incandescent bulb heating and UV-C irradiation treated, **(4)** UV-C irradiation treated, **(5)** incandescent bulb heating treated, and **(6)** steam exposure treated polypropylene fiber sample

Table 5.3 Average UTS values of polypropylene fiber in untreated and differently disinfected sample

S. N.	Sample	Average UTS (with standard deviation in bracket) (MPa)
1	untreated	5.43 (0.30)
2	Alcohol immersion	4.35 (0.24)
3	Incandescent bulb heating	3.54 (0.42)
4	Steam exposure	3.47 (0.34)
5	UV-C irradiation	3.77 (0.35)
6	Combined incandescent bulb heating and UV-C irradiation	4.26 (0.39)

5.3.4 Study of Scratch Resistance in Both Untreated and Disinfected Fibers

Scratch resistance test was carried out in a scratch tester (model: TR-101, make: DUCOM) with start load 20 N, stroke length 5 mm, and scratch velocity 0.10 mm/sec. Five scratch tests were performed for each sample. The polypropylene fiber samples are under the category of thin film sample. Scratch tip made the scratches in the samples. When the scratch tip pierced the fiber sample completely, load reduced to zero. Table 5.4 lists the average values with standard deviation of distance travelled by scratch tip for both untreated as well as disinfected fiber samples. Figure 5.5 shows the resistive load-distance travelled graph of single test for each sample. More the distance covered by scratch tip before fully penetrating the fiber, more was the scratch resistant. Scratch tip covered an average distance of 4.29 mm in untreated sample, which showed the highest scratch resistant among all the samples. Moreover, it was observed that combined incandescent bulb heat and UV-C treated samples were more scratch resistant than both incandescent bulb heat and UV-C treated sample alone.

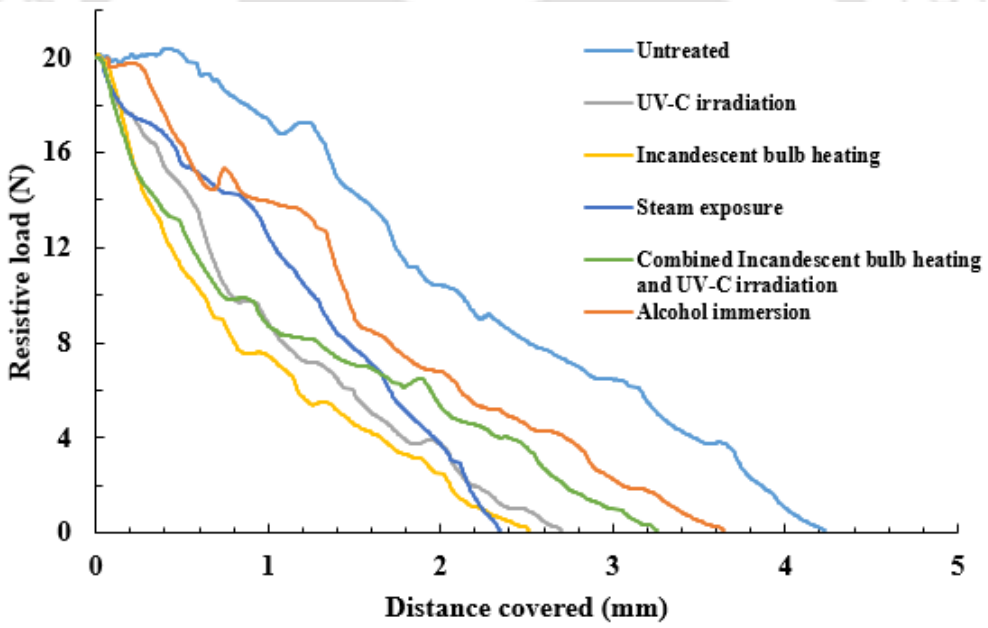

Figure 5.5 Resistive load-distance travelled graph of untreated and all disinfected polypropylene fiber sample

Table 5.4 Average distance travelled by scratch tip for 20 N load in untreated and all disinfected fiber sample

S. N.	Sample	Average distance travelled (with standard deviation in bracket) (mm)
1	untreated	4.30 (0.19)
2	Alcohol immersion	3.67 (0.16)
3	Incandescent bulb heating	2.55 (0.11)
4	Steam exposure	2.35 (0.1)
5	UV-C irradiation	2.76 (0.18)
6	Combined incandescent bulb heating and UV-C irradiation	3.22 (0.1)

5.3.5 XRD Study in Both Untreated and Disinfected Fibers

XRD study was carried out to check the chemical changes in the surfaces of disinfected fiber samples as compared to untreated sample. Figure 5.6 shows the intensity–angle graphs for both untreated as well as disinfected fiber samples. For all the samples, peaks were found in almost the same angle. However, intensity values got changed for different disinfection treatment. With increase in treatment temperature, peaks were showing more intensity. An increase in peak intensity with increase in heating temperature was reported (Wang et al., 2015). In this study, intensity value for the steam treatment was more than that of all other treatment methods. Peak areas for all differently treated as well as untreated fibers are also compared from the intensity–angle graphs (Figure 5.6). The peak area is the highest in the case of steam treated fiber as fiber got subjected to the highest temperature. When the annealing temperature for polypropylene was slightly more than 100 °C, molecular chains were easier to loosen, rearrange or to create microstructural evolution at the molecular level. Remarkable change in crystallinity of polypropylene could not be noticed during annealing temperature below 145 °C. Phase transformation and secondary crystallization process can only be observed at enough high temperature (Wang et al., 2015). No significant changes were observed in all the disinfected fiber sample as compared to the untreated sample.

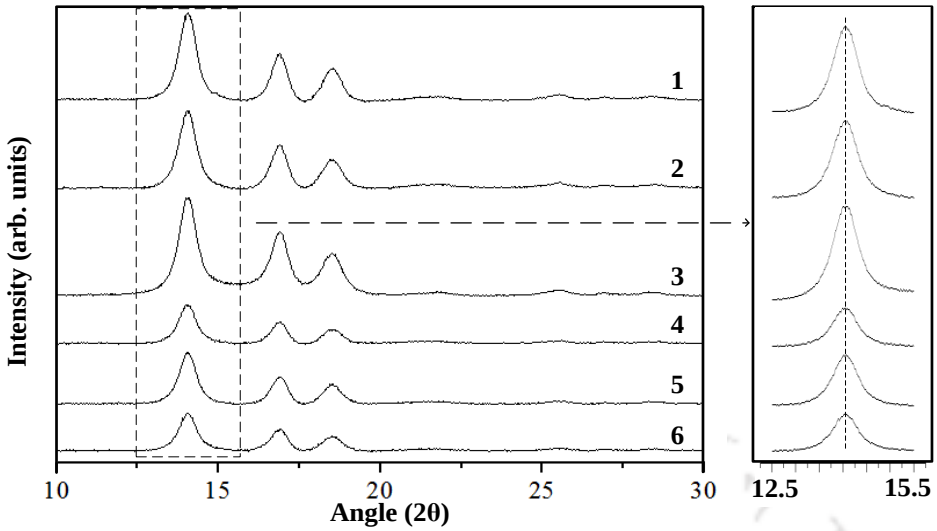

Figure 5.6 XRD plot of **(1)** incandescent bulb heating treated, **(2)** combined incandescent bulb heating and UV-C irradiation treated, **(3)** steam exposure treated, **(4)** alcohol immersion treated, **(5)** UV-C irradiation treated, and **(6)** untreated polypropylene fiber sample

5.4 Conclusion

In this work, the effects of five disinfection methods— incandescent bulb heating, UV-C irradiation, alcohol immersion, steam exposure, and combination of incandescent bulb heating and UV-C irradiation treatment— on the mechanical properties of polypropylene fibers were studied. Mechanical properties viz., diameter, R_a, UTS, and scratch resistance of fibers were investigated using FESEM, AFM, UTM, and scratch tester, respectively. Chemical changes in the surface of the disinfected polypropylene fiber were also investigated using XRD analysis. The salient observations are as follows:

1. Fibers treated with alcohol and UV-C irradiation became wider and rougher than the untreated fiber sample. Incandescent bulb heating, steam exposure, and combined incandescent bulb heating and UV-C irradiation made fiber thinner and smoother than the untreated sample. Smoother fibers make better respirator as micro-organism get less chance to hide in pores.
2. Combined incandescent bulb heating and UV-C treatment caused less reduction in UTS than incandescent bulb heating and UV-C treatment alone. Moreover, combined incandescent bulb heating and UV-C treated samples were more scratch resistant than incandescent bulb heating and UV-C treated sample alone. Thus, combined

incandescent bulb heating and UV-C irradiation disinfection showed the least degradation after 20 cycles.

3. No matter what disinfection method is used, there is some degradation of the respirator.
4. XRD analysis indicated no change in the chemical structure of the surface.

Chapter 6

Design of a Pedagogical Gadget for Teaching Heat Transfer

6.1 Introduction

A heat-based sterilization box is transformed into a pedagogical gadget to develop minimum viable products (MVPs). There have been a lot of research activities on engineering pedagogy in recent years. Pedagogy is the art and science of teaching-learning strategies that encompasses the interaction between students and teachers, the learning environment, and the learning task. In November 1951, Hans Lohmann established the Institute for Engineering Pedagogy for teaching and research in this field (Kersten, 2018). In a sense, engineering pedagogy is more challenging than pedagogy of other disciplines, because of unique nature of engineering education. An engineer needs to be adept both in theory and practice. In addition, leadership, creativity, self-initiative, and resource optimization are the required qualities for an engineer. It is not easy to impart these qualities only through lectures or well-structured plan of laboratory experiments. Education needs to be supplemented by means to encourage hands-on practices.

Engineering is basically an experiential profession. Students should inculcate the habit of learning through hands-on practices and relating their experiences with theory. Training the students through hands-on practices requires sufficient resources and efforts. Lectures can be delivered in classroom or through online mode, whereas hands-on practices are performed only in physical laboratories. Laboratories in science and engineering education are paramount for imparting knowledge and honing skills. Feisel and Rosa (2005) highlighted the importance of a laboratory in engineering and science education for undergraduate students. Tiwari and Singh (2011) mentioned the usefulness of well-developed internet-based remote laboratory (RL) experiments into an engineering curriculum. Feedback was collected for further improvements of the content with effective learning and knowledge transfer. Gadzhanov and Nafalski (2010) described the pedagogical effectiveness of RLs showing involvement of students in the entire teaching process.

Gamification, e-learning, and flipped classrooms are the tools of collaborative, cooperative, and non-competitive learning that motivate the students towards teamwork and

decision making. Gamification, e-learning, and flipped classrooms can be important tools for imparting such type of learning. Main purpose of gamifying a course is to motivate students and inspire them to engage with the course in learning surroundings. Markopoulos et al. (2015) observed a beneficial effect of gamification in engineering education by making difficult subjects more enjoyable and interesting. "Learning by doing" played an important role in both teaching and learning process with gamification.

Baker (2013) mentioned that hands-on laboratory experiments and active participation improved girls' achievement in physical sciences. It is also essential to obtain proper feedback regarding the students' experience. Hands-on learning is also called 'experiential learning', 'learning by doing', and 'active learning' in engineering and science education. Renner et al. (1985) interviewed students about their interest in learning physics using laboratory work. Students mentioned hands-on experience in laboratory as interesting method of learning as compared to listening to teachers in classroom. Ato and Wilkinson (1986) found that school students using science equipment showed more interest in science as well as a positive attitude towards scientific inquiry and science profession than students with low usage of science equipment. Holstermann et al. (2010) focused on hands-on experience in four different activity related to biology and observed that students with hands-on experience reported higher interest in the respective activity than students without hands-on experience. Gadola and Chindamo (2019) carried out a case study in designing a motorbike for a small racing competition. This design competition provided all the knowledge and exposure that define the idea of experiential learning.

Researchers also attempted to provide a feel of engineering to school level children by organizing engineering Work Experience Week (WEW) sessions, in which students learn by doing. Gonzalez-Buelga et al. (2022) studied the impact of WEW program at the University of Bristol, UK. Engineering WEW created opportunities for the participants to work as engineering researchers by experiencing hands-on activities. Main objective of WEW program was to motivate secondary school students towards engineering profession. Results from the student-feedback in the form of response to questionnaire were used to analyze the impact of WEW program. Tauro et al. (2017) developed a problem-based learning program based on mechatronics for Malaysian high-school students and carried out pre- and post-assessment surveys to examine the impact of the program on engagement of students in science,

technology, engineering, and mathematics (STEM) fields. Before attending the program, 21% of the participants showed their willingness to work as an engineer, whereas it increased to 34.55% after attending the program. An increase of 44% student-enrollment in mechanical engineering program was reported after starting STEM event in high school (Karkoub and Abdulla, 2020). Using solid modeling, software, and hands-on experimental activities, researchers tried to attract high school children towards mechanical engineering (Musto et al., 2004). Cirenza et al. (2018) conducted hands-on workshops to help undergraduate mechanical engineering students for conceptual understanding of heat transfer. Students reported that workshop enhanced their learning abilities by offering real, hands-on experience. Penney and Clausen (2018) described a number of hands-on experiments on fluid mechanics or heat transfer that can be carried out either in engineering laboratory or as classroom demonstration.

Researchers also explored the usage of toys and simple models in teaching-learning practices. Billard (2003) developed a doll-shaped robot to use in the introductory classes of robotics. Paul and Dixit (2011) developed simple toys for understanding some basic concepts of mechanical engineering, e.g., vibration, coefficient of friction, functioning of mechanisms. Meng et al. (2019) fabricated inexpensive and easy to use experimental setup using computer-aided design, vacuum forming, and 3D printers for undergraduate students to carry out two fluid mechanics-based experiments; one was related to venturimeter and other nozzle experiment and other was for studying frictional losses in flow through pipes. Such pedagogical gadgets aid in the development of a scientific spirit among students. Unfortunately, pedagogical gadgets are not widely available as consumer products. Thus, there is a tremendous need for developing easily affordable products for teaching the scientific principles in a simplified manner.

In this chapter, development of a pedagogical gadget for conducting a number of hands-on experiments related to heat transfer is presented. The gadget can be useful for pre-engineering as well as engineering students. Feedback obtained from different groups of students and teachers were analyzed. The main purpose of collecting feedback was to check the pedagogical effectiveness of the gadget and obtain the feedback for its improvement. Educational assessment of the gadget was carried out among the newly graduated students to check its efficacy for learning heat transfer concept. These students were doing preparation for

graduate aptitude test in engineering and had taken a course on heat transfer during their B.Tech. program.

6.2 Design of a Pedagogical Gadget

In this chapter, a pedagogical gadget is designed from a heat-based sterilization box to develop MVPs. A simple, easy to handle, and low-cost pedagogical gadget of size 27 cm × 17 cm × 17 cm was developed at Indian Institute of Technology Guwahati for teaching the concepts of heat transfer. The gadget was made of a wooden box containing a 100 W incandescent bulb, a mercury free liquid in glass thermometer for measuring the temperature, and a detachable box made of aluminium to act as inner layer of the wooden box. Air-gap between the inner wooden surfaces and outer surfaces of the aluminium box acted as insulator. An incandescent bulb was used for heating. A Data Acquisition (DAQ) system and thermocouple were used to measure and download the temperature data at the center and surface of the aluminium sample. Figure 6.1(a) and Figure 6.1(b) show the schematic diagram and photograph of the pedagogical gadget, respectively.

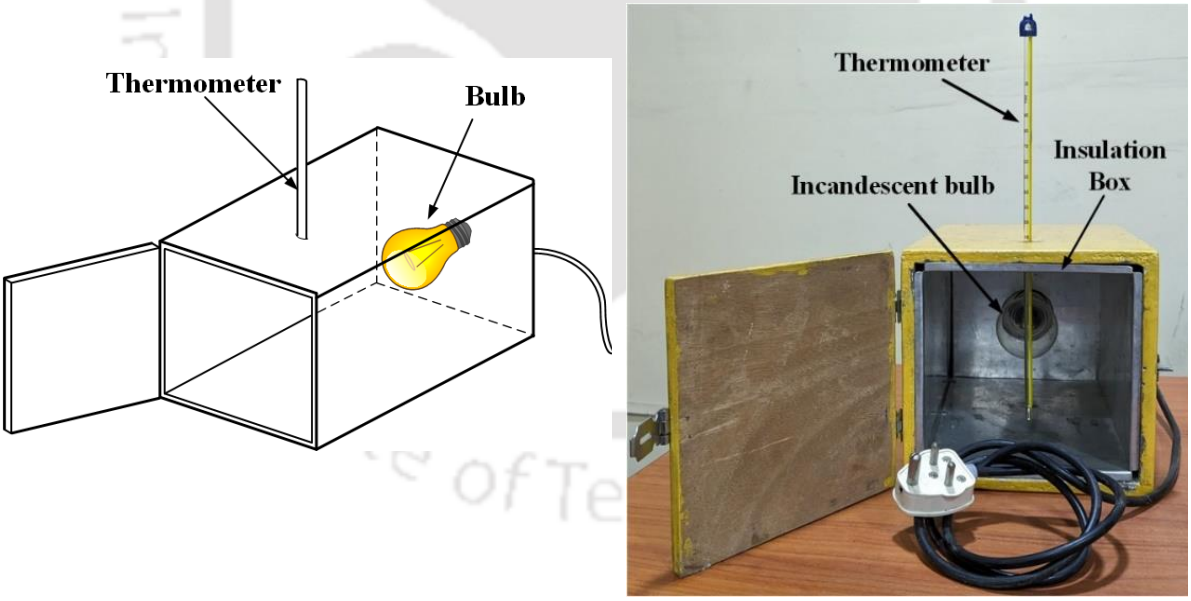

Figure 6.1 Pedagogical gadget: **(a)** schematic diagram and **(b)** photograph showing different parts

6.3 Possible Experiments in Designed Pedagogical Gadget

Some experiments are carried out in the designed pedagogical gadget for teaching heat transfer. Experiments help the teaching-learning process by engaging the students in hands-on activities. Some possible experiments are described in sequel.

6.3.1 Newton's Law of Cooling

Newton's law of cooling states that the rate of heat loss from a body is directly proportional to the difference in the temperatures of the body and its surrounding. This means that a hot body will initially cool rapidly and then the rate of cooling gets slower. To demonstrate this law, the air inside the wooden box is first heated to a temperature above the ambient temperature. Temperature inside the box is measured using type-K thermocouple connected with a DAQ. After reaching a pre-decided temperature, the bulb is switched off. Temperature readings are recorded after a fixed interval of time using DAQ, till the temperature inside the box reaches almost the ambient temperature. Students were asked to plot a graph to show the variation of temperature with time. A typical plot obtained from this gadget is shown in Figure 6.2. In the case of lumped mass, variation of temperature with time is given by the following expression (Bergman et al., 2011):

$$\theta = \theta_i \exp\left(-\frac{t}{\tau_t}\right), \tag{6.1}$$

where the temperature differences θ and θ_i are given by

$$\theta = T - T_\infty \text{ and } \theta_i = T_i - T_\infty. \tag{6.2}$$

In Eq. 6.2, T is the temperature at time t, T_i is the initial temperature and T_∞ is the ambient temperature. In Eq. 6.1, τ_t is called thermal time constant given by

$$\tau_t = \frac{\rho V C}{h A_s}, \tag{6.3}$$

where ρ is the density of the material, V the volume, C the specific heat, h the convective heat transfer coefficient and A_s is the surface area. In the present case, density and specific heat are not uniform thorough out the box. Moreover, the convective heat transfer coefficient varies with temperature. Hence, Eq. 6.1 is only an approximate representation of true variation of

temperature with time. In Figure 6.2, solid curve depicts experimental results. Students were asked to fit an exponential curve based on this experimental data of the form given in Eq. 6.1.

During a typical demonstration day, ambient temperature was 29 ℃. The air inside the box was heated up to 90 ℃ and was allowed to cool. Hence, θ_i is 61 ℃. Thus, Eq. 6.1 contains only one parameter, i.e., τ_t. This parameter was obtained matching the experimental and fitted temperature at 5 min, 35 min and 65 min. Accordingly three exponential curves were obtained as shown in Figure 6.2. It is observed that when experimental and fitted temperatures are matched at 5 min, there is a good agreement between fitted and experimental temperatures up to 5 min. However, later on, fitted temperature values are much less than experimental values. In other words, this type of fitting provides faster-than-actual cooling. It indicates that actual convective heat transfer coefficient reduces with temperature, thus slowing the cooling rate. When the fitting was done based on the matching of fitted and experimental temperature at 35 min, the overall agreement between fitted and experimental curves is better. Nevertheless, actual cooling rate is faster up to 35 min and slower afterwards. This again ascertains that actual convective heat transfer coefficient is high at high temperature and low at low temperature. When the fitting was done based on the matching of fitted and experimental temperature at 65 min, the fitted curve shows slower cooling, i.e., it underestimates the convective heat transfer coefficient.

Students were encouraged to discuss their observations and describe what they learnt. Some academically bright students pointed out the following lessons they learnt through this experiment:

(i) In general, the natural convective heat transfer coefficient for air is a function of temperature; it is high at high temperature.

(ii) By taking some representative average value of thermal time constant, an exponential curve can still be fitted to describe the variation of temperature with time. For obtaining overall good fitting, time constant should not be calculated based on the early or late data during cooling.

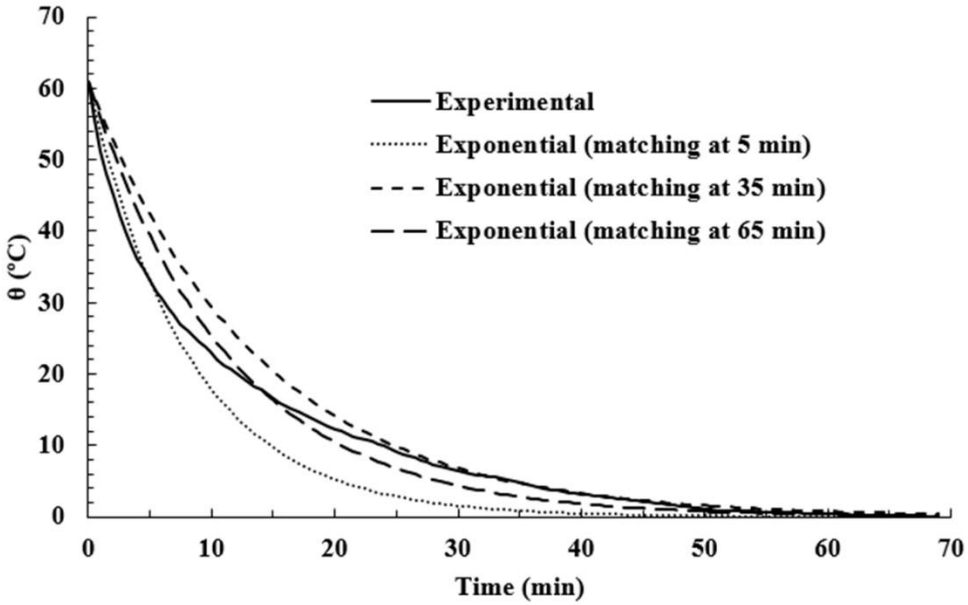

Figure 6.2 Variation of temperature with time during cooling

6.3.2 Concept of Specific Heat Capacity

Specific heat capacity of a body is defined as the amount of heat required per unit mass of the body to raise its temperature by one unit. This means that for a given value of heat, temperature rise in the same amount of two different types of substance will be different. It is due to the difference in specific heat capacities of the two substances. To understand this concept, air inside the wooden box was heated to a temperature above the room temperature. Using stopwatch, time required to raise the temperature of air from the room temperature to pre-decided temperature was noted. After reaching the pre-decided temperature, heating was stopped. After cooling the wooden box to room temperature, keeping some aluminium pieces inside the wooden box, similar experiment was repeated. Time required to raise same amount of temperature in the latter case was more. Figure 6.3 shows the temperature-time graph of a typical experiment of heating empty box and aluminium filled box to illustrate the concept of specific heat.

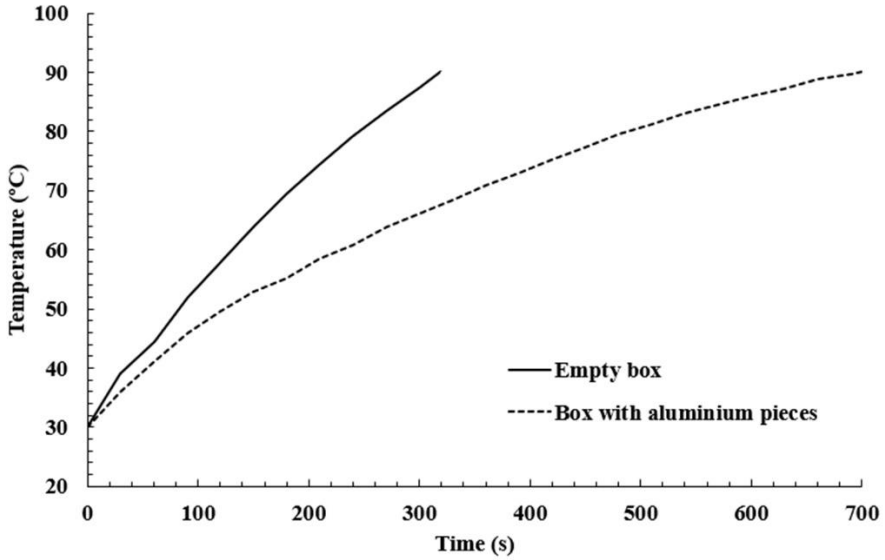

Figure 6.3 Variation of temperature with time during heating

Using this gadget, a rough estimate of specific heat capacity of a substance could be made. For example, both empty box and box filled with aluminium pieces were heated to 90 ºC from room temperature and time required to raise the temperature was noted in both the cases. For empty box, time t_1 required to reach 90 ºC from room temperature of 30 ºC is 319 s using a 100 W incandescent bulb.

For empty box,

$$m_{eq}(C_p)_{eq}\Delta T = 100t_1, \tag{6.4}$$

where m_{eq} is the equivalent mass corresponding to empty box, $(C_p)_{eq}$ is the equivalent specific heat capacity and ΔT is the increase in temperature. Now, similar experiment was repeated by keeping 0.7 kg amount of aluminium pieces inside the wooden box. Seven pieces of an aluminium cylinder of diameter 19 mm and length 135 mm made up a mass of 0.7 kg. Time t_2 required to reach 90 ºC from room temperature was 700 s using the same 100 W incandescent bulb. For box with aluminium pieces,

$$m_{eq}(C_p)_{eq}\Delta T + m_{al}(C_p)_{al}\Delta T = 100t_2 \tag{6.5}$$

Substituting Eq. 6.4 in Eq. 6.5,

$$100(t_2 - t_1) = m_{al}(C_p)_{al}\Delta T, \tag{6.6}$$

which provides the specific heat capacity of aluminium as 907 J/(kg.°C). The value of specific heat of AA6061 (which was similar to aluminium used in the experiments) is 900 J/(kg.°C) at 25 °C (Aval et al., 2012), which is very close to experimental observation. Similarly, specific heat value of steel was experimentally measured as 478 J/(kg.°C), which is close to specific heat capacity of hot rolled AISI 1018 as 475 J/(kg.°C) (Nandan et al., 2007). Generally, the specific heat of metals increased with temperature. This effect can also be studied by varying the maximum temperature during heating.

This experiment was repeated by several groups of students and there was some small variation in the results. However, one group obtained the specific heat capacity of aluminium as 411 J/(kg.°C), which is quite different from the values reported in literature and obtained by other groups. A brain-storming session was held between instructor and students to identify the cause of this variation. It was observed that this particular group used different pieces of aluminium, although the total mass was 0.7 kg only. The students used a single piece of aluminium of diameter 60 mm and length 95 mm. To raise the temperature of the box to 90 ºC from room temperature of 30 ºC, it required 492 s against about 700 s required by other groups. It was decided to calculate Biot number for different types of aluminium pieces. The Biot number is a non-dimensional parameter defined by

$$B_i = \frac{hL_c}{k}, \tag{6.7}$$

where k is the thermal conductivity and L_c is the characteristic length, often taken as ratio of volume of solid to its surface area. Taking typical value of h as 10 W/(m^2.°C) and k as 200 W/(m.°C), B_i is obtained as 0.57×10^{-3} for aluminium piece of diameter 60 mm and length 95 mm. On the other hand, for aluminium pieces of diameter 19 mm and length 135 mm, B_i is obtained as 0.22×10^{-3}. Larger the Biot number, the more is the deviation from the lumped capacitance method. Hence, in the second case, with B_i of 0.57×10^{-3}, a large error is introduced. Using type-K thermocouple, temperatures at surface and center of the aluminium sample were measured. For temperature measurement at the center, a 47.5 mm deep and 1.5 mm diameter hole was made in the center of the circular part to insert the thermocouple in the aluminium piece of 60 mm diameter. A temperature difference was found in both the places of

bigger diameter aluminium piece. Temperature reading of 88 °C and 45.2 °C were recorded at surface and center, respectively. Thus, internal temperature of the solid was quite low, although the surface temperature became close to 90 °C. It showed the presence of temperature gradient inside the aluminium piece with bigger diameter, which violated the assumption of lumped capacitance. Hence, a deceptively small value of specific heat capacity was obtained. However, temperature gradient was not present in case of smaller diameter aluminium pieces. Position of the samples inside the box was also important. The samples should be kept near to heat source, i.e., incandescent bulb.

6.3.3 Insulation Effect

Thermal insulators are used to prevent the flow of heat. To demonstrate the effect of the insulator, air inside the wooden box (without a detachable insulating aluminium box) was first heated to a temperature well-above the ambient temperature. Time to reach a pre-decided temperature (90 ºC) was recorded through a stopwatch. The experiment was repeated by placing the detachable box made of highly polished thin aluminium sheet inside the wooden box. The temperature of the air inside the detachable box fitted within the wooden box was recorded. A thin layer of air between wooden and detachable box acted as a thermal insulator, avoiding heat loss. This reduced the time to achieve the pre-decided temperature. It also enhanced the time of cooling from the maximum temperature to room temperature. Figure 6.4 shows the results of a typical experiment of heating wooden box and wooden box with thermal insulator to illustrate the concept of insulation effect. It is clearly seen that with detachable box (i.e., with enhanced insulation), the temperature of 90 °C could be attained in 320 s, while normally it took 920 s.

6.3.4 Absorptivity of Black Color

Black color absorbs almost all the visible radiation incident on it. To describe the absorptivity of black color, two measuring cylinders of same amount of water (3 mL each) was heated inside the wooden box. One cylinder contained normal water while the other cylinder contained black colored water. Measuring cylinder with normal water was first heated to 100 ºC and time to raise the temperature was recorded using a stopwatch. Thermometer was dipped under water to record the temperature of water in the measuring cylinder. The experiment was repeated by heating the black colored water to reach 100 ºC and the time was recorded. It was

observed that the black colored water required less time to reach 100 ºC temperature than the normal water. Figure 6.5 shows the results of a typical experiment of heating normal water and black colored water in a measuring cylinder to illustrate the concept of absorptivity of black color.

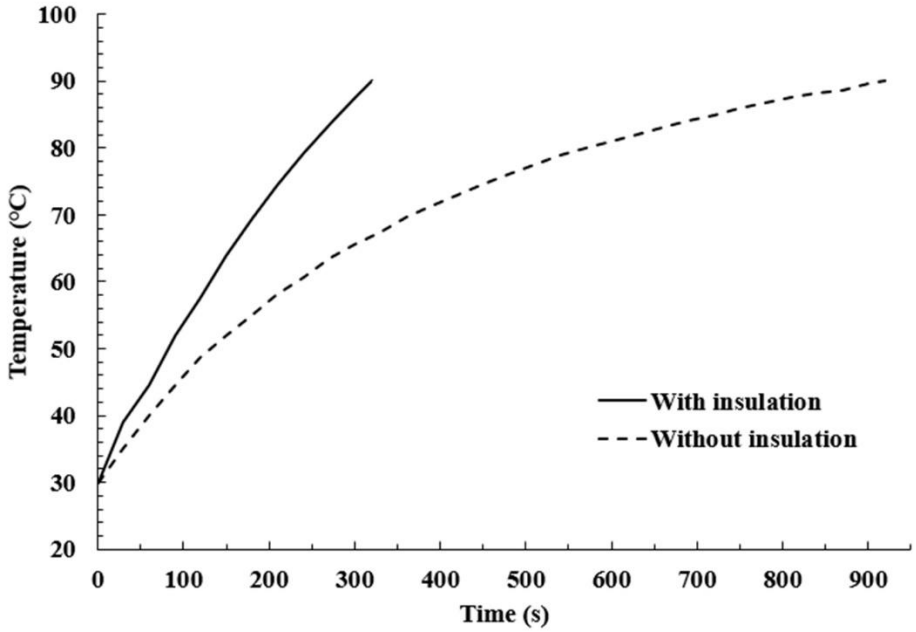

Figure 6.4 Temperature-time graph during heating the normal box and box with detachable aluminium box

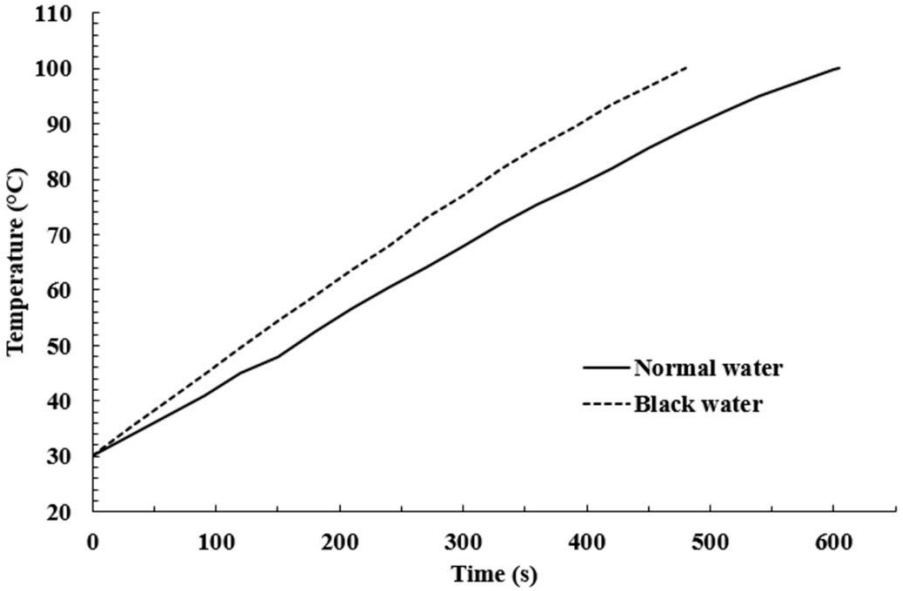

Figure 6.5 Temperature-time graph during heating normal water and black water

6.3.5 Change in Diffusion with Temperature

Diffusion is defined as the movement of molecules from an area of high concentration to an area of low concentration. To describe the effect of temperature on diffusion, following experiment was carried out. Same amount of water (200 mL each) was taken in two identical glass beakers. In both the beakers, same amount of ink is added without stirring. One beaker is heated inside the wooden box above the room temperature and the other one is kept at room temperature. Temperature was recorded through a thermometer. After reaching a pre-decided temperature of 45 ºC, heating is stopped. It was observed that the ink in the heated beaker is mixed properly with water while the ink in beaker at room temperature. The movement of the water molecules inside the heated beaker increases due to conversion of heat energy into kinetic energy. This helps in faster intermixing of fluids in the heated beaker as compared to the beaker at room temperature. Figure 6.6 shows the mixing of ink with water kept in room temperature and heated wooden box. In beaker kept in room temperature, ink got settled down at the bottom of the beaker, whereas proper mixing of ink was observed in case of beaker kept in heated wooden box.

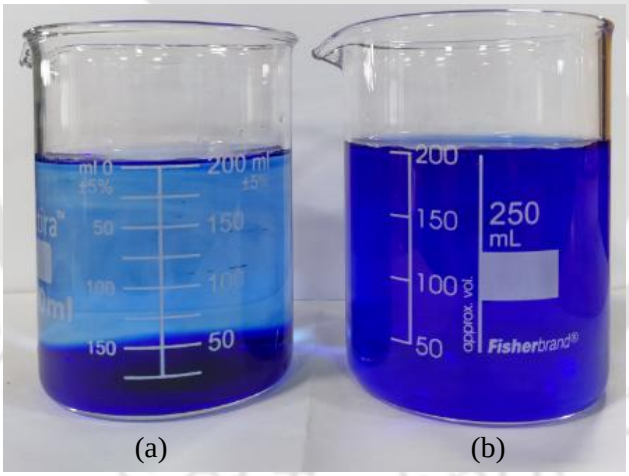

Figure 6.6 Water added with ink kept in **(a)** room temperature **(b)** heated pedagogical gadget

6.4 Survey and Feedback on Pedagogical Gadget

A survey was carried out for collecting the information regarding the pedagogical effectiveness of the gadget among the students and teachers. Many researchers conducted survey to confirm the effectiveness of their pedagogical tools viz., project-based learning (PjBL), RL,

engineering WEW, and experiential learning for improvement of teaching-learning methods in engineering education (Gadola and Chindamo, 2019; Gonzalez-Buelga et al., 2022; Tauro et al., 2017; Musto et al., 2004). The main purpose of this survey was to gauge the capability of the gadget to help the students in learning some basic heat transfer concepts, engaging in hands-on practices, developing interest in engineering, developing a team spirit, and developing collaborative skills. The survey helped the researchers by providing feedback of pedagogical gadget and its utilization.

This survey was designed for different groups of students. A feedback form with a set of written statement and questions was made for the survey purpose. The feedback forms were made in local language (Assamese) as well as in English. Table 6.1 shows the statements that participants had to rate between 1 to 10 and questions that were asked in the survey. The rating scale varies from 1 to 10, where 1 meant "totally disagree" and 10 meant "totally agree". Feedback statements and questions were related to various aspects of the gadget e.g., its pedagogical effectiveness and differing views of the researchers. A feedback about product design, required further modifications and opportunities to use such gadgets was also obtained.

Table 6.1 Questions for survey

Q1.	This gadget is useful for the improvement of teaching-learning process. (Answer in a scale of 1 to 10.)
Q2.	I did not carry out this type of experiment before. (Answer in a scale of 1 to 10.)
Q3.	I learnt something new from it. (Answer in a scale of 1 to 10.)
Q4.	It is an effective way of learning the basic concepts. (Answer in a scale of 1 to 10.)
Q5.	Other similar types of pedagogical gadgets should be made. (Answer in a scale of 1 to 10.)
Q6.	Have you come across this type of pedagogical gadgets before? (Yes/No)
Q7.	Any suggestions for further modifications of this gadget? (Answer in a paragraph.)

Additionally, a multiple-choice question (MCQ)— "This gadget is suitable for (a) High school students (b) Higher secondary students (c) Undergraduate science and engineering students" was added for teachers to know the suitability of the gadget within the framework of

course curricula. Total 712 people comprising teachers and students from different institutes viz., (1) Indian Institute of Technology Guwahati, (2) Nowgong Polytechnic, Nagaon, (3) Ganesh Das High School, Sualkuchi, (4) Sankardev Sishu Vidya Niketan, Sualkuchi, (5) Gateway Academy, Baihata Chariali, (6) Ram Saraswati Academy, Pachim Dadara, and (7) Sualkuchi Budram Madhab Satradhikar College, Sualkuchi participated in this survey. Participants were requested to carry out the experiments to promote hands-on practices and rigorous engagement with experiment. Students were grouped into five categories—undergraduate (23 Mechanical Engineering and 125 Bachelor of Science students), diploma (157 Mechanical Engineering students), high school (150 ninth and tenth class students), higher secondary (152 eleventh and twelfth class students), and post-graduate (72 Mechanical Engineering students). Experiments were carried out in groups of participants i.e., one group comprising three participants was asked to carry out experiment with the help of pedagogical gadget. Main purpose of survey conducted among high school and higher secondary level students was to attract them towards careers in engineering education and develop aptitude for experimental science in general and engineering in particular. In the past also, several researchers and educationist conducted WEW program mainly to attract high school and higher secondary students; they conducted sessions on mechatronics in PjBL and solid modeling related to mechanical engineering (Gonzalez-Buelga et al., 2022; Tauro et al., 2017; Karkoub and Abdulla, 2020; Musto et al., 2004). Table 6.2 lists the number of respondents in different groups.

Table 6.2 Number of respondents from different groups

Group	Number of respondents
Undergraduate Mechanical Engineering and Science student	148
Diploma Mechanical Engineering student	157
High school student	150
Higher secondary student	152
Post-graduate Mechanical Engineering student	72
Teacher	33

6.4.1 Response to Statement 1

Statement 1 was “This gadget is useful for the improvement of teaching-learning process”. Out of a total of 712 respondents, 312 respondents provided 10 points to this statement. It means that 42.4% respondents totally agreed with this statement. They found this gadget to be a useful one for the improvement of teaching-learning process. On an average, this statement got 8.76 point out of 10. Only two high school students, two higher secondary students, and 4 diploma students rated the product as less than 5 point without providing any reason. The response to this statement should be interpreted with caution as this statement related to pedagogical aspect of the gadget. Usually the respondents participating in the survey have a friendly attitude towards the pedagogical gadget and its designer and tend to give positive feedbacks and comments. However, authors could gauge the enthusiasm of the participants during hands-on practices and accordingly assessed the worth of the pedagogical gadget. In this case, participants showed great interest and enthusiasm towards team-work (working in a group of 3), thus affirming that gadget can be indeed useful as a pedagogical tool.

6.4.2 Response to Statement 2

Statement 2 was “I did not carry out this type of experiment before”. Overall, 278 respondents entered 10 points for this statement. It means that 39.04% respondents totally agreed with statement 2. On an average, this statement earned 8.28 point out of 10. Among all the teachers participated in survey, only 12 out of 33 had carried out similar experiments. Only 4 out of 150 high school students and 19 out of 152 higher secondary students did not agree with this statement. Among the graduation level, diploma level, and post-graduate level students, about 14.9%, 12.1%, and 23.6% students had rated the statement below 5. This indicates huge potential to introduce such type of pedagogical gadgets in the science education curriculum.

6.4.3 Response to Statement 3 and 4

Statement 3 was “I learnt something new from it” and Statement 4 was “It is an effective way of learning these basic concepts”. A total of 36.7% participants responded that they had totally agreed with statement 3 i.e., they had learnt something new from this pedagogical approach. On an average, statement 3 got 8.67 point out of 10. Most of the high school and higher secondary students mentioned about their interest in experiments related to the black body radiation and concept of specific heat. Undergraduate and post-graduate students were also

amazed with the fact that time required for heating equal amount of aluminium but of different dimension was different. Some of the post-graduate students shared the idea of pedagogical approach related to their research work to make it easily understandable and attractive to undergraduate students. Total 80.9% of the respondents totally agreed with the statement 4 by giving 10 point in the rating scale. Students and teachers showed their satisfaction for learning the basic concepts of heat transfer experimentally using this gadget as a pedagogical tool. On an average, statement 4 got 9.36 point. The feedback indicated the gadget as effective one for learning basic heat transfer concepts by improving student-instructor engagement level.

6.4.4 Response to Statement 5 and Questions 6 and 7

Statement 5 was "Other similar types of pedagogical gadgets should be made". Following two questions were asked:

Question 6: Have you come across this type of pedagogical gadgets before?

Question 7: Any suggestions for further modifications of this gadget?

Overall 84.7% respondents totally agreed with the statement 5. This statement earned 9.36 point on an average. However, high school and higher secondary level students gave more 10 points on rating scale as compared to undergraduate and post-graduate students. Maximum number of respondents wanted the authors to develop similar type of other pedagogical gadgets for better understanding of science and engineering education. An 87.4% of total respondents agreed that they did not use this type of pedagogical gadgets in their teaching-learning processes. Hence, it is concluded that there is sufficient originality in the developed gadget. However, very few participants provided any useful suggestions. Only teachers and post-graduate students could provide some useful suggestions. One suggestion was regarding enhancing the safety; it may be of concern to very small children, not for high school and onwards level students. For younger children, the maximum temperature can easily be limited to 35 ºC. Other two suggestions were replacing the glass thermometer with a digital thermometer and use of glass instead of wood in one side of the box for better visualization of interior of the box. Responses for Statement 5, Questions 6 and 7 showed the necessity of design and modification of such pedagogical gadget for the improvement of teaching-learning process.

6.4.5 Response of Teachers to MCQ

Teachers were asked to provide response to following MCQ: This gadget is suitable for (a) High school students, (b) Higher secondary students, and (c) Undergraduate engineering and science students. They could choose more than two options. Among all the teachers (from high school, higher secondary, diploma, and undergraduate levels) who responded to this question, 30% teachers felt that this product is suitable for undergraduate students. On the other hand, 80% of all the teachers felt that it can be useful for higher secondary level students and 90% felt that it can be useful for high school level students. In contrast to it, all undergraduate students felt that this product can be useful for them in the learning process. This brings out the difference in the perception of teachers and students. In this case, need for this type of pedagogical gadget was overlooked to some extent by the teachers; however, the undergraduate students strongly recommended its use in their learning process.

6.5 Educational Assessment Based on Test

To check the effectiveness of the pedagogical gadget for learning outcomes, a written test was conducted among the newly graduated engineering students. These students were doing preparation for a graduate aptitude test in engineering, which include the topics from heat transfer. Students had studied the subject during their B.Tech. Program as a full course of 3 one-hour lecture per week (total 42 lectures). Students were divided in two groups with 6 students in each group. In one group, heat transfer was taught by providing the theoretical study material while the other group was provided with additional hands-on experiment in the pedagogical gadget along with the study material. Questions based on the concepts, viz., lumped capacitance method, Biot number, calculation of cooling time were asked in the test. It was observed that students provided with only theoretical study material scored less marks than the students exposed to hands-on experiential learning. Out of 20 marks, students with the pedagogical gadget scored an average mark of 16 with a standard deviation of 2.19 marks while the student from other group scored 11.83 mark on an average with a standard deviation of 2.93 marks.

It is clear that the students exposed to pedagogical gadgets scored better in an average sense. A test of significance was also conducted. For this purpose, a null hypothesis is made: “There is no impact of the pedagogical gadget”. The alternative hypothesis is “The pedagogical

gadget improves the average test score". The test statistic is calculated using the following formula:

$$t = \frac{\bar{x} - \bar{y}}{s\sqrt{\frac{1}{n_1} + \frac{1}{n_2}}}, \tag{6.8}$$

where $\bar{x}$ is the average mark of first group, i.e., 16 and $\bar{y}$ is the average mark of second group, i.e., 11.83. In both the groups, the sample size is 6, i.e., n_1=n_2=6. The parameter s is computed from the following equation:

$$s^2 = \frac{(n_1 - 1)s_1^2 + (n_2 - 1)s_2^2}{n_1 + n_2 - 2}, \tag{6.9}$$

where s_1 and s_2 are the sample standard deviations, 2.19 and 2.93, respectively; the denominator is degree of freedom. This provides a student's t value of 2.79. From the table of one-tailed critical values of t, for degree of freedom equal to 10, at 1% level of significance, the critical value is 2.764 (Mendenhall et al., 2009). As the obtained t value is more than the critical value, the null hypothesis is rejected. Thus, it can be said with 99% confidence that pedagogical gadget improves learning. This educational assessment shows the importance of hands-on activities using pedagogical gadget for better learning of heat transfer concepts.

6.6 Conclusion

In this chapter, a pedagogical gadget was designed and its effectiveness for providing a better teaching-learning was assessed through a survey. Considering the survey results as well as the enthusiasm shown by the participants towards engagement with experiential learning using the gadget, it is concluded that this gadget can be quite successful in enhancing the interest of engineering students in heat transfer. Further, it can motivate school students to learn mechanical engineering. Educational assessment was also carried out by conducting a test among newly graduated students. On an average, students exposed to hands-on experiential learning scored more marks than students without hands-on experience.

Standard branded laboratory instruments make the experimental study monotonous and boring. On the other hand, this gadget is more amenable to carry out a number of hands-on activities and add several innovative experiments. In the process of conducting survey, it was

realized that learning is more enjoyable and effective if experimental gadgets have some imperfection because student learn from errors. For example, in the estimation of specific heat capacity of solid, freedom was provided to students in choosing the samples. In the process, they learnt the importance of Biot number in the applicability of lumped capacitance method. Also, being simple, inexpensive, and portable, gadget looked like a toy, which attracted the interest of the students towards experimental field. In future, it is planned to develop similar other pedagogical gadgets. As a part of outreach activate and for disseminating the knowledge, some institutes were given offer to purchase the gadget. Total twelve numbers of gadgets were procured by technical institutes. Institutes were also provided with a video demonstrating the experiments. The faculty members showed their satisfaction with the gadgets. Feedback from the learners is awaited.

Chapter 7

Artificial Ageing of Rice Using a Sterilization Box Equipped with Infrared Heating and Ultraviolet-C Radiation

7.1 Introduction

Rice (*Oryza sativa*) is a principal food for the majority of the world's population, and it is consumed in many parts of the world. It is a major source of carbohydrates and also has various other macromolecules like proteins and fats, apart from minerals, vitamins as well as phytochemicals (Vici et al., 2021). It supplies 35–60% of the calories consumed by three billion people in Asian nations (Omar et al., 2016). India is the second largest producer and consumer of rice after China. Over 60% of the Indian population depends on rice as a staple food, making it the most significant crop (Chatterjee and Das, 2019). Rice is mainly used for consumption after hydrothermal cooking. Raw rice is also used as an important ingredient in many processed foods around the world. The continuous usage requires the storage of rice after production. Assam is one of the principal states in the country associated with rice growing and consumption. Bahadur and Ranjit are the two popular varieties of rice produced in the state (Gautam et al., 2018).

Storage of rice affects cooking and eating qualities due to changes in nutritional contents and physical properties. These changes in the properties of rice during storage are commonly termed as ageing (Keawpeng and Venkatachalam, 2015). Ageing takes place from pre-harvest to consumption of rice. Changes occurring in rice grain affect the milling, cooking, and eating values of rice. Monitoring the changes in physical properties, nutrient contents, milling quality, and cooking quality of rice due to ageing were reported. Saikrishna et al. (2018) reported the beneficial changes in cooking, physicochemical, sensory as well as pasting properties during ageing of rice, which further led to higher economic value along with customer preferences. Excluding moisture content, no significant changes in chemical composition of one year stored milled rice and freshly milled rice were observed (Thanompolkrung et al., 2017).

Ageing can be carried out by both natural and artificial means. Natural ageing is a slow process. It requires more storehouse space as well as higher maintenance and operational costs. Several biotic factors (for example, fungi, insects, rodents, and birds) and abiotic factors (for example, temperature, moisture content, and relative humidity) affect the quality of rice during the longer storage period (Moses et al., 2015). Careful monitoring as well as an appropriate safe storage environment for a longer period (3–6 months) are the two essential requirements for the natural ageing of rice, which could be quite unmanageable sometimes. Another way of ageing is artificial ageing, also known as accelerated ageing of rice. It causes the physicochemical changes in rice in a shorter time period, providing cooking properties comparable to naturally aged rice (Gujral and Kumar, 2003). Artificial ageing can be carried out in many ways e.g., (1) drying cum curing, (2) hydrothermal treatment, (3) thermal treatment, (4) microwave (MW) treatment, and (5) heat treatment by radiofrequency (Saikrishna et al., 2018).

In drying cum curing, paddy was dried by roasting with sand at 95–155 ºC for 1 to 1.5 min followed by tempering in a metal bin for 1.5 to 2 h and finally air cooled (Srinivas et al., 1981). In hydrothermal treatment, freshly harvested paddy was preconditioned for 24 h in a refrigerator for moisture balance. Conditioned paddy was steamed at atmospheric pressure in an autoclave for 30 min, followed by drying in shade to 9–11% of moisture content (Gujral and Kumar, 2003). In thermal treatment, fresh paddy was thermally treated at 90–100 ºC in an oven for a few (1 to 9) h (Faruq et al., 2003). In the case of microwave treatment, microwave radiation of frequency 2450 MHz was used on harvested rice at 60, 70, and 80 ºC for 0, 1, and 3 min. Treated rice was dried and stored at 40 ºC in airtight K-coated nylon polyethylene film bags for six months (Nguyen and Goto, 2009). In radiofrequency heat treatment, fresh paddy was exposed to a radiofrequency generator operated at 17.12 MHz frequency and 70–85 ºC temperatures for 5, 10, and 15 min (Vearasilp et al., 2011).

In this chapter, a sterilization box equipped with both IR lamp and UV-C lamp was used for artificial ageing of rice. For performance study, synergistic effect of IR radiation heating and UV-C irradiation over artificial ageing of Ranjit rice was investigated. A conceptual design of an artificial ageing box is also presented in this chapter. Artificial ageing of rice was carried out using IR radiation heating at 70 ℃ for 1, 3, 5, and 7 h simultaneously combined with UV-C irradiation. This work accomplished simple, cost-effective, easy to

handle, energy efficient, and rapid artificial ageing as well as surface disinfection of rice. Kernel expansion and water uptake (WU) were measured to investigate the cooking quality of the treated rice. Nutrient value (starch, protein, and fat) as well as moisture contents after ageing were investigated. Fourier Transform Infrared Spectroscopy (FTIR) analysis was carried out to check the presence of starch in naturally as well as artificially aged rice sample. Microscopic evaluation was carried out to investigate the structures of starch granules. Surface decontamination of Ranjit rice using IR radiation heating and UV-C irradiation was also tested for antimicrobial activity.

7.2 Previous Work on Improvement of Food Quality by Irradiation Technology

Irradiation technology was used for the improvement of rice quality and other physio-chemical properties. Irradiation is an environment friendly, efficient, energy saving, and easy to control post-harvest treatment. Irradiation is beneficial to maintain product quality with an increase in nutritional value, against microbiological degradation without using any chemicals (Indiarto and Nurannisa, 2021; Indiarto and Qonit, 2020). There are two types of radiation— ionizing radiation (viz., x-rays, gamma rays) and non-ionizing radiation (viz., ultraviolet (UV), infrared (IR), radio waves) (Indiarto and Qonit, 2020). UV type-C (UV-C) rays (200–280 nm wavelength) are non-ionizing radiation with the ability to alter genetic material in cells, making them effective in inactivating a wide range of microbial pathogens such as bacteria, viruses, fungi, and yeasts.

Applications of UV radiation in disinfecting water, milk and dairy products, shelf life improvement of fresh products, and processing of solid as well as liquid foods were reported (Singh et al., 2021a). Moreover, the effectiveness of UV-C irradiation on different beverages viz., tender coconut water (Gautam et al., 2017), cranberry-flavored water (Gopisetty et al., 2019), melon juice, orange-carrot juice, orange-tangerine juice (Fenoglio et al., 2020), isotonic sports drinks made from orange or orange-strawberry-mango-kiwi-banana-lemon juice, (Kozono et al., 2023) and green juice blends for microbial inactivation was reported (Biancaniello et al., 2018). Further, Ferreira et al. (2021) evaluated the effect of UV-C radiation in brown, red as well as black rice during six months of storage and reported the effectiveness of UV-C radiation for the fungal decontamination and photodegradation of mycotoxins without

affecting color and cooking properties. Similar to UV radiation, the effectiveness of IR radiation heating to inactivate spores, bacteria, mold, and yeast in solid as well as liquid food was reported (Aboud et al., 2019). Complete mortality of regularly found insects in rice using IR heating was reported in the temperature range of 65–70 ℃ (Pan et al., 2008). IR radiation heating was used to investigate milling quality, drying characteristics as well as disinfestation effectiveness of rough rice. IR heating resulted in a quick removal of moisture due to fast and uniform heating (Pan et al., 2008). Using IR radiation heating, rough rice was heated to a temperature range of 35.9–71.4 ℃ and the drying characteristics as well as the milling quality of rice were investigated. Rapid IR heating to 60 ℃ followed by tempering and slow cooling resulted in higher milling quality of rice as well as rapid removal of moisture due to its high heating rate (Khir et al., 2007). Moisture removal characteristic was studied using IR heating on thin layered rough rice; an increase in moisture removal as well as rice temperature with an increase in heating time and intensity of radiation was observed (Khir et al., 2014). Ding et al. (2015) recommended IR heating to 60 ℃ followed by tempering and natural cooling for higher moisture removal rate, milling quality, heating rate, moisture diffusivity as well as storage lives for both brown rice and rough rice. The cooking, color, texture gelatinization, microstructure, and pasting properties of stored brown rice were all improved by IR heating method with excellent drying as well as heating efficiencies (Ding et al., 2018). Ratseewo et al. (2022) reported both positive as well negative impacts of far-IR (FIR) treatment of normal rice and pigmented rice. Increase in total phenolic, anthocyanin, flavonoid contents as well as antioxidant activity, were reported as positive impacts of FIR treatment. In addition, negative impacts viz., reduction in rutin and sinapic acid contents were reported. Higher heat transfer rate, fast drying by instant heating due to direct heat penetration, higher energy efficiency, simplicity as well as compactness of the equipment, easy process control, and superior product quality with less chances of flavor losses are the advantages of IR heating (Khir et al., 2014; Yadav et al., 2020). The synergistic effect of IR radiation heating and UV irradiation was reported to inhibit the growth of mold and yeast, resulting in reduced number of damaged fig fruits (Hamanaka et al., 2011).

7.3 Performance Study of the Sterilization Box

To carry out the performance study, synergistic effect of IR heating and UV-C radiation over artificial ageing of Ranjit rice was examined. Kernel expansion, water uptake (WU), moisture content removal, and nutrient value (starch, protein, and fat) of the rice were investigated. Surface decontamination of the treated rice using IR radiation heating and UV-C irradiation was also investigated for antimicrobial activity.

7.3.1 Materials and Methods

Bovine serum albumin (BSA, A2153) and Bicinchoninic acid assay (BCA Assay kit, QPBCA) were procured from Sigma Aldrich, (St Louis, USA). Other chemicals viz., Sulphuric acid (11760L8M50), Hexane (20749LC250) and Methanol (66930LM250) were procured from Finar, Ahmedabad, India. Phenol (CDH Laboratory, 029477, Kanpur, India), HCl (Sigma Aldrich, 320331, St Louis, USA), NaOH (Himedia, GRM-467 500MG, Thane, India) and milli-Q water of resistivity 18 MΩ-cm at 25 °C were used. The media Nutrient broth (NB, M002), Potato dextrose agar (PDA, MH096-500G) and Yeast extract powder (RM027-500G) were procured from Himedia (Thane, India).

7.3.2 Raw Materials

Freshly harvested rice kernels, used within 60 days were considered as non-aged kernels and kernels kept at room temperature (25 ºC to 28 ºC) for twelve months were considered as naturally aged kernels (Faruq et al., 2015). Freshly harvested Ranjit rice was purchased from the local cultivator in Assam, India. One-year old (naturally aged) Ranjit rice was also collected as a control. The rice samples were kept in an air-tight glass container for carrying out the experiments.

7.3.3 Artificial Ageing Using Sterilization Box

Each sample was treated at a predefined temperature and time in the sterilization boxes designed in chapter 3 and chapter 4. Two heating methods viz., IR radiation and incandescent bulb were applied separately for artificial ageing. In addition, UV-C irradiation was applied for the disinfection. Samples to be aged were kept at a distance of 10 cm from the heating source and 8 cm from the UV-C source in the case of both sterilization boxes. Kernels treated at 70 ºC for four different time durations (1, 3, 5, and 7 h) were considered as artificially aged

kernels. The aged samples were kept for 60 min at room temperature to be cooled down and used for different experiments. The power density of IR irradiation was estimated as 3.18 × 10^4 W/m^2 as discussed in chapter 4. Further, UV-C dose was calculated as 49.24 J/cm^2-h using Eq. 4.1.

7.3.4 Moisture Removal with IR and Incandescent Heating Methods

Using IR radiation heating, a high rate of rice drying could be achieved by spreading the rice in a thin layer (Khir et al., 2014). Samples of 60 gm were kept at a distance of 10 cm from the heating source (IR or incandescent bulb) in the sterilization boxes at 70 °C for 1, 3, 5, and 7 h in the presence of UV-C irradiation. The treated samples were cooled at room temperature for 60 min and weighed. The loss of weight in the rice kernels due to heating revealed the removal of moisture content (Talpur et al., 2011) as follows:

$$\text{Moisture removal}\,(\%) = \frac{W_i - W_f}{W_i} \times 100\%, \tag{7.1}$$

where W_i and W_f denote weights of untreated and heated rice kernels, respectively.

7.3.5 Measurement of Kernel Expansion

Ten rice kernels from each group viz., non-aged, naturally aged and artificially aged were randomly selected. The initial length and breadth of rice kernels were calculated using a stainless hardened Vernier caliper (make: Mitutoyo, Japan) with the least count of 0.02 mm. The kernels were soaked with 5 mL of water in a 20 mL glass test tube for 20 min (Faruq et al., 2015). The test tubes with soaked rice kernels were submerged in a boiling water bath for 20 min. Boiled rice kernels were kept in a petri dish at ambient temperature for 50 min to remove the extra surface moisture. The final length and breadth of boiled rice kernels were calculated using the same Vernier caliper. Proportionate change (PC) was calculated as follows (Faruq et al., 2015):

$$\text{PC} = \frac{\left(\frac{L_f}{B_f} - \frac{L_i}{B_i}\right)}{\frac{L_i}{B_i}}, \tag{7.2}$$

where L_i and B_i denote the length and breadth of rice kernel before cooking, respectively, and L_f and B_f denote the length and breadth of rice kernel after cooking, respectively. Elongation ratio (ER) and actual elongation (AE) were calculated as (Faruq et al., 2015; Faruq et al., 2003)

$$\mathrm{ER} = \frac{L_c}{L_r}, \tag{7.3}$$

$$\mathrm{AE} = L_c - L_r, \tag{7.4}$$

where L_c and L_r denote the average length of cooked kernels and average length of raw kernels, respectively.

7.3.6 Measurement of Water Uptake (WU)

Twenty rice kernels were randomly selected from each group viz., non-aged, naturally aged and artificially aged rice samples. Rice kernels were cooked in a glass test tube as discussed in Section 7.3.5. The cooked kernels were placed on filter paper to remove the surface water. The WU (%) was calculated as follows (Faruq et al., 2015):

$$\mathrm{WU}\,(\%) = \frac{W_c - W_{uc}}{W_{uc}} \times 100, \tag{7.5}$$

where W_c and W_{uc} denote the weight of twenty cooked and uncooked rice kernels, respectively.

7.3.7 Estimation of Starch Content

Phenol-sulphuric acid method was employed to estimate starch content. This colorimetric method is the most used method for the analysis of carbohydrate content in an aqueous solution (Quero-Jiménez et al., 2019; McCleary et al., 2020). In this method, carbohydrate is dehydrated by reacting with concentrated sulphuric acid, producing furfural derivatives. These furfural derivatives further react with phenol and develop an orange-golden hue, the absorbance of which can be measured at 490 nm. Ground rice of 25 mg was taken from each rice group, viz., non-aged, naturally aged, and artificially aged rice samples. Absolute ethanol and distilled water were used to wet the ground rice samples followed by the addition of hot ethanol which was heated in a hot plate through boiling water. It was then mixed using a vortex and was centrifuged at 2000 g for 10 min to separate the supernatant and sediment. This collected sediment was then used for the analysis of starch. To the sediment, 1 N HCl solution was added and incubated it at 95 °C for 45 min. Then, the mixture was centrifuged at 2000 g to separate the supernatant and sediment. The supernatant was diluted appropriately and 1 ml sample was taken. To this, 0.5 mL, 5% phenol was added, followed by mixing. Finally, 2.5 mL of

concentrated sulphuric acid was added and left at room temperature for 10 min. Absorbance was measured at 490 nm using a multi-plate reader (infinite 200 PRO, Tecan).

Starch content was determined using the following expression,

$$\text{Starch}\,(\%, \text{wet basis}) = 100 \times \frac{(A - I) \times DF \times V \times 0.9}{B \times W}, \tag{7.6}$$

where A is the absorbance, DF is the dilution factor, V is the volume in mL, W is the initial weight of the ground rice sample in mg and I and B are the intercept and slope of the standard curve in mL/µg, respectively.

7.3.8 FTIR analysis of Starch

Fourier transform infrared spectroscopy (FTIR) was performed to confirm the presence of functional groups using an IR spectrophotometer (Shimadzu IR Affinity S1) in attenuated total reflectance (ATR) mode. The sample of 10 µl was placed upon the ZnSe crystal and the spectra were collected in the range 400–3000 cm^{-1} at ambient condition. A total of 64 scans and a 4 cm^{-1} resolution were set for the experiment (Sharma and Pandey, 2021b).

7.3.9 Estimation of Protein Content

The protein content in the rice was determined using the NaOH extraction method (Sadaiah et al., 2018). Alkali solution has the ability to solubilize rice proteins effectively by breaking the amide, hydrogen as well as disulfide bonds in proteins (Fabian and Ju, 2011). The rigid structure of rice starch becomes loose in highly alkaline conditions due to the interaction between rice and alkali, leading to the dissolving of covered protein in starch from rice particles (Cai et al., 2023). Moisture free, dried rice sample was ground properly to powder. Powdered rice of 25 mg was taken separately from each rice groups, viz., non-aged, naturally aged and the artificially aged rice samples. To wet the rice sample, ethanol was added and subsequently, 4.5 mL of 1 N NaOH was added to the mixture, followed by incubation in hot water bath at 95 °C for 15 min for the total dissolution of the sample. Sample was then cooled at room temperature and protein content was determined using BCA assay. It is a colorimetric Cu based protein quantification assay. In a basic solution condition, BCA forms a Cu^{2+} protein complex and then gets reduced to Cu^{+}. The amount of reduction in Cu^{2+} is proportional to the presence of protein content in the solution. Thus, BCA chelate of each Cu^{+} ion resulting in the change of green color to purple color, which strongly absorbs the light at 562 nm (Otieno et al., 2016).

BSA at different concentrations was used for plotting the standard curve graph (Hasan et al., 2018b).

7.3.10 Estimation of Fat Content

To determine the fat content, soxhlet extraction method was carried out using hexane and methanol sequentially for 12 h to remove the fats from each of the three different rice groups, viz., non-aged, naturally aged and artificially aged rice (Hewavitharana et al., 2020; Sowbhagya and Bhattacharya, 1971). For the extraction process, 5 gm of powdered rice was placed in the thimble and 400 mL solvent was placed in the round bottom flask, which was heated over the mantle. After extraction, the samples were filtered through Whatman filter paper, and the solvent was removed properly through a rotary evaporator. After removing the final solvent, the dried fats were weighed by subtracting the weight of the initial round bottom flask from the one containing the dried fats.

7.3.11 Scanning Electron Microscopy

In this work, microscopic evaluation was carried out to analyze the change in the microstructure of rice grain due to artificial ageing using IR radiation heat and UV-C irradiation. The non-aged, naturally aged and artificially aged rice were washed properly with distilled water followed by washing with ethanol (100%). Washed rice kernels were dried at 50 °C as described by Shih et al. (2014). Field emission scanning electron microscopy (FESEM) (model Sigma, make Zeiss) was used to investigate the effect of artificial ageing on the microstructure of Ranjit rice.

7.3.12 Antimicrobial Effect of Combined IR Heat and UV-C Treatment Using Spread Plate Assay

The agar spread plate assay aimed to investigate the antibacterial effect of IR heating and UV-C irradiation over the surface of real rice samples. For this, 15 gm of naturally aged rice kernels were surface swabbed with a sterile cotton swab and incubated into 1 mL of the autoclaved Milli-Q water to suspend the bacteria. 100 µL of this suspension was spread-plated on sterile NB agar plates and incubated statically overnight at 37 °C. A similar study was performed using 15 gm of artificially aged rice. The bacterial growth (colony) for both cases was examined. For antifungal, PDA and yeast extract were used in the spread plate assay. A similar

procedure was followed as antibacterial activity and fungal growth on plates were examined after 3 days (Gaber et al., 2023; Mishra et al., 2023).

7.4 Results and Discussion

Removal of moisture content, kernel expansion, WU and nutritional values (starch, protein and fat) were investigated. Microscopic analysis and antimicrobial activity were also carried out. The detailed results are described in the following subsections.

7.4.1 Removal of Moisture Content

The experiment was carried out to analyze the moisture removal content in rice kernels for different intervals of time with two different types of heating methods viz., IR radiation heating and incandescent bulb heating. In the case of IR radiation heating, the results showed moisture removal of 3.15 ± 0.1%, 6.60 ± 0.06%, 8.09 ± 0.09% and 8.26 ± 0.14% in 1, 3, 5 and 7 h, respectively. The moisture removal using incandescent bulb heating was found to be relatively lower i.e. 2.84 ± 0.08%, 6.02 ± 0.08%, 7.12 ± 0.13% and 7.32 ± 0.17% in 1, 3, 5 and 7 h, respectively. Moreover, the time required to heat 60 gm of rice kernels from room temperature to 70 ℃ was 156 s and 311 s for IR radiation heating and incandescent bulb heating, respectively. The temperature of rice was measured by a thermometer, similar to Khir et al. (2007). IR radiation heating showed less time requirement to reach 70 ℃ as well as a higher percentage of moisture removal from the rice kernels due to its fast heating. Results showed the effectiveness of IR radiation heating over incandescent bulb heating for the removal of moisture content. Similar to this work, a surge in moisture removal of rice with an increase in heating time during IR radiation heating was reported (Khir et al., 2014). IR heating provides better results due to better penetration of heat. In further studies, artificial ageing using only IR radiation heating and UV-C irradiation was considered.

7.4.2 Measurement of Kernel Expansion

Kernel expansion of different groups of Ranjit rice viz., non-aged (freshly harvested), naturally aged, and artificially aged at 70 ℃ for different time periods (1, 3, 5, and 7 h) was studied. Table 7.1 shows the analysis of PC, ER, and AE of non-aged, naturally aged, and artificially aged Ranjit rice kernels. PC values were found to increase with time in the case of artificial ageing up to 5 h and further decreased at 7 h due to morphological changes as discussed in the microstructure analysis section. Artificial ageing for 5 h showed the highest value of PC as

0.21, followed by naturally aged (0.15) and non-aged (0.08). ER and AE values were also found to increase with time in the case of artificial ageing as listed in Table 7.1. The highest value of ER was calculated as 1.68 in the case of artificial ageing for 7 h, followed by naturally aged (1.54) and non-aged (1.42). A similar trend of PC as well as ER was reported for four Malaysian rice varieties (Mahsuri, NS 9192, Mahsuri Mutant and Putri), wherein the highest PC and ER values were observed for thermally treated artificially aged rice samples followed by naturally aged and non-aged (Faruq et al., 2003). In another study, an increase in ER value was reported in the case of sun-dried aged rice as compared to non-aged rice (Yerragopu and Palanimuthu, 2019). The highest AE value was calculated as 3.68 mm in artificial ageing for 7 h, followed by naturally aged (2.83 mm) and non-aged (2.26 mm). Similar positive impact of temperature in AE value of Malaysian rice varieties was reported (Faruq et al., 2003; Faruq et al., 2015). The results of PC, ER, and AE values revealed the effectiveness of artificial ageing over natural ageing using IR radiation heating. Therefore, cooking quality of Ranjit rice improved by artificial ageing using IR radiation heating.

Table 7.1 Analysis of PC, ER and AE of non-aged, naturally aged and artificially aged Ranjit rice kernel (*n*=10)

Rice type	PC	ER	AE (mm)
Non-aged	0.08	1.42	2.26
Naturally aged	0.15	1.54	2.83
Artificially aged for 1 h	0.12	1.54	2.96
Artificially aged for 3 h	0.15	1.56	2.99
Artificially aged for 5 h	0.21	1.60	3.24
Artificially aged for 7 h	0.18	1.68	3.68

7.4.3 Measurement of WU

WU is the measurement of the amount of water absorbed during cooking. A greater value of WU (%) due to boiling indicates good cooking quality of rice (Faruq et al., 2015). Figure 7.1 shows the analysis of WU (%) of non-aged, naturally aged, and artificially aged Ranjit rice kernels. In this investigation, artificially aged for 5 h showed the highest value of WU (%) as

89.62% followed by naturally aged (68.45%) and non-aged (59.93%). An increase in WU (%) from non-aged to naturally aged and the highest for artificially aged was reported for two Malaysian rice cultivars viz., Mahsuri and Puteri (Faruq et al., 2015). In another study, WU (%) was reported to be greater for a higher temperature (37 °C) storage of rice for 16 months compared to a lower temperature (4 °C) storage (Saikrishna et al., 2018). Improvement of cooking quality of Ranjit rice can be observed by increasing the WU (%) by artificial ageing using IR radiation heating. Results of artificial ageing for 5 h showed the best cooking quality of Ranjit rice. In further studies, artificial ageing at 70 °C using IR radiation heating and UV-C irradiation for 5 h was considered.

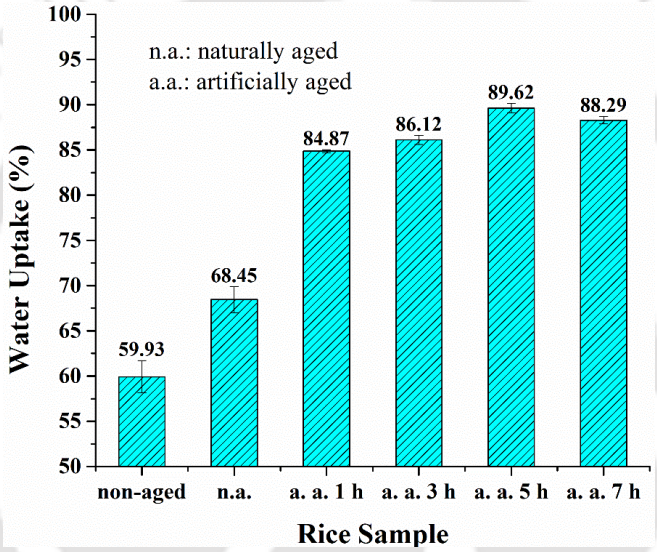

Figure 7.1 WU (%) of non-aged, naturally aged and artificially aged Ranjit rice

7.4.4 Starch Content

The starch content in the rice sample was analyzed using phenol-sulphuric acid. Starch content obtained from non-aged, naturally aged, and artificially aged rice samples were 67.55 ± 2.1%, 65.54 ± 1.79%, and 62.96 ± 0.66%, respectively. A similar value of starch content in the non-aged Ranjit rice was reported as 65.17 ± 0.27% (Chatterjee and Das, 2019). A slight decrease in total starch content after storage also agreed with the previous study (Peng et al., 2019). A decline in starch content and a simultaneous increase in amylose were reported during the storage of rice (Peng et al., 2019). From the investigation, it was observed that ageing caused a slight decrease in starch content. Moreover, the difference in starch content between natural ageing and artificial ageing was found to be less than 5%.

Figure 7.2 shows the FTIR analysis of naturally aged and artificially aged rice samples to validate the presence of starch. The fingerprint region of starch can be clearly observed in the region of 500–1500 cm^{-1} (Sharma et al., 2020). The characteristic peaks at around 865 cm^{-1} to 1120 cm^{-1} show the stretching of the O=C of the anhydrous glucose ring, and the peak at about 2820 cm^{-1} indicates the presence of C-H stretching. Moreover, peaks corresponding to the pyranose ring of glucose unit can be seen in the region below 800 cm^{-1} (Raungrusmee and Anal, 2019). FTIR spectra depicted the presence of similar structural elements of starch in both rice samples.

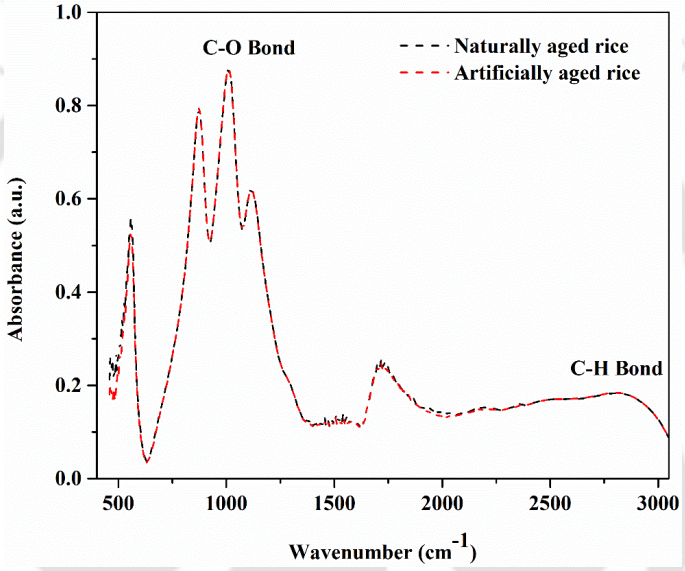

Figure 7.2 FTIR spectra of starch present in naturally aged and artificially aged rice sample

7.4.5 Protein and Fat Content

The protein content in the rice samples was extracted using alkali and further analyzed using BCA assay. The protein contents obtained using this method were found to be 2.25 ± 0.003%, 2.20 ± 0.004%, and 2.07 ± 0.004% from the non-aged, naturally aged, and artificially aged rice samples, respectively. The protein contents obtained from all the rice samples are shown graphically in Figure 7.3. A similar value of protein content in Ranjit rice was reported (Kalita et al., 2021). The results indicated no significant change in the total protein content before and after ageing (Peng et al., 2019).

The fat content was analyzed by the soxhlet method using two solvents for the efficient extraction of the fats from the rice grain. The fat contents measured were 1.97 ± 0.03%, 1.91

± 0.02%, and 1.84 ± 0.01% for the non-aged, naturally aged, and artificially aged rice samples, respectively. Figure 7.3 shows the fat content obtained from all the rice samples. The fat content obtained from Ranjit rice was similar to the reported data (Chatterjee and Das, 2019). Almost equal amount of fat was obtained from all three rice samples. The difference in fat contents in natural-aged and artificial-aged rice samples was less than 5%. In a previous study, Thanompolkrung et al. (2017) compared the chemical composition of freshly and one-year-aged milled rice; an insignificant difference was found, except for moisture content. These observations indicate that the nutritional values of the artificial-aged rice are comparable with natural-aged one, highlighting the practical utility of the designed box.

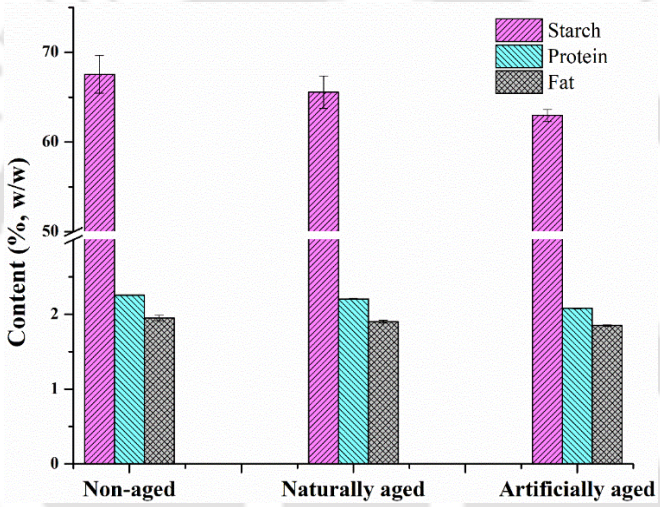

Figure 7.3 Starch, protein and fat contents obtained from non-aged, naturally aged and artificially aged rice samples

7.4.6 Microscopic Analysis

The microscopic evaluation of the non-aged, naturally aged, and artificially aged rice was carried out using FESEM. Figure 7.4 shows the whole (a, c, e; magnification factor: X125) and segments transverse sections (b, d, f; magnification factor: X5000) of the rice samples. Starch granules extracted from rice samples were found to be of size around 5 μm and polyhedral in shape, similar to the data reported by Ramos et al. (2019). In a separate study, Ding et al. (2015) carried out microscopic analyses of IR drying (IRD), hot air drying (HAD), and ambient air drying (AAD) rice grain to check the effect of IR heating on starch granules. No structural changes of starch granules were observed in IRD, HAD, and AAD rice grain, further indicated no adverse effect of IR heating on rice microstructure (Ding et al., 2015). In the present study, the structures of starch granules were also observed to be similar in all the rice samples, i.e.,

the non-aged, naturally aged, and artificially aged showing no significant differences. These findings suggest that the microstructure of the rice is unaffected by IR heating.

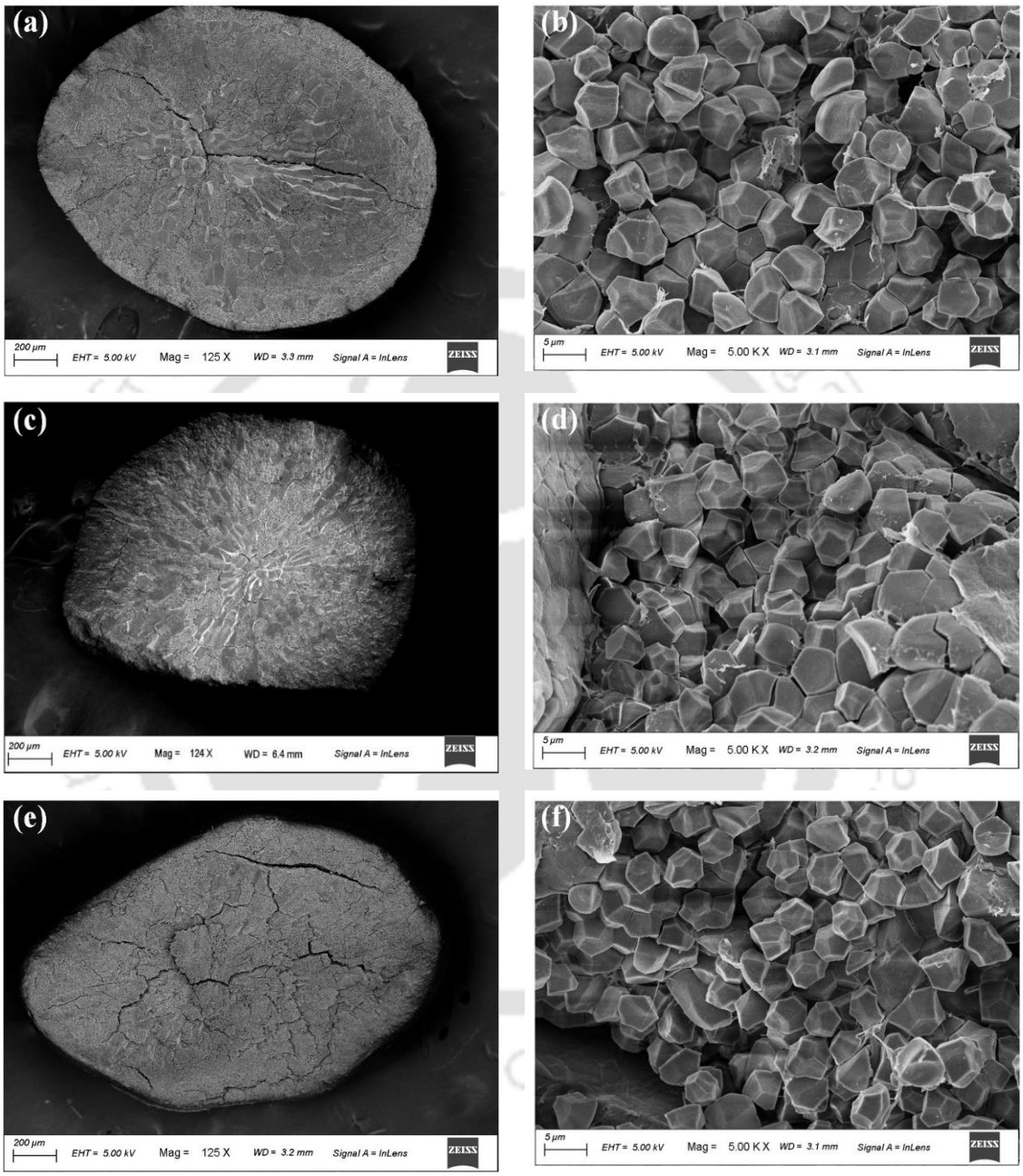

Figure 7.4 Microscopic evaluation of **(a, b)** non-aged, **(c, d)** naturally aged and **(e, f)** artificially aged rice for 5 h showing starch granules

7.4.7 Antimicrobial Effect of IR Radiation Heat and UV-C Irradiation Treatment on Rice

In this work, the antibacterial effect of IR radiation heating and UV-C irradiation over rice samples was examined by spread plate assay of isolated bacterial cells from the surface of 15 gm of each naturally aged and artificially aged (70 ℃ for 5 h) rice kernels. The spread samples were kept for overnight in undiluted conditions. No bacteria colonies were found in artificially aged rice as shown in Figure 7.5(a) and Figure 7.5(b). This indicated the bacterial disinfection ability of combined IR radiation heating and UV-C irradiation. The effectiveness of the combined IR heating and UV-C irradiation for the inactivation of microbial spores viz., *Aspergillus niger, Bacillus subtilis* as well as the killing of bacterial spores was reported (Hamanaka et al., 2011). Further, plates were checked for antifungal activity after 3 days of incubation. A significant decline in the number of fungal colonies was observed in the case of artificially aged rice as compared to that of naturally aged rice (Figure 7.5(c) and Figure 7.5(d)). These results show the potential of IR heating and UV-C for antimicrobial activity. In a previous study, a rice sample was sterilized by conduction heating rotary dryer, which was found to reduce the fungal mortality (Matouk et al., 2014). The surface of wheat (grain) was sterilized using UV radiation and a decrease in mold colonies with an increase in UV irradiation time was reported (Hidaka and Kubota, 2006). In another study, the heating of rice by IR radiation at 60 °C followed by tempering and slow cooling were suggested for drying and disinfestation of freshly harvested rice (Pan et al., 2008). The synergistic effect of incandescent bulb heating and UV-C irradiation at 70 ℃ for 15 min to sterilize day-to-day life items viz., belt, watch, and wallet with 100% antibacterial and antiviral efficiency has been reported chapter 3. In chapter 4, the combined effect of IR radiation heating and UV-C irradiation together at 65.61 °C for 13.54 min was reported to be effective for killing both Gram-positive (*S. aureus*) and Gram-negative (*S. typhi*) bacteria. These results suggest the effectiveness of artificial ageing at 70 ℃ for 5 h over natural ageing for decontamination of Ranjit rice. These observations demonstrated the potential of IR heating to decontaminate the surfaces of grains, fruits, and vegetables.

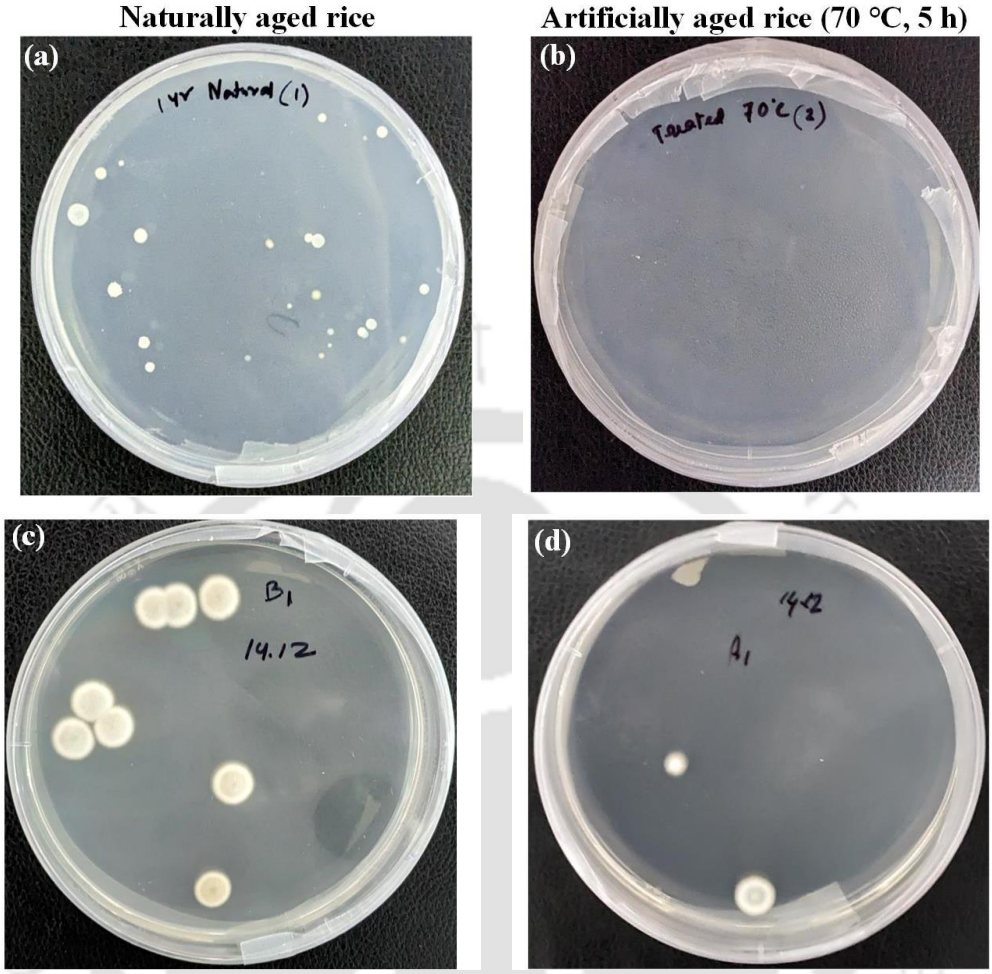

Figure 7.5 Bacterial culture of **(a)** naturally aged rice, **(b)** artificially aged rice by IR radiation heat and UV-C irradiation treatment at 70 ℃ for 5 h. Fungal culture of **(c)** naturally aged and **(d)** artificially aged rice. The samples were incubated in NB agar at 37 °C for 24 h for bacteria culture while PD agar media was used for fungal culture at 30 °C for 72 h

7.4.8 Comparison of Various Ageing Methods to Present Study Applied to Different Rice Varieties

Table 7.2 shows the various ageing methods applied to different types of rice varieties as well as their effects on rice quality. PC values of different rice samples treated with various artificial ageing methods varied from 0.13 to 0.90. Similarly, researchers reported AEs and ERs in the ranges of 3.3 mm to 8.5 mm and 1.06 to 2.3, respectively. For all the rice varieties, PCs, AEs and ERs got increased due to artificial ageing, similar to present work (Faruq et al., 2003; Faruq et al., 2015; Soponronnarit et al., 2008). An increase in WU (%) due to artificial ageing

was reported in this work, similarly reported by other researchers for differently aged rice samples (Gujral and Kumar, 2003; Faruq et al., 2015; Soponronnarit et al., 2008; Devraj et al., 2020). Moisture content removal (%) increased in the range of 0.7% to 11.2% in all the different varieties of rice due to artificial ageing (Vearasilp et al., 2011; Khir et al., 2007; Khir et al., 2014; Ding et al., 2015). Present work reported the range of moisture content removal as 2.72% to 8.52%, depending on the treating intervals. In addition, the artificially aged samples resulted in the antimicrobial properties. Thus, artificial ageing using both IR heating and UV-C irradiation could be an efficient ageing method with a faster heating rate and disinfection facilities. In addition, a preliminary sensory test was also conducted, which indicated a better experience of participants regarding taste and appearance in the case of artificially aged rice than naturally aged one (Appendix A).

Table 7.2 Effect of different ageing methods on the quality of various treated rice samples

Rice	Method of ageing	Treatment	Properties							Reference
			PC	AE (mm)	ER	WU	Moisture Removal	Protein (%)	Fat (%)	
IR-8	Hydrothermal treatment	Steamed for 30 min	NA	NA	NA	29.14% increase	NA	NA	NA	(Gujral and Kumar, 2003)
Sharbati			NA	NA	NA	41.18% increase	NA	NA	NA	
Govinda			NA	NA	NA	69.04% increase	NA	NA	NA	
Mahsuri	Thermal treatment	90–110 °C for 1–9 h	0.13–0.23	3.3–4.6	1.64–1.84	NA	NA	NA	NA	(Faruq et al., 2003)
Mahsuri Mutant			0.41–0.65	4.3–8.5	1.77–2.3	NA	NA	NA	NA	
NS9192			0.27–0.60	3.6–6.75	1.53–2.29	NA	NA	NA	NA	
Putri			0.34–0.90	3.8–8.1	1.61–2.08	NA	NA	NA	NA	
KDML105	Radiofrequency heat treatment (17.12 MHz)	70–85 ºC for 5–15 min	NA	NA	1.35–1.37	NA	11.2%	NA	NA	(Vearasilp et al., 2011)

M202	IR radiation drying	35.9–71.4 ℃ for 15–120 s	NA	NA	NA	NA	0.7–1.6%	NA	NA	(Khir et al., 2007)
Thin layer rough rice	IR radiation heating	35–70 ℃ for 30–120 s	NA	NA	NA	NA	1.5–2.5%	NA	NA	(Khir et al., 2014)
M206	IR radiation drying	60 ℃ followed by 4 h tempering and natural cooling	NA	NA	NA	NA	2.17%	NA	NA	(Ding et al., 2015)
Mahsuri	Thermal treatment	90–110 ℃ for 1–9 h	0.14–0.23	3–4.6	1.64–1.84	17.05–38.20%	NA	NA	NA	(Faruq et al., 2015)
Puteri			0.4–0.9	3.8–8.1	1.68–2.20	25.67–45.63%	NA	NA	NA	
Sana Masuri	MW treatment	950 and 1,400 W for 72 and 91 s	NA	NA	1.06–1.72	87.98–92.9%	NA	NA	NA	(Soponronnarit et al., 2008)
RNR-15048			NA	NA	1.06–1.8	88.11–92.89%	NA	NA	NA	

KDML 105	Hot air drying	130–150 ℃ for 30–120 min	NA	NA	1.68–1.85	331.04–402.5%	NA	NA	NA	(Devraj et al., 2020)
KDML 105	Thermal treatment	Air drying at 27 ℃	NA	NA	NA	NA	NA	7.68	0.40	(Thanompolkrung et al., 2017)
Ranjit	IR radiation heating and UV-C irradiation	70 ℃ for 5 h	0.08–0.21	2.26–3.68	1.42–1.68	59.93–89.62%	2.72–8.52%	2.07–2.25	1.84–1.97	Present study

7.5 Conceptual Design of an Artificial Ageing Box

An artificial ageing box with both IR heating and UV-C irradiation is conceptually designed. It was provided the same facility as the sterilization box used for artificial ageing of rice. It comprised a wooden box with four chambers, separated by plates. Plates were used for keeping rice in a spread-out manner. Each chamber comprised a 250 W IR lamp and two 11 W UV-C lamps. IR lamp was used for heating the rice and UV-C lamp was used for surface disinfection of rice. A Digital Temperature Controller (DTC) was used to measure and control the temperature inside the box, as discussed in chapter 3. A limit switch controlled covering door was used to prevent the direct exposure of UV-C light to the human skin as well as eye. High reflecting galvanized iron (GI) sheet was used to reduce the heat loss from the wooden box. Thin layer of air between the walls of the wooden box and GI sheet acted as thermal insulator. Moreover, inner layer of the GI sheet was covered with aluminium foil adhesive tape to increase the reflectivity of the GI sheet. Figure 7.6 shows the schematic diagram of the conceptually designed artificial ageing box.

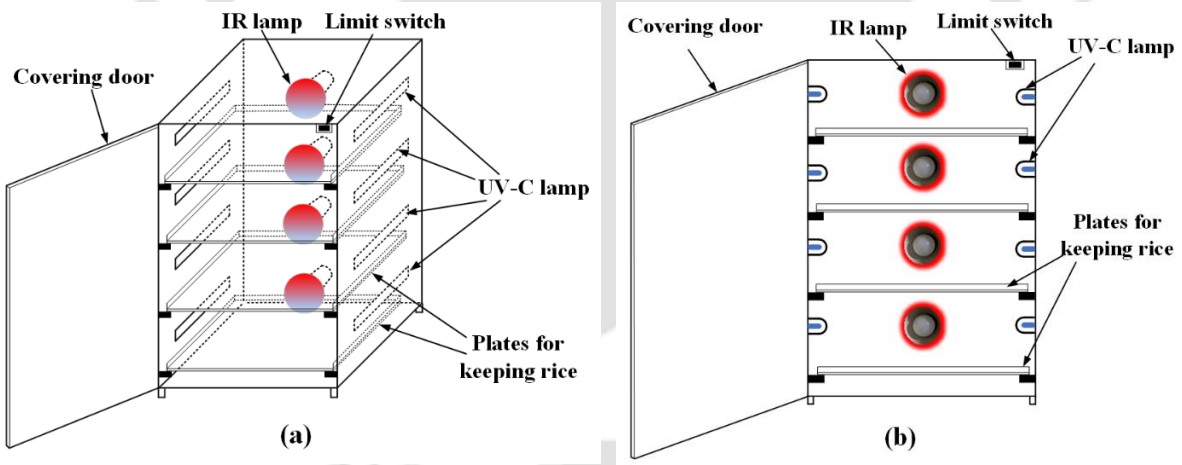

Figure 7.6 Schematic diagram of the artificial ageing box **(a)** isometric view and **(b)** front view

7.6 Conclusion

Artificial ageing of Ranjit rice was carried out by treating rice kernels at 70 ºC with UV-C irradiation for four different time durations (1, 3, 5, and 7 h). Two heating methods viz., IR radiation heating and incandescent bulb heating, were applied for the 70 ºC treatment of rice. IR radiation heating was more efficient than incandescent bulb heating for removing moisture content. Kernel expansion and WU were measured to investigate the cooking quality of rice.

Artificial ageing at 70 ºC using IR radiation heating and UV-C irradiation for 5 h showed the best cooking quality of rice. WU (%) was found to vary as artificially aged (89.62%) > naturally aged (68.45%) > non-aged (59.93%). Further, nutritional values were compared among the non-aged, naturally aged, and artificially aged rice samples, and no significant difference in starch, protein, and fat contents was observed between artificially aged and naturally aged rice. The microscopic evaluation using FESEM confirmed no adverse effect of IR radiation heating on the microstructure of rice. In addition, artificial ageing using IR heating and UV-C irradiation at 70 ℃ for 5 h was found to decontaminate the surface of Ranjit rice, as confirmed by spread plate assay. This aspect positively aids towards the disinfection of grains while storing aged rice. Thus, artificial ageing using IR heating and UV-C irradiation could be a cheap, fast and yet effective method without compromising the cooking quality and nutritional values. An artificial ageing box was also conceptually designed for ageing large amount of rice in one-shot. A detailed sensory test involving a representative number of consumers will be carried out in future research.

Chapter 8
Epilogue

8.1 Introduction

This thesis involves the process of conceptualizing, designing, and development of a product as well its adventure of integrating various engineering fields with creative vision, problem solving, and user-centric thinking. The extensive research explores the essence of a new product and its minimum viable products (MVPs) with different functionalities. A sterilization box with ultraviolet-C (UV-C) irradiation and incandescent bulb heating is designed. Its performance study over inactivation of coronavirus and bacteria is carried out. Unfolding of glycoprotein IgG confirms the inactivation of coronavirus as IgG is used as the model material in lieu of SARS-CoV-2. Moreover, its effectiveness to sterilize day-to-day life accessories is also investigated. Another sterilization box with infrared (IR) heating and UV-C facility is designed. For its performance assessment, broad-spectrum antibacterial activity as well as inactivation of coronavirus by unfolding SARS-CoV-2 spike protein are tested. Furthermore, N95 respirators are disinfected using the designed sterilization box to see the impact of heat and radiation on the functionalities. Fiber diameter, surface roughness (R_a), ultimate tensile strength (UTS), scratch resistance, and X-ray diffraction (XRD) of the fibers are studied. Another MVP, a pedagogical gadget is designed with heat-based sterilization box as the basis. Surveys and educational assessments are carried out to predict the pedagogical effectiveness of the gadget for providing a better teaching-learning environment among students as well as teachers. As a further application of the same technology, artificial ageing of Ranjit rice is carried out using a designed sterilization box to explore another application. Cooking qualities, microscopic evaluation as well as nutrient values (starch, protein, and fat) of artificially aged rice are compared with non-aged and one-year naturally aged rice. A preliminary sensory test is also conducted. Surface disinfection of rice confirms the antimicrobial activity of the sterilization box. To handle large amount of rice, an artificial ageing box is conceptually designed as another MVP. The overall conclusions of the thesis are discussed in the following section.

8.2 Overall Conclusions

The salient aspects of the present thesis are summarized as follows:

- A sterilization box equipped with incandescent bulb heating and UV-C irradiation facility was effective to fight against COVID-19. Incubation of heat and UV-C together at 70 °C for 15 min unfolds the glycoprotein (IgG) to a required extent as well as inactivate *E. coli*.
- Dry heat at 70 °C along with the UV-C incubation for 15 min was found to be a suitable condition to sterilize items of daily use with 100% antiviral and antibacterial efficiency.
- A sterilization box having IR heating and UV-C irradiation facility was sufficient to kill both Gram-positive (*S. aureus*) and Gram-negative (*S. typhi*) bacteria.
- Simultaneous IR heating and UV-C irradiation at 65.61 °C for 13.54 min was sufficient to unfold SARS-CoV-2 spike protein followed by inactivating the coronavirus.
- N95 FFRs were successfully disinfected using the designed sterilization box. Fibers treated with alcohol and UV-C irradiation became wider and rougher than the untreated fiber sample. Incandescent bulb heating, steam exposure, and combined incandescent bulb heating and UV-C irradiation made fiber thinner and smoother than the untreated sample. Smoother fibers make better respirator as micro-organism get less chance to hide in pores.
- Heat-based sterilization box was successfully transformed into a pedagogical gadget. Effectiveness of this gadget was assessed through a survey. In the process of conducting survey, it was realized that learning is more enjoyable and effective through hand-on experience using pedagogical gadget. Feedbacks from the students and teachers revealed the usefulness and necessity of such pedagogical gadget to attract students towards science education.
- Combined incandescent bulb heating and UV-C treatment caused less reduction in UTS than incandescent bulb heating and UV-C treatment alone. Moreover, combined incandescent bulb heating and UV-C treated samples were more scratch resistant than incandescent bulb heating and UV-C treated sample alone. Thus, combined incandescent bulb heating and UV-C irradiation disinfection showed the least degradation after 20 cycles.

- An efficient, inexpensive, and easy to handle artificial ageing combined with surface disinfection of rice was successfully accomplished using the designed sterilization box without compromising its cooking quality as well as nutrient value (starch, protein, and fat). The conceptually designed artificial ageing box can be used for artificial ageing of large amount rice.

Overall, a product with many variants has been developed. The variants are sterilization box, pedagogical gadget, and artificial ageing box. Core design and components remaining the same, each variant can be produced with minimal changes. This type of approach is helpful for operating an industry producing the variants.

8.3 Scope for Future Work

Based on the literature survey conducted and work carried out during this thesis, there are some possibilities for further exploration and investigation. Some of these are as follows:

- **Design and development of different sizes of sterilization boxes for various applications:** Considering the overall economy, sterilization boxes have to be sized according to the requirement. There is a requirement of sterilization boxes in homes, offices, hospitals, and market places. A pass-through type sterilization box with objects moving in a conveyor can be designed for processing large-sized objects. Overall, product design should consider the application. For large scale sterilization, there may be a requirement of chemicals also along with radiation. This aspect needs thorough investigation.
- **Artificial ageing of rice using sterilization box and its sensory test:** In this work, only limited study was carried out on the quality of artificial aged rice. Various attributes viz., glossiness, whiteness, looseness, hot-rice aroma, cold-rice aroma, sweetness, hardness, cohesiveness, stickiness, chewiness, and roughness can be studied. It is preferable that number of human subjects should be more than 100 with enough diversity in the samples.
- **Inactivation of spore forming bacteria viz., Bacillus and Clostridium, under the synergistic effects of UV-C irradiation and heat in the designed sterilization box:** Spores can survive extreme conditions, such as high temperature, alcohol, ultraviolet radiation, acidity, and nutrient deprivation. It is necessary to validate the instrument's

ability to eliminate spore-forming bacteria, by which it meets the necessary standards for commercialization to biomedical sectors.

- **Drying of various agricultural products using the designed sterilization box:** The sterilization box can be adopted for drying of various agricultural products with optimum heating cycle.
- **Development of solar powered sterilization box:** Solar energy can be used directly in place of the bulbs by properly concentrating the light. It can also be stored in batteries, which in turn can supply the energy to the bulbs used in this study. There is a requirement of a dedicated study in this area.
- **Computational analysis of heat transfers inside the designed sterilization box:** The designs presented here are based on the approximate analysis. A more rigorous study of heat transfer will help to optimize the products.

References

- Abdussamad, T.R., Rasco, B.A. and Sablani, S.S., 2016. Ultraviolet-C light sanitization of English cucumber (Cucumis sativus) packaged in polyethylene film. Journal of food Science, 81(6), E1419–E1430.
- Aboud, S.A., Altemimi, A.B., RS Al-HiIphy, A., Yi-Chen, L. and Cacciola, F., 2019. A comprehensive review on infrared heating applications in food processing. Molecules, 24(22), 4125.
- Abraham, J.P., Plourde, B.D. and Cheng, L., 2020. Using heat to kill SARS-CoV-2. Reviews in Medical Virology, 30(5), e2115.
- Aknyede, O.A., Mohan, R., Kelkar, A. and Sankar, J., 2010. Static and Dynamic Loading Behavior of Hybrid Epoxy Composite with Alumina Nanoparticles. In 16th International Conference on Composite Materials.
- Alarifi, I.M., 2021. Investigation into the Structural, Chemical and High Mechanical Reforms in B4C with Graphene Composite Material Substitution for Potential Shielding Frame Applications. Molecules, 26(7), 1921.
- Al-Sayah, M.H., 2020. Chemical disinfectants of COVID-19: an overview. Journal of Water and Health, 18(5), 843–848.
- Alonso, S., Kalinowski, M., Ferreira, B., Barbosa, S.D. and Lopes, H., 2023. A systematic mapping study and practitioner insights on the use of software engineering practices to develop MVPs. Information and Software Technology, 156, 107144.
- Anand, U., Jakhmola, S., Indari, O., Jha, H.C., Chen, Z.S., Tripathi, V. and Perez de la Lastra, J.M., 2021. Potential therapeutic targets and vaccine development for SARS-CoV-2/COVID-19 pandemic management: a review on the recent update. Frontiers in Immunology, 12, 658519.
- Arfat, M.Y., Ashraf, J.M., Arif, Z. and Alam, K. 2014. Fine characterization of glucosylated human IgG by biochemical and biophysical methods. International Journal of Biological Macromolecules, 69, 408–415.
- Ashraf, S., Sood, M., Bandral, J.D., Trilokia, M. and Manzoor, M., 2019. Food irradiation: A review. International Journal of Chemical Studies, 7(2), 131–136.

- Ato, T. and Wilkinson, W.J., 1986. Relationships between the availability and use of science equipment and attitudes to both science and sources of scientific information in Benue State, Nigeria. Research in Science and Technological Education, 4(1), 19–28.
- Aval, H.J., Serajzadeh, S. and Kokabi, A.H., 2012. Experimental and theoretical evaluations of thermal histories and residual stresses in dissimilar friction stir welding of AA5086-AA6061. The International Journal of Advanced Manufacturing Technology, 61(1), 149–160.
- Ayrilmis, N., Jarusombuti, S., Fueangvivat, V. and Bauchongkol, P., 2011. Effect of thermal-treatment of wood fibres on properties of flat-pressed wood plastic composites. Polymer Degradation and Stability, 96(5), 818–822.
- Babb, J.R., Bradley, C.R. and Ayliffe, G.A.J., 1980. Sporicidal activity of glutaraldehydes and hypochlorites and other factors influencing their selection for the treatment of medical equipment. Journal of Hospital Infection, 1(1), 63–75.
- Back, K.H., Kim, S.O., Park, K.H., Chung, M.S. and Kang, D.H., 2012. Spray method for recovery of heat-Injured Salmonella Typhimurium and Listeria monocytogenes. Journal of Food Protection, 75(10), 1867–1872.
- Baker, D., 2013. What works: Using curriculum and pedagogy to increase girls' interest and participation in science. Theory Into Practice, 52(1), 14–20.
- Baker, N., Williams, A.J., Tropsha, A. and Ekins, S., 2020. Repurposing quaternary ammonium compounds as potential treatments for COVID-19. Pharmaceutical Research, 37, 1–4.
- Banerjee, R., Roy, P., Das, S. and Paul, M.K., 2021. A hybrid model integrating warm heat and ultraviolet germicidal irradiation might efficiently disinfect respirators and personal protective equipment. American Journal of Infection Control, 49(3), 309–318.
- Bang, J., Kim, H., Kim, H., Beuchat, L.R. and Ryu, J.H., 2011. Combined effects of chlorine dioxide, drying, and dry heat treatments in inactivating microorganisms on radish seeds. Food Microbiology, 28(1), 114–118.

- Bari, M.L., Nei, D., Enomoto, K., Todoriki, S. and Kawamoto, S., 2009. Combination treatments for killing Escherichia coli O157: H7 on alfalfa, radish, broccoli, and mung bean seeds. Journal of Food Protection, 72(3), 631–636.
- Bergman, T.L., Lavine, A.S., Incropera, F.P. and DeWitt, D.P., 2011. Introduction to heat transfer. 6th ed., Hoboken: John Wiley and Sons, 280–285.
- Bharti, B., Li, H., Ren, Z., Zhu, R. and Zhu, Z., 2022. Recent advances in sterilization and disinfection technology: A review. Chemosphere, 136404.
- Biancaniello, M., Popović, V., Fernandez-Avila, C., Ros-Polski, V. and Koutchma, T., 2018. Feasibility of a novel industrial-scale treatment of green cold-pressed juices by UV-C light exposure. Beverages, 4(2), 29.
- Billard, A., 2003. Robota: Clever toy and educational tool. Robotics and Autonomous Systems, 42(3–4), 259–269.
- Blanchard, E.L., Lawrence, J.D., Noble, J.A., Xu, M., Joo, T., Ng, N.L., Schmidt, B.E., Santangelo, P.J. and Finn, M.G., 2020. Enveloped virus inactivation on personal protective equipment by exposure to ozone. MedRxiv.
- Block, S.S. ed., 2001. Disinfection, sterilization, and preservation. Lippincott Williams and Wilkins.
- Bopp, N.E., Bouyer, D.H., Gibbs, C.M., Nichols, J.E., Ntiforo, C.A. and Grimaldo, M.A., 2020. Multicycle autoclave decontamination of N95 filtering facepiece respirators. Applied Biosafety, 25(3), 150–156.
- Boudam, M.K. and Moisan, M., 2010. Synergy effect of heat and UV photons on bacterial-spore inactivation in an N2–O2 plasma-afterglow sterilizer. Journal of Physics D: Applied Physics, 43(29), 295202.
- Cadnum, J.L., Li, D.F., Jones, L.D., Redmond, S.N., Pearlmutter, B., Wilson, B.M. and Donskey, C.J., 2020. Evaluation of ultraviolet-C Light for rapid decontamination of airport security bins in the era of SARS-CoV-2. Pathogens and Immunity, 5(1), 133.
- Cai, Y., Li, Q., Li, D., Sun, C., Bao, Y., Li, F. and Jiang, S., 2023. Optimizing the extraction of protein from broken rice using response surface methodology and comparing the protein functional properties. Journal of Cereal Science, 113, 103726.

- Calderón-Miranda, M.L., Barbosa-Cánovas, G.V. and Swanson, B.G., 1999. Transmission electron microscopy of Listeria innocua treated by pulsed electric fields and nisin in skimmed milk. International Journal of Food Microbiology, 51(1), 31–38.
- Campos, R.K., Jin, J., Rafael, G.H., Zhao, M., Liao, L., Simmons, G., Chu, S., Weaver, S.C., Chiu, W. and Cui, Y., 2020. Decontamination of SARS-CoV-2 and other RNA viruses from N95 level meltblown polypropylene fabric using heat under different humidities. ACS nano, 14(10), 14017–14025.
- Cela-Dablanca, R., Santás-Miguel, V., Fernández-Calviño, D., Arias-Estévez, M., Fernández-Sanjurjo, M.J., Álvarez-Rodríguez, E. and Núñez-Delgado, A., 2021. SARS-CoV-2 and other main pathogenic microorganisms in the environment: Situation in Galicia and Spain. Environmental Research, 197, 111049.
- Chatterjee, L. and Das, P., 2019. Chemical properties of six indigenous rice varieties of Assam. International Journal of Chemical Studies, 7, 2515–2519.
- Chatterley, C. and Linden, K., 2010. Demonstration and evaluation of germicidal UV-LEDs for point-of-use water disinfection. Journal of Water and Health, 8(3), 479–486.
- Cheon, H.L., Shin, J.Y., Park, K.H., Chung, M.S. and Kang, D.H., 2015. Inactivation of foodborne pathogens in powdered red pepper (Capsicum annuum L.) using combined UV-C irradiation and mild heat treatment. Food Control, 50, 441–445.
- Chin, A.W., Chu, J.T., Perera, M.R., Hui, K.P., Yen, H.L., Chan, M.C., Peiris, M. and Poon, L.L., 2020. Stability of SARS-CoV-2 in different environmental conditions. The Lancet Microbe, 1(1), e10.
- Choi, S., Beuchat, L.R., Kim, H. and Ryu, J.H., 2016. Viability of sprout seeds as affected by treatment with aqueous chlorine dioxide and dry heat, and reduction of Escherichia coli O157: H7 and Salmonella enterica on pak choi seeds by sequential treatment with chlorine dioxide, drying, and dry heat. Food Microbiology, 54, 127–132.
- Chotiprasitsakul, D., Kitiyakara, T., Jongkaewwattana, A., Santanirand, P., Jiaranaikulwanich, A., Prahsarn, C., Monmaturapoj, N., Wadwongsri, P., Jeendum, N. and Watcharananan, S., 2020. Approach of using a household device in decontaminating respirators with ultraviolet C during the scarcity in the COVID-19 pandemic, Research Square.

- Cirenza, C.F., Diller, T.E. and Williams, C.B., 2018. Hands-On Workshops to Assist in Students' Conceptual Understanding of Heat Transfer. Journal of Heat Transfer, 140(9), 092001.
- Cramer, A., Tian, E., Yu, S.H., Galanek, M., Lamere, E., Li, J., Gupta, R. and Short, M.P., 2020. Disposable N95 masks pass qualitative fit-test but have decreased filtration efficiency after cobalt-60 gamma irradiation. MedRxiv, 2020–03.
- Crini, G. and Lichtfouse, E., 2019. Advantages and disadvantages of techniques used for wastewater treatment. Environmental Chemistry Letters, 17, 145–155.
- Collins, F.M. and Montalbine, V.I.N.C.E.N.T., 1976. Mycobactericidal activity of glutaraldehyde solutions. Journal of Clinical Microbiology, 4(5), 408–412.
- Conde-Cid, M., Arias-Estévez, M. and Núñez-Delgado, A., 2021a. How to study SARS-CoV-2 in soils?. Environmental Research, 198, 110464.
- Conde-Cid, M., Arias-Estévez, M. and Núñez-Delgado, A., 2021b. SARS-CoV-2 and other pathogens could be determined in liquid samples from soils. Environmental Pollution, 273, 116445.
- Coohill, T.P. and Sagripanti, J.L., 2008. Overview of the inactivation by 254 nm ultraviolet radiation of bacteria with particular relevance to biodefense. Photochemistry and Photobiology, 84(5), 1084–1090.
- Costa, P., Gomes, A.T., Braz, M., Pereira, C. and Almeida, A., 2021. Application of the resazurin cell viability assay to monitor Escherichia coli and Salmonella typhimurium inactivation mediated by phages. Antibiotics, 10(8), 974.
- Coulthard, C.E. and Sykes, G., 1936. The germicidal effect of alcohol with special reference to its action on bacterial spores. Pharmaceutical Journal, 137, 79–81.
- Damit, B., Lee, C. and Wu, C.Y., 2011. Flash infrared radiation disinfection of fibrous filters contaminated with bioaerosols. Journal of Applied Microbiology, 110(4), 1074–1084.
- Darmady, E.M., Hughes, K.E.A., Jones, J.D., Prince, D. and Tuke, W., 1961. Sterilization by dry heat. Journal of Clinical Pathology, 14(1), 38–44.
- de Groot, T., Chowdhary, A., Meis, J.F. and Voss, A., 2019. Killing of Candida auris by UV-C: Importance of exposure time and distance. Mycoses, 62(5), 408–412.

- Deepa, A., Kuppan, P. and Krishnan, P., 2020. A comparative study of structural changes in conventional and unconventional machining and mechanical properties evaluation of polypropylene based self-reinforced composites. Science and Engineering of Composite Materials, 27(1), 108–118.
- DeLeo, P.C., Huynh, C., Pattanayek, M., Schmid, K.C. and Pechacek, N., 2020. Assessment of ecological hazards and environmental fate of disinfectant quaternary ammonium compounds. Ecotoxicology and Environmental Safety, 206, 111116.
- Devraj, L., Natarajan, V., Vadakkeppulpara Ramachandran, S., Manicakam, L. and Sarvanan, S., 2020. Influence of microwave heating as accelerated aging on physicochemical, texture, pasting properties, and microstructure in brown rice of selected Indian rice varieties. Journal of Texture Studies, 51(4), 663–679.
- Ding, C., Khir, R., Pan, Z., Wood, D.F., Venkitasamy, C., Tu, K., El-Mashad, H. and Berrios, J., 2018. Influence of infrared drying on storage characteristics of brown rice. Food Chemistry, 264, 149–156.
- Ding, C., Khir, R., Pan, Z., Zhao, L., Tu, K., El-Mashad, H. and McHugh, T.H., 2015. Improvement in shelf life of rough and brown rice using infrared radiation heating. Food and Bioprocess Technology, 8, 1149–1159.
- Dixit, P.M. and Dixit, U.S., 2008. Modeling of Metal Forming and Machining Processes: By Finite Element and Soft Computing Methods, Springer-Verlag; London.
- Duong, T.N., Hien, N.T., Nghia, N.D., Khoa, N.T., Tuan, N.H., Tu, T.A., Tu, N.H., Phuong, H.V.M. and Anh, D.D., 2021. The first community outbreak of COVID-19 in Viet Nam: description and lessons learned. Western Pacific Surveillance and Response Journal: WPSAR, 12(2), 42.
- Eggers, M., Koburger-Janssen, T., Eickmann, M. and Zorn, J., 2018. In vitro bactericidal and virucidal efficacy of povidone-iodine gargle/mouthwash against respiratory and oral tract pathogens. Infectious Diseases and Therapy, 7, 249–259.
- Eppinger, S.D. and Ulrich, K., 1995. Product Design and Development.
- Fabian, C. and Ju, Y.H., 2011. A review on rice bran protein: its properties and extraction methods. Critical reviews in food science and nutrition, 51(9), 816–827.

- Faruq, G., Mohamad, O., and Meisner, M., 2003. Kernel ageing: An analysis in four Malaysian rice varieties. International Journal of Agriculture and Biology, 5(3), 230–232.
- Faruq, G., Prodhan, Z.H. and Nezhadahmadi, A., 2015. Effects of ageing on selected cooking quality parameters of rice. International Journal of food properties, 18(4), 922–933.
- Feisel, L.D. and Rosa, A.J., 2005. The role of the laboratory in undergraduate engineering education. Journal of Engineering Education, 94(1), 121–130.
- Feldmann, F., Shupert, W.L., Haddock, E., Twardoski, B. and Feldmann, H., 2019. Gamma irradiation as an effective method for inactivation of emerging viral pathogens. The American Journal of Tropical Medicine and Hygiene, 100(5), 1275.
- Fenoglio, D., Ferrario, M., García Carrillo, M., Schenk, M. and Guerrero, S., 2020. Characterization of microbial inactivation in clear and turbid juices processed by short-wave ultraviolet light. Journal of Food Processing and Preservation, 44(6), e14452.
- Ferreira, C.D., Lang, G.H., da Silva Lindemann, I., da Silva Timm, N., Hoffmann, J.F., Ziegler, V. and de Oliveira, M., 2021. Postharvest UV-C irradiation for fungal control and reduction of mycotoxins in brown, black, and red rice during long-term storage. Food Chemistry, 339, 127810.
- Fischer, B., Knabbe, C. and Vollmer, T., 2020. SARS-CoV-2 IgG seroprevalence in blood donors located in three different federal states, Germany, March to June. Eurosurveillance, 25(28), 2001285.
- Fowler, C.B., Evers, D.L., O'Leary, T.J. and Mason, J.T., 2011. Antigen retrieval causes protein unfolding: evidence for a linear epitope model of recovered immunoreactivity. Journal of Histochemistry and Cytochemistry, 59(4), 366–381.
- Gaber, S.E., Hashem, A.H., El-Sayyad, G.S. and Attia, M.S., 2023. Antifungal activity of myco-synthesized bimetallic ZnO-CuO nanoparticles against fungal plant pathogen Fusarium oxysporum. Biomass Conversion and Biorefinery, 1–15.
- Gadola, M. and Chindamo, D., 2019. Experiential learning in engineering education: The role of student design competitions and a case study. International Journal of Mechanical Engineering Education, 47(1), 3–22.

- Gadzhanov, S. and Nafalski, A., 2010. Pedagogical effectiveness of remote laboratories for measurement and control. World Transactions on Engineering and Technology Education, 8(2), 162–167.
- Gautam, A., Chetia, S.K., Modi, M.K. and Ahmed, T., 2018. Phenotypic screening and evaluation of Sub1 introgressed lines in popular rice varieties ranjit and bahadur of Assam, India. International Journal of Current Microbiology and Applied Sciences, 7(9), 1744–1755.
- Gautam, D., Umagiliyage, A.L., Dhital, R., Joshi, P., Watson, D.G., Fisher, D.J. and Choudhary, R., 2017. Nonthermal pasteurization of tender coconut water using a continuous flow coiled UV reactor. LWT-Food Science and Technology, 83, 127–131.
- Gayán, E., García-Gonzalo, D., Álvarez, I. and Condón, S., 2014. Resistance of Staphylococcus aureus to UV-C light and combined UV-heat treatments at mild temperatures. International Journal of Food Microbiology, 172, 30–39.
- Gayán, E., Mañas, P., Álvarez, I. and Condón, S., 2013. Mechanism of the synergistic inactivation of Escherichia coli by UV-C light at mild temperatures. Applied Environmental Microbiology, 79(14), 4465–4473.
- Gayán, E., Serrano, M., Raso, J., Álvarez, I. and Condón, S., 2012. Inactivation of Salmonella enterica by UV-C light alone and in combination with mild temperatures. Applied Environmental Microbiology, 78(23), 8353–8361.
- Gerba, C.P., 2015. Quaternary ammonium biocides: efficacy in application. Applied and Environmental Microbiology, 81(2), 464–469.
- Ghisaidoobe, A.B. and Chung, S.J., 2014. Intrinsic tryptophan fluorescence in the detection and analysis of proteins: a focus on Förster resonance energy transfer techniques. International journal of Molecular Sciences, 15(12), 22518–22538.
- Gonzalez-Buelga, A., Renaud-Assemat, I., Selwyn, B., Ross, J. and Lazar, I., 2022. Development and delivery of a work experience week programme for mechanical engineering. International Journal of Mechanical Engineering Education, 50(2), 349–363.
- González, C.M., 2021. Cleaning with UV Light. Mechanical Engineering, 143(1), 32–33.

- Gopisetty, V.V.S., Patras, A., Pendyala, B., Kilonzo-Nthenge, A., Ravi, R., Pokharel, B., Zhang, L., Si, H. and Sasges, M., 2019. UV-C irradiation as an alternative treatment technique: Study of its effect on microbial inactivation, cytotoxicity, and sensory properties in cranberry-flavored water. Innovative food science & emerging technologies, 52, 66–74.
- Gouma, M., Álvarez, I., Condón, S., Gayán, E. and Technologies, E., 2015. Modelling microbial inactivation kinetics of combined UV-H treatments in apple juice. Innovative Food Science, 27, 111–120.
- Govindaraj, S. and Muthuraman, M.S., 2015. Systematic review on sterilization methods of implants and medical devices. International Journal of ChemTech Research, 8(2), 897–911.
- Goyal, S.M., Chander, Y., Yezli, S. and Otter, J.A., 2014. Evaluating the virucidal efficacy of hydrogen peroxide vapour. Journal of Hospital Infection, 86(4), 255–259.
- Gujral, H.S. and Kumar, V., 2003. Effect of accelerated aging on the physicochemical and textural properties of brown and milled rice. Journal of Food Engineering, 59(2–3), 117–121.
- Halls, N., 1992. The microbiology of irradiation sterilization. Medical Device Technology, 3(6), 37–45.
- Hamanaka, D., Norimura, N., Baba, N., Mano, K., Kakiuchi, M., Tanaka, F. and Uchino, T., 2011. Surface decontamination of fig fruit by combination of infrared radiation heating with ultraviolet irradiation. Food Control, 22(3–4), 375–380.
- Harrell, C.R., Djonov, V., Fellabaum, C. and Volarevic, V., 2018. Risks of using sterilization by gamma radiation: the other side of the coin. International Journal of Medical Sciences, 15(3), 274.
- Hasan, A., Waibhaw, G. and Pandey, L.M., 2018a. Conformational and organizational insights into serum proteins during competitive adsorption on self-assembled monolayers. Langmuir, 34(28), 8178–8194.
- Hasan, A., Saxena, V. and Pandey, L.M., 2018b. Surface functionalization of Ti6Al4V via self-assembled monolayers for improved protein adsorption and fibroblast adhesion. Langmuir, 34(11), 3494–3506.

- Hawe, A., Hulse, W.L., Jiskoot, W. and Forbes, R.T., 2011. Taylor dispersion analysis compared to dynamic light scattering for the size analysis of therapeutic peptides and proteins and their aggregates. Pharmaceutical Research, 28(9), 2302–2310.
- Heilingloh, C.S., Aufderhorst, U.W., Schipper, L., Dittmer, U., Witzke, O., Yang, D., Zheng, X., Sutter, K., Trilling, M., Alt, M. and Steinmann, E., 2020. Susceptibility of SARS-CoV-2 to UV irradiation. American Journal of Infection Control, 48(10), 1273–1275.
- Henwood, A.F., 2020. Coronavirus disinfection in histopathology. Journal of Histotechnology, 43(2), 102–104.
- Herzog, A.B., Pandey, A.K., Reyes-Gastelum, D., Gerba, C.P., Rose, J.B. and Hashsham, S.A., 2012. Evaluation of sample recovery efficiency for bacteriophage P22 on fomites. Applied and Environmental Microbiology, 78(22), 7915–7922.
- Hewavitharana, G.G., Perera, D.N., Navaratne, S.B. and Wickramasinghe, I., 2020. Extraction methods of fat from food samples and preparation of fatty acid methyl esters for gas chromatography: A review. Arabian Journal of Chemistry, 13(8), 6865–6875.
- Hidaka, Y. and Kubota, K., 2006. Study on the Sterilization of Grain Surface Using UV Radiation—Development and Evaluation of UV Irradiation Equipment—. Japan Agricultural Research Quarterly: JARQ, 40(2), 157–161.
- Hiep, N.T., Nguyen, M.K., Nhut, H.T., Hung, N.T.Q., Manh, N.C., Lin, C., Chang, S.W., Um, M.J. and Nguyen, D.D., 2023. A review on sterilization methods of environmental decontamination to prevent the coronavirus SARS-CoV-2 (COVID-19 virus): A new challenge towards eco-friendly solutions. Science of The Total Environment, 904, 166021.
- Holstermann, N., Grube, D. and Bögeholz, S., 2010. Hands-on activities and their influence on students' interest. Research in Science Education, 40(5), 743–757.
- Hsu, B.B., Wong, S.Y., Hammond, P.T., Chen, J. and Klibanov, A.M., 2011. Mechanism of inactivation of influenza viruses by immobilized hydrophobic polycations. Proceedings of the National Academy of Sciences, 108(1), 61–66.
- Hu, Y. and Ma, L., 2021. Effect of surface treatment of polypropylene (PP) fiber on the sulfate corrosion resistance of cement mortar. Materials, 14(13), 3690.

- Hubbard, R.E. and Haider, M.K., 2010. Hydrogen bonds in proteins: role and strength. eLS.
- Hugo, W.B., 1991. A brief history of heat and chemical preservation and disinfection. Journal of Applied Bacteriology. Oxford, 71(1), 9–18.
- Iannazzo, D., Pistone, A., Ziccarelli, I. and Galvagno, S., 2018. Graphene-based materials for application in pharmaceutical nanotechnology. In Fullerens, Graphenes and Nanotubes, 297–329, William Andrew Publishing.
- Ijaz, M.K., Nims, R.W., Zhou, S.S., Whitehead, K., Srinivasan, V., Kapes, T., Fanuel, S., Epstein, J.H., Daszak, P., Rubino, J.R. and McKinney, J., 2021. Microbicidal actives with virucidal efficacy against SARS-CoV-2 and other beta-and alpha-coronaviruses and implications for future emerging coronaviruses and other enveloped viruses. Scientific Reports, 11(1), 5626.
- Inagaki, H., Saito, A., Sugiyama, H., Okabayashi, T. and Fujimoto, S., 2020. Rapid inactivation of SARS-CoV-2 with deep-UV LED irradiation. Emerging Microbes and Infections, 9(1), 1744–1747.
- Indiarto, R. and Nurannisa, R.L., 2021. Aging technique of rice and its characteristics. International Journal of Scientific & Technology Research, 10(1), 27–31.
- Indiarto, R. and Qonit, M.A.H., 2020. A review of irradiation technologies on food and agricultural products. International Journal of Scientific and Technology Research, 9(1), 4411–4414.
- Jildeh, Z.B., Wagner, P.H. and Schöning, M.J., 2021. Sterilization of objects, products, and packaging surfaces and their characterization in different fields of industry: The status in 2020. physica status solidi (a), 218(13), 2000732.
- Jinia, A.J., Sunbul, N.B., Meert, C.A., Miller, C.A., Clarke, S.D., Kearfott, K.J., Matuszak, M.M. and Pozzi, S.A., 2020. Review of sterilization techniques for medical and personal protective equipment contaminated with SARS-CoV-2. IEEE Access, 8, 111347–111354.

- Kalita, T., Gohain, U.P. and Hazarika, J., 2021. Effect of different processing methods on the nutritional value of rice. Current Research in Nutrition and Food Science Journal, 9(2), 683–691.
- Kampf, G., Todt, D., Pfaender, S. and Steinmann, E., 2020a. Persistence of coronaviruses on inanimate surfaces and their inactivation with biocidal agents. Journal of Hospital Infection, 104(3), 246–251.
- Kampf, G., Voss, A. and Scheithauer, S., 2020b. Inactivation of coronaviruses by heat. Journal of Hospital Infection, 105(2), 348–349.
- Karami, Z., Youssefi, M. and Borhani, S., 2013. The effects of UV irradiation exposure on the structure and properties of polypropylene/ZnO nanocamposite fibers. Fibers and Polymers, 14, 1627–1634.
- Kariwa, H., Fujii, N. and Takashima, I., 2006. Inactivation of SARS coronavirus by means of povidone-iodine, physical conditions and chemical reagents. Dermatology, 212 (Suppl. 1), 119–123.
- Karkoub, M. and Abdulla, S., 2020. Transformative learning experiences in mechanical engineering through mechatronics: From high school to college. International Journal of Mechanical Engineering Education, 48(1), 3–31.
- Keawpeng, I. and Venkatachalam, K., 2015. Effect of aging on changes in rice physical qualities. International Food Research Journal, 22(6), 2180–2187.
- Kersten, S., 2018. Approaches of engineering pedagogy to improve the quality of teaching in engineering education. In vocational Teacher Education in Central Asia, edited by J. Dummer et al., Springer, Cham, 129–139.
- Khir, R., Pan, Z., Salim, A., Hartsough, B.R. and Mohamed, S., 2011. Moisture diffusivity of rough rice under infrared radiation drying. LWT-Food Science and Technology, 44(4), 1126–1132.
- Khir, R., Pan, Z., Salim, A. and Thompson, J.F., 2007. Drying characteristics and quality of rough rice under infrared radiation heating. ASAE Annual Meeting (p.1). American Society of Agricultural and Biological Engineers.
- Khir, R., Pan, Z., Thompson, J.F., El-Sayed, A.S., Hartsough, B.R. and El-Amir, M.S., 2014. Moisture removal characteristics of thin layer rough rice under sequenced

infrared radiation heating and cooling. Journal of Food Processing and Preservation, 38(1), 430–440.

- Kong, J. and Yu, S., 2007. Fourier transform infrared spectroscopic analysis of protein secondary structures. Acta biochimica et biophysica Sinica, 39(8), 549–559.
- Kowacz, M. and Warszyński, P., 2018. Effect of infrared light on protein behavior in contact with solid surfaces. Colloids and Surfaces A: Physicochemical and Engineering Aspects, 557, 94–105.
- Kozono, L., Fenoglio, D., Ferrario, M. and Guerrero, S., 2023. Inactivation of Alicyclobacillus acidoterrestris spores, single or composite Escherichia coli and native microbiota in isotonic fruit-flavoured sports drinks processed by UV-C light. International Journal of Food Microbiology, 386, 110024.
- Kratzel, A., Todt, D., V'kovski, P., Steiner, S., Gultom, M., Thao, T.T.N., Ebert, N., Holwerda, M., Steinmann, J., Niemeyer, D. and Dijkman, R., 2020. Inactivation of severe acute respiratory syndrome coronavirus 2 by WHO-recommended hand rub formulations and alcohols. Emerging Infectious Diseases, 26(7), 1592.
- Krishnamurthy, K., Tewari, J.C., Irudayaraj, J. and Demirci, A., 2010. Microscopic and spectroscopic evaluation of inactivation of Staphylococcus aureus by pulsed UV light and infrared heating. Food and Bioprocess Technology, 3, 93–104.
- Kumar, S., Thambiraja, T.S., Karuppanan, K. and Subramaniam, G., 2022. Omicron and Delta variant of SARS-CoV-2: a comparative computational study of spike protein. Journal of Medical Virology, 94(4), 1641–1649.
- Lakowicz, J.R. ed., 2006. Principles of fluorescence spectroscopy. Boston, MA: springer US.
- Lan, J., Ge, J., Yu, J., Shan, S., Zhou, H., Fan, S., Zhang, Q., Shi, X., Wang, Q., Zhang, L. and Wang, X., 2020. Structure of the SARS-CoV-2 spike receptor-binding domain bound to the ACE2 receptor. Nature, 581(7807), 215–220.
- Lancaster, M.V. and Fields, R.D., Alamar Biosciences Laboratory Inc, 1996. Antibiotic and cytotoxic drug susceptibility assays using resazurin and poising agents. U.S. Patent 5,501,959.

- Lauritano, D., Moreo, G., Limongelli, L., Nardone, M. and Carinci, F., 2020. Environmental disinfection strategies to prevent indirect transmission of SARS-CoV2 in healthcare settings. Applied Sciences, 10(18), 6291.
- Lee, J., Bong, C., Lim, W., Bae, P.K., Abafogi, A.T., Baek, S.H., Shin, Y.B., Bak, M.S. and Park, S., 2021. Fast and easy disinfection of coronavirus-contaminated face masks using ozone gas produced by a dielectric barrier discharge plasma generator. Environmental Science and Technology Letters, 8(4), 339–344.
- Lee, J.W., Daly, S.R., Huang-Saad, A., Rodriguez, G. and Seifert, C.M., 2020. Cognitive strategies in solution mapping: How engineering designers identify problems for technological solutions. Design Studies, 71, 100967.
- Lee, Y.N., Chen, L.K., Ma, H.C., Yang, H.H., Li, H.P. and Lo, S.Y., 2005. Thermal aggregation of SARS-CoV membrane protein. Journal of Virological Methods, 129(2), 152–161.
- Lenarduzzi, V. and Taibi, D., 2016. MVP explained: A systematic mapping study on the definitions of minimal viable product. In 2016 42th Euromicro Conference on Software Engineering and Advanced Applications (SEAA), August, (112–119). IEEE.
- Li, S., Gu, A., Xue, J., Liang, G. and Yuan, L., 2013. The influence of the short-term ultraviolet radiation on the structure and properties of poly (p-phenylene terephthalaramide) fibers. Applied Surface Science, 265, 519–526.
- Li, Z. and Hirst, J.D., 2020. Computed optical spectra of SARS-CoV-2 proteins. Chemical Physics Letters, 758, 137935.
- Liao, L., Xiao, W., Zhao, M., Yu, X., Wang, H., Wang, Q., Chu, S. and Cui, Y., 2020. Can N95 respirators be reused after disinfection? How many times?. ACS nano, 14(5), 6348–6356.
- Linden, K.G., Hull, N. and Speight, V., 2019. Thinking outside the treatment plant: UV for water distribution system disinfection. Accounts of Chemical Research, 52(5), 1226–1233.
- Liu, H., Du, Y., Wang, X. and Sun, L., 2004. Chitosan kills bacteria through cell membrane damage. International Journal of Food Microbiology, 95(2), 147–155.

- Liu, H., Elkin, I., Chen, J. and Klibanov, A.M., 2015. Why do some immobilized N-alkylated polyethylenimines far surpass others in inactivating influenza viruses? Biomacromolecules, 16(1), 351–356.
- Lokman, S.M., Rasheduzzaman, M., Salauddin, A., Barua, R., Tanzina, A.Y., Rumi, M.H., Hossain, M.I., Siddiki, A.Z., Mannan, A. and Hasan, M.M., 2020. Exploring the genomic and proteomic variations of SARS-CoV-2 spike glycoprotein: a computational biology approach. Infection, Genetics and Evolution, 84, 104389.
- Ludwig-Begall, L.F., Wielick, C., Dams, L., Nauwynck, H., Demeuldre, P.F., Napp, A., Laperre, J., Haubruge, E. and Thiry, E., 2020. The use of germicidal ultraviolet light, vaporized hydrogen peroxide and dry heat to decontaminate face masks and filtering respirators contaminated with a SARS-CoV-2 surrogate virus. Journal of Hospital Infection, 106(3), 577–584.
- Magrab, E.B., Gupta, S.K., McCluskey, F.P. and Sandborn, P., 2009. Integrated product and process design and development: the product realization process. CRC Press.
- Maris, A., Jacobs, J., Van Horn, G., Stratton, C.W. and Schmitz, J., 2020. Microbiologic proof-of-concept: a novel device combining UV light and ozone for human skin antisepsis. American Journal of Clinical Pathology, 154(Supplement_1), S132–S133.
- Markopoulos, A.P., Fragkou, A., Kasidiaris, P.D. and Davim, J.P., 2015. Gamification in engineering education and professional training. International Journal of Mechanical Engineering Education, 43(2), 118–131.
- Martin, N., Ma, D., Herbet, A., Boquet, D., Winnik, F.M. and Tribet, C., 2014. Prevention of thermally induced aggregation of IgG antibodies by noncovalent interaction with poly (acrylate) derivatives. Biomacromolecules, 15(8), 2952–2962.
- Martins, C.V., Xavier, C.S. and Cobrado, L., 2022. Disinfection methods against SARS-CoV-2: a systematic review. Journal of Hospital Infection, 119, pp.84–117.
- Martinelli, M., Giovannangeli, F., Rotunno, S., Trombetta, C.M. and Montomoli, E., 2017. Water and air ozone treatment as an alternative sanitizing technology. Journal of Preventive Medicine and Hygiene, 58(1), E48.

- Matouk, M.M., El-Kholy, M.M., Tharwat, A. and Shabban, A.S.M., 2014. Drying and sterilization of high moisture rough rice using conduction heating rotary dryer. Journal of Soil Sciences and Agricultural Engineering, 5(3), 295–310.
- McCleary, B.V., McLoughlin, C., Charmier, L.M. and McGeough, P., 2020. Measurement of available carbohydrates, digestible, and resistant starch in food ingredients and products. Cereal Chemistry, 97(1), 114–137.
- McDevitt, J.J., Lai, K.M., Rudnick, S.N., Houseman, E.A., First, M.W. and Milton, D.K., 2007. Characterization of UVC light sensitivity of vaccinia virus. Applied and Environmental Microbiology, 73(18), 5760–5766.
- McDonnell, G. and Russell, A.D., 1999. Antiseptics and disinfectants: activity, action, and resistance. Clinical Microbiology Reviews, 12(1), 147–179.
- Mecha, A.C. and Chollom, M.N., 2020. Photocatalytic ozonation of wastewater: a review. Environmental Chemistry Letters, 18, 1491–1507.
- Mendenhall, W., Beaver, R.J. and Beaver, B.M., 2009. Probability and statistics. New Delhi: Cengage Learning, 525.
- Meng, F., Van Wie, B.J., Thiessen, D.B. and Richards, R.F., 2019. Design and fabrication of very-low-cost engineering experiments via 3-D printing and vacuum forming. International Journal of Mechanical Engineering Education, 47(3), 246–274.
- Meyers, C., Kass, R., Goldenberg, D., Milici, J., Alam, S. and Robison, R., 2021. Ethanol and isopropanol inactivation of human coronavirus on hard surfaces. Journal of Hospital Infection, 107, 45–49.
- Militello, V., Vetri, V. and Leone, M., 2003. Conformational changes involved in thermal aggregation processes of bovine serum albumin. Biophysical Chemistry, 105(1), 133–141.
- Miller, A., Brown, C. and Warner, G., 2019. Guidance on the use of existing ASTM polymer testing standards for ABS parts fabricated using FFF. Smart and Sustainable Manufacturing Systems, 3(1).
- Mishra, R.K., Pandey, S., Hazra, K.K., Mishra, M., Naik, S.S., Bohra, A., Parihar, A.K., Rathore, U.S., Kumar, K., Singh, B. and Singh, N.P., 2023. Biocontrol efficacy and induced defense mechanisms of indigenous Trichoderma strains against Fusarium

wilt [F. udum (Butler)] in pigeonpea. Physiological and molecular plant pathology, 127, 102122.

- Mohr, H., Gravemann, U., Bayer, A. and Müller, T.H., 2009. Sterilization of platelet concentrates at production scale by irradiation with short-wave ultraviolet light. Transfusion, 49(9), 1956–1963.
- Molin, G. and Östlund, K., 1975. Dry-heat inactivation of Bacillus subtilis spores by means of infra-red heating. Antonie van Leeuwenhoek, 41(1), 329–335.
- Molina-Chavarria, A., Félix-Valenzuela, L., Silva-Campa, E. and Mata-Haro, V., 2020. Evaluation of gamma irradiation for human norovirus inactivation and its effect on strawberry cells. International Journal of Food Microbiology, 330, p.108695.
- Moses, J.A., Jayas, D.S. and Alagusundaram, K., 2015. Climate change and its implications on stored food grains. Agricultural Research, 4, 21–30.
- Mubarak, M.T., Ozsahin, I. and Ozsahin, D.U., 2019, March. Evaluation of sterilization methods for medical devices. Advances in Science and Engineering Technology International Conferences (ASET),1–4, IEEE.
- Musto, J.C., Howard, W.E. and Rather, S.S., 2004. Using solid modeling and rapid prototyping in a mechanical engineering outreach program of high school students. International Journal of Mechanical Engineering Education, 32(4), 283–291.
- Nandan, R.G.G.R., Roy, G.G., Lienert, T.J. and Debroy, T., 2007. Three-dimensional heat and material flow during friction stir welding of mild steel. Acta Materialia, 55(3), 883–895.
- Narita, F., Wang, Z., Kurita, H., Li, Z., Shi, Y., Jia, Y. and Soutis, C., 2021. A review of piezoelectric and magnetostrictive biosensor materials for detection of COVID-19 and other viruses. Advanced Materials, 33(1), 2005448.
- Nguyen, T.Q. and Goto, K., 2009. Effects of heat shock treatment on rice quality during storage (Part 2): nutritional and pasting properties changes. Engineering in Agriculture, Environment and Food, 2(3), 89–95.
- Núñez-Delgado, A., 2020. SARS-CoV-2 in soils. Environmental Research, 190, 110045.
- Ochi, S., Takagi, H. and Niki, R., 2002. Mechanical properties of heat-treated natural fibers. WIT Transactions on The Built Environment, 59, 117–125.

- Omar, K.A., Salih, B.M., Abdulla, N.Y., Hussin, B.H. and Rassul, S.M., 2016. Evaluation of starch and sugar content of different rice samples and study their physical properties. Indian Journal of Natural Sciences, 6(36), 11084–11088.
- Omidbakhsh, N. and Sattar, S.A., 2006. Broad-spectrum microbicidal activity, toxicologic assessment, and materials compatibility of a new generation of accelerated hydrogen peroxide-based environmental surface disinfectant. American Journal of Infection Control, 34(5), 251–257.
- Oppenheimer, J.A., Jacangelo, J.G., Laîné, J.M. and Hoagland, J.E., 1997. Testing the equivalency of ultraviolet light and chlorine for disinfection of wastewater to reclamation standards. Water Environment Research, 69(1), 14–24.
- Otieno, B.A., Krause, C.E. and Rusling, J.F., 2016. Bioconjugation of antibodies and enzyme labels onto magnetic beads. In Methods in enzymology, 571, 135–150. Academic Press.
- Pan, Z., Khir, R., Bett-Garber, K.L., Champagne, E.T., Thompson, J.F., Salim, A., Hartsough, B.R. and Mohamed, S., 2011. Drying characteristics and quality of rough rice under infrared radiation heating. Transactions of the ASABE, 54(1), 203–210.
- Pan, Z., Khir, R., Godfrey, L.D., Lewis, R., Thompson, J.F. and Salim, A., 2008. Feasibility of simultaneous rough rice drying and disinfestations by infrared radiation heating and rice milling quality. Journal of Food Engineering, 84(3), 469–479.
- Pandey, L.M., 2020a. Design of engineered surfaces for prospective detection of SARS-CoV-2 using quartz crystal microbalance-based techniques. Expert Review of Proteomics, 17(6), 425–432.
- Pandey, L.M., 2020b. Surface engineering of personal protective equipments (PPEs) to prevent the contagious infections of SARS-CoV-2. Surface Engineering, 36(9), 901–907.
- Pandey, L.M., 2022. Physicochemical factors of bioprocessing impact the stability of therapeutic proteins. Biotechnology Advances, 107909.
- Park, M.J., Kim, J.H. and Oh, S.W., 2019. Inactivation effect of UV-C and mild heat treatment against Salmonella Typhimurium and Escherichia coli O157: H7 on black pepper powder. Food Science and Biotechnology, 28, 599–607.

- Patel, M., 2003. Medical sterilization methods. Lemo USA Inc.
- Patterson, E.I., Prince, T., Anderson, E.R., Casas-Sanchez, A., Smith, S.L., Cansado-Utrilla, C., Solomon, T., Griffiths, M.J., Acosta-Serrano, Á., Turtle, L. and Hughes, G.L., 2020. Methods of inactivation of SARS-CoV-2 for downstream biological assays. The Journal of Infectious Diseases, 222(9), 1462–1467.
- Paul, P. and Dixit, U.S., 2011. Development of Toys for Teaching and Learning of Mechanical Engineering. National Conference on Advanced Design and Manufacture, January 6–7, Einstein College of Engineering, Tirunelveli, Tamil Nadu, India.
- Pecher, P. and Arnold, U., 2009. The effect of additional disulfide bonds on the stability and folding of ribonuclease A. Biophysical Chemistry, 141(1), 21–28.
- Pendyala, B., Patras, A., Pokharel, B. and D'Souza, D., 2020. Genomic modeling as an approach to identify surrogates for use in experimental validation of SARS-CoV-2 and HuNoV inactivation by UV-C treatment. Frontiers in Microbiology, 11, 572331.
- Peng, B., He, L.L., Tan, J., Zheng, L.T., Zhang, J.T., Qiao, Q.W., Wang, Y., Gao, Y., Tian, X.Y., Liu, Z.Y. and Song, X.H., 2019. Effects of rice aging on its main nutrients and quality characters. Journal of Agricultural Science, 11(17), 44.
- Penney, W.R. and Clausen, E.C. eds., 2018. Fluid mechanics and heat transfer: inexpensive demonstrations and laboratory exercises. CRC Press, Taylor and Francis Group.
- Pithon, M.M., dos Santos, R.L., Martins, F.O., Romanos, M.T.V. and Araújo, M.T., 2010. Cytotoxicity of orthodontic elastic chain bands after sterilization by different methods. orthodontic waves, 69(4), 151–155.
- Quero-Jiménez, P.C., Montenegro, O.N., Sosa, R., Pérez, D.L., Rodríguez, A.S., Méndez, R.R., Alonso, A.C., Corrales, A.J., de la Torre, J.B., Acosta, J.V. and Hernández, N.B., 2019. Total carbohydrates concentration evaluation in products of microbial origin. Afinidad, 76(587), 83–90.
- Quevedo, R., Bastías, J.M., Espinoza, T., Ronceros, B., Balic, I. and Muñoz, O., 2020. Inactivation of Coronaviruses in food industry: The use of inorganic and organic disinfectants, ozone, and UV radiation. Scientia Agropecuaria, 11(2), 257–266.

- Rabenau, H.F., Cinatl, J., Morgenstern, B., Bauer, G., Preiser, W. and Doerr, H.W., 2005a. Stability and inactivation of SARS coronavirus. Medical Microbiology and Immunology, 194, 1–6.
- Rabenau, H., Kampf, G., Cinatl, J. and Doerr, H.W., 2005b. Efficacy of various disinfectants against SARS coronavirus. Journal of Hospital Infection, 61(2), 107–111.
- Racioppi, F., Daskaleros, P.A., Besbelli, N., Borges, A., Deraemaeker, C., Magalini, S.I., Arrifta, R.M., Pulce, C., Ruggerone, M.L. and Vlachos, P., 1994. Household bleaches based on sodium hypochlorite: review of acute toxicology and poison control center experience. Food and Chemical Toxicology, 32(9), 845–861.
- Ramos, A.H., Rockenbach, B.A., Ferreira, C.D., Gutkoski, L.C. and de Oliveira, M., 2019. Characteristics of flour and starch isolated from red rice subjected to different drying conditions. Starch-Stärke, 71(7–8), 1800257.
- Rath, S.L. and Kumar, K., 2020. Investigation of the effect of temperature on the structure of SARS-CoV-2 spike protein by molecular dynamics simulations. Frontiers in Molecular Biosciences, 7, 583523.
- Ratseewo, J., Warren, F.J., Meeso, N. and Siriamornpun, S., 2022. Effects of Far-Infrared Radiation Drying on Starch Digestibility and the Content of Bioactive Compounds in Differently Pigmented Rice Varieties. Foods, 11(24), 4079.
- Raungrusmee, S. and Anal, A.K., 2019. Effects of lintnerization, autoclaving, and freeze-thaw treatments on resistant starch formation and functional properties of pathumthani 80 rice starch. Foods, 8(11), 558.
- Reader, P.P., Olkhov, R.V., Reeksting, S., Lubben, A., Hyde, C.J. and Shaw, A.M., 2019. A rapid and quantitative technique for assessing IgG monomeric purity, calibrated with the NISTmAb reference material. Analytical and Bioanalytical Chemistry, 411(24), 6487–6496.
- Reed, N.G., 2010. The history of ultraviolet germicidal irradiation for air disinfection. Public Health Reports, 125(1), 15–27.
- Renner, J.W., Abraham, M.R. and Birnie, H.H., 1985. Secondary School Students' Beliefs about the Physics Laboratory. Science Education, 69(5), 649–663.
- Ries, E., 2009. Minimum viable product: a guide. Startup Lessons Learned, 3(1).

- Ries, E., 2011. The lean startup: How today's entrepreneurs use continuous innovation to create radically successful businesses. Currency.
- Rubbo, S.D., Gardner, J.F. and Webb, R.L., 1967. Biocidal activities of glutaraldehyde and related compounds. Journal of Applied Bacteriology, 30(1), 78–87.
- Rubio-Romero, J.C., del Carmen Pardo-Ferreira, M., Torrecilla-García, J.A. and Calero-Castro, S., 2020. Disposable masks: Disinfection and sterilization for reuse, and non-certified manufacturing, in the face of shortages during the COVID-19 pandemic. Safety Science, 129, 104830.
- Rutala, W.A. and Weber, D.J., 1999. Infection control: the role of disinfection and sterilization. Journal of Hospital Infection, 43, S43–S55.
- Rutala, W.A. and Weber, D.J., 2008. Guideline for disinfection and sterilization in healthcare facilities. US Centers for Disease Control.
- Rutala, W.A. and Weber, D.J., 2013. Disinfection and sterilization: an overview. American journal of infection control, 41(5), S2–S5.
- Rutala, W.A., Gergen, M.F., Sickbert-Bennett, E.E. and Weber, D.J., 2020. Comparative evaluation of the microbicidal activity of low-temperature sterilization technologies to steam sterilization. Infection Control and Hospital Epidemiology, 41(4), 391–395.
- Sabino, C.P., Ball, A.R., Baptista, M.S., Dai, T., Hamblin, M.R., Ribeiro, M.S., Santos, A.L., Sellera, F.P., Tegos, G.P. and Wainwright, M., 2020. Light-based technologies for management of COVID-19 pandemic crisis. Journal of Photochemistry and Photobiology B: Biology, 212, 111999.
- Sadaiah, K., Veronica, N., Nagendra, V., Niharika, G., Neeraja, C.N., Surekha, K., Subrahmanyam, D., Ravindra, B.V. and Sanjeeva, R.D., 2018. Methods of Protein Estimation and the Influence of Heat Stress on Rice Grain Protein. International Journal of Pure and Applied Bioscience, 6(3), 159–168.
- Saikrishna, A., Dutta, S., Subramanian, V., Moses, J.A. and Anandharamakrishnan, C., 2018. Ageing of rice: A review. Journal of Cereal Science, 81, 161–170.
- Saini, V., Sikri, K., Batra, S.D., Kalra, P. and Gautam, K., 2020. Development of a highly effective low-cost vaporized hydrogen peroxide-based method for disinfection

of personal protective equipment for their selective reuse during pandemics. Gut Pathogens, 12, 1–11.

- Salazar, E., Kuchipudi, S.V., Christensen, P.A., Eagar, T., Yi, X., Zhao, P., Jin, Z., Long, S.W., Olsen, R.J., Chen, J. and Castillo, B., 2020. Convalescent plasma anti–SARS-CoV-2 spike protein ectodomain and receptor-binding domain IgG correlate with virus neutralization. The Journal of Clinical Investigation, 130(12), 6728–6738.
- Sarada, B.V., Vijay, R., Johnson, R., Rao, T.N. and Padmanabham, G., 2020. Fight against COVID-19: ARCI's technologies for disinfection. Transactions of the Indian National Academy of Engineering, 5, 349–354.
- Saxena, V., Chandra, P. and Pandey, L.M., 2018. Design and characterization of novel Al-doped ZnO nanoassembly as an effective nanoantibiotic. Applied Nanoscience, 8, 1925–1941.
- Schaeffer, A.J., Jones, J.M. and Amundsen, S.K., 1980. Bacterial effect of hydrogen peroxide on urinary tract pathogens. Applied and Environmental Microbiology, 40(2), 337–340.
- Schmidt, S.B., Grüter, L., Boltzmann, M. and Rollnik, J.D., 2020. Prevalence of serum IgG antibodies against SARS-CoV-2 among clinic staff. PloS One, 15(6), e0235417.
- Schuit, M.A., Larason, T.C., Krause, M.L., Green, B.M., Holland, B.P., Wood, S.P., Grantham, S., Zong, Y., Zarobila, C.J., Freeburger, D.L. and Miller, D.M., 2022. SARS-CoV-2 inactivation by ultraviolet radiation and visible light is dependent on wavelength and sample matrix. Journal of Photochemistry and Photobiology B: Biology, 233, 112503.
- Sharma, L.G. and Pandey, L.M., 2021a. Thermomechanical process induces unfolding and fibrillation of bovine serum albumin. Food Hydrocolloids, 112, 106294.
- Sharma, L.G. and Pandey, L.M., 2021b. Shear-induced aggregation of amyloid β (1–40) in a parallel plate geometry. Journal of Biomolecular Structure and Dynamics, 39(17), 6415–6423.
- Sharma, N., Kamni, Singh, V.K., Kumar, S., Lee, Y., Rai, P.K. and Singh, V.K., 2020. Investigation of molecular and elemental changes in rice grains infected by false smut disease using FTIR, LIBS and WDXRF spectroscopic techniques. Applied Physics B, 126, 1–12.

- Shih, C.H., Lee, T.T., Kuo, W.H.J. and Yu, B., 2014. Growth performance and intestinal microflora population of broilers fed aged brown rice. Annals of Animal Science, 14(4), 897–909.
- Shivaprasad, D., Taneja, N.K., Lakra, A. and Sachdev, D., 2021. In vitro and in situ abrogation of biofilm formation in E. coli by vitamin C through ROS generation, disruption of quorum sensing and exopolysaccharide production. Food Chemistry, 341, 128171.
- Shomali, M., Opie, D., Avasthi, T. and Trilling, A., 2015. Nitrogen dioxide sterilization in low-resource environments: a feasibility study. PloS One, 10(6), e0130043.
- Simmons, S.E., Carrion, R., Alfson, K.J., Staples, H.M., Jinadatha, C., Jarvis, W.R., Sampathkumar, P., Chemaly, R.F., Khawaja, F., Povroznik, M. and Jackson, S., 2021. Deactivation of SARS-CoV-2 with pulsed-xenon ultraviolet light: Implications for environmental COVID-19 control. Infection Control and Hospital Epidemiology, 42(2), 127–130.
- Singh, H., Bhardwaj, S.K., Khatri, M., Kim, K.H. and Bhardwaj, N., 2021a. UVC radiation for food safety: An emerging technology for the microbial disinfection of food products. Chemical Engineering Journal, 417, 128084.
- Singh, D., Majumdar, A.G., Gamre, S. and Subramanian, M., 2021b. Membrane damage precedes DNA damage in hydroxychavicol treated E. coli cells and facilitates cooperativity with hydrophobic antibiotics. Biochimie, 180, 158–168.
- Singh, H., Jakhar, R. and Sehrawat, N., 2020. Designing spike protein (S-Protein) based multi-epitope peptide vaccine against SARS COVID-19 by immunoinformatics. Heliyon, 6(11), e05528.
- Singh, S., Kumar, V., Kapoor, D., Dhanjal, D.S., Bhatia, D., Jan, S., Singh, N., Romero, R., Ramamurthy, P.C. and Singh, J., 2021. Detection and disinfection of COVID-19 virus in wastewater. Environmental Chemistry Letters, 19, 1917–1933.
- Sinha, R.P. and Häder, D.P., 2002. UV-induced DNA damage and repair: a review. Photochemical and Photobiological Sciences, 1(4), 225–236.

- Sivakumar, S., Naveen, R., Dhabliya, D., Shankar, B.M. and Rajesh, B.N., 2021. Electronic currency note sterilizer machine. Materials Today: Proceedings, 37, 1442–1444.
- Soponronnarit, S., Chiawwet, M., Prachayawarakorn, S., Tungtrakul, P. and Taechapairoj, C., 2008. Comparative study of physicochemical properties of accelerated and naturally aged rice. Journal of Food Engineering, 85(2), 268–276.
- Sowbhagya, C.M. and Bhattacharya, K.R., 1971. A simplified colorimetric method for determination of amylose content in rice. Starch-Stärke, 23(2), 53–56
- Sozzi, E., Baloch, M., Strasser, J., Fisher, M.B., Leifels, M., Camacho, J., Mishal, N., Elmes, S.F., Allen, G., Gadai, G. and Valenti, L., 2019. A bioassay-based protocol for chemical neutralization of human faecal wastes treated by physico-chemical disinfection processes: A case study on benzalkonium chloride. International Journal of Hygiene and Environmental Health, 222(2), 155–167.
- Spicher, G. and Peters, J., 1976. Microbial resistance to formaldehyde. I. Comparative quantitative studies in some selected species of vegetative bacteria, bacterial spores, fungi, bacteriophages and viruses. Zentralblatt fur Bakteriologie, Parasitenkunde, Infektionskrankheiten und Hygiene. Erste Abteilung Originale. Reihe B: Hygiene, Praventive Medizin, 163(5–6), 486–508.
- Srinivas, T., Bhashyam, M.K., Shankara, R., Vasudeva, S. and Desikachar, H.S.R., 1981. Drying-cum-curing of freshly harvested high moisture paddy by roasting with hot sand. Journal of Food Science and Technology, 18(5), 184–187.
- Stelea, S.D., Pancoska, P., Benight, A.S. and Keiderling, T.A., 2001. Thermal unfolding of ribonuclease A in phosphate at neutral pH: Deviations from the two–state model. Protein Science, 10(5), 970–978.
- Stoll, H.W., 1999. Product design methods and practices. CRC Press.
- Szeto, W., Yam, W.C., Huang, H. and Leung, D.Y., 2020. The efficacy of vacuum-ultraviolet light disinfection of some common environmental pathogens. BMC Infectious Diseases, 20(1), 1–9.
- Takamure, K., Sakamoto, Y., Iwatani, Y., Amano, H., Yagi, T. and Uchiyama, T., 2022. Characteristics of collection and inactivation of virus in air flowing inside a

winding conduit equipped with 280 nm deep UV-LEDs. Environment International, 170, 107580.

- Talpur, M.A., Changying, J., Chandio, F.A., Junejo, S.A. and Mari, I.A., 2011. Application of oven drying method on moisture content of ungrounded and grounded (long and short) rice for storage. Journal of Stored Products and Postharvest Research, 2(12), 245–247.
- Tanaka, N. and Nakajima, A., 1972. Partial melting, recrystallization and thermal shrinkage of polypropylene fibers. Bulletin of the Institute for Chemical Research, Kyoto University, 49(6), 382–389.
- Tanaka, Y., Tsunemi, Y., Kawashima, M. and Nishida, H., 2013. The impact of near-infrared in plastic surgery. Plastic Surgery: An International Journal, 2013, g1–13.
- Tauro, F., Cha, Y., Rahim, F., Sattar Rasul, M., Osman, K., Halim, L., Dennisur, D., Esner, B. and Porfiri, M., 2017. Integrating mechatronics in project-based learning of Malaysian high school students and teachers. International Journal of Mechanical Engineering Education, 45(4), 297-320.
- Thanompolkrung, T., Yongsawatdigul, J. and Tongta, S., 2017. Protein characteristics in relation to textural and pasting properties of rice after storage. Suranaree Journal of Science & Technology, 24(1), 51–62.
- Tilley, F.W. and Schaffer, J.M., 1926. Relation between the chemical constitution and germicidal activity of the monohydric alcohols and phenols. Journal of Bacteriology, 12(5), 303–309.
- Tiwari, R. and Singh, K., 2011. Virtualisation of engineering discipline experiments for an Internet-based remote laboratory. Australasian Journal of Educational Technology, 27(4), 671–692.
- Tizaoui, C., 2020. Ozone: a potential oxidant for COVID-19 virus (SARS-CoV-2). Ozone: Science and Engineering, 42(5), 378–385.
- Trujillo, R. and David, T.J., 1972. Sporostatic and sporocidal properties of aqueous formaldehyde. Applied Microbiology, 23(3), 618–622.
- Unluturk, S., Atılgan, M.R., Baysal, A.H. and Tari, C., 2008. Use of UV-C radiation as a non-thermal process for liquid egg products (LEP). Journal of Food Engineering, 85(4), 561–568.

- Vearasilp, S., Chaisathidvanich, K., Thanapornpoonpong, S., von Hörsten, D. and Lücke, W., 2011. Aging milled rice by radio frequency heat treatment. In Proceedings of the Conference on International Research on Food Security, Natural Resource Management and Rural Development, Stuttgart, Germany (5–7).
- Vermeer, A.W., Bremer, M.G. and Norde, W., 1998. Structural changes of IgG induced by heat treatment and by adsorption onto a hydrophobic Teflon surface studied by circular dichroism spectroscopy. Biochimica et Biophysica Acta (BBA) - General Subjects, 1425(1), 1–12.
- Vermeer, A.W.P. and Norde, W., 2000. The Thermal Stability of Immunoglobulin: Unfolding and Aggregation of a Multi-Domain Protein. Biophysical Journal, 78(1), 394–404.
- Vici, G., Perinelli, D.R., Camilletti, D., Carotenuto, F., Belli, L. and Polzonetti, V., 2021. Nutritional properties of rice varieties commonly consumed in Italy and applicability in Gluten free diet. Foods, 10(6), 1375.
- Vilhunen, S., Särkkä, H. and Sillanpää, M., 2009. Ultraviolet light-emitting diodes in water disinfection. Environmental Science and Pollution Research, 16, 439–442.
- Viscusi, D.J., Bergman, M.S., Eimer, B.C. and Shaffer, R.E., 2009. Evaluation of five decontamination methods for filtering facepiece respirators. Annals of Occupational Hygiene, 53(8), 815–827.
- Viscusi, D.J., King, W.P. and Shaffer, R.E., 2007. Effect of decontamination on the filtration efficiency of two filtering facepiece respirator models. Journal of the International Society for Respiratory Protection, 24(3/4), 93.
- Wallace, C.A., 2016. New developments in disinfection and sterilization. American Journal of Infection Control, 44(5), e23–e27.
- Wang, D., Sun, B.C., Wang, J.X., Zhou, Y.Y., Chen, Z.W., Fang, Y., Yue, W.H., Liu, S.M., Liu, K.Y., Zeng, X.F. and Chu, G.W., 2020. Can masks be reused after hot water decontamination during the COVID-19 pandemic? Engineering, 6(10), 1115–1121.
- Wang, W., Zhao, G., Wu, X. and Zhai, Z., 2015. The effect of high temperature annealing process on crystallization process of polypropylene, mechanical properties,

and surface quality of plastic parts. Journal of Applied Polymer Science, 132(46), 42773, 1–12.

- Wang, Y., Wu, X., Wang, Y., Li, B., Zhou, H., Yuan, G., Fu, Y. and Luo, Y., 2004. Low stability of nucleocapsid protein in SARS virus. Biochemistry, 43(34), 11103–11108.
- Watanabe, A., Iwagami, M., Yasuhara, J., Takagi, H. and Kuno, T., 2023. Protective effect of COVID-19 vaccination against long COVID syndrome: A systematic review and meta-analysis. Vaccine, 41(1), 1783–1790.
- Wigginton, K.R., Menin, L., Sigstam, T., Gannon, G., Cascella, M., Hamidane, H.B., Tsybin, Y.O., Waridel, P. and Kohn, T., 2012. UV Radiation Induces Genome-Mediated, Site-Specific Cleavage in Viral Proteins. ChemBioChem, 13(6), 837–845.
- Xu, Q., Zhang, L., Chen, L., Zhao, X., Wang, X., Hu, M., Le, Y., Xue, F., Li, X. and Zheng, J., 2022. SARS-CoV-2 might transmit through the skin while the skin barrier function could be the mediator. Medical Hypotheses, 159, 110752.
- Yadav, G., Gupta, N., Sood, M., Anjum, N. and Chib, A., 2020. Infrared heating and its application in food processing. The Pharma Innovation Journal, 9(2), 142–151.
- Yang, S., Zhang, Q., Yang, H., Shi, H., Dong, A., Wang, L. and Yu, S., 2022. Progress in infrared spectroscopy as an efficient tool for predicting protein secondary structure. International Journal of Biological Macromolecules. 206, 175–187.
- Yerragopu, P.S. and Palanimuthu, V., 2019. Effect of steaming on accelerated ageing of rice (Oryza sativa L.). International Journal of Current Microbiology and Applied Sciences, 8(02), 358–375.
- Yoo, J.H., 2018. Review of disinfection and sterilization–back to the basics. Infection & Chemotherapy, 50(2), 101–109.
- Yue, C.Y., Sui, G.X. and Looi, H.C., 2000. Effects of heat treatment on the mechanical properties of Kevlar-29 fibre. Composites Science and Technology, 60(3), 421–427.
- Yujie, M., Rae, Z., Kurt, R. and Kelly, B., 2020. Effect of ultraviolet C disinfection treatment on the nanomechanical and topographic properties of N95 respirator filtration microfibers. MRS Advances, 5(56), 2863–2872.

- Zare, M., Amin, M.M., Nikaeen, M., Bina, B., Pourzamani, H., Fatehizadeh, A. and Taheri, E., 2015. Resazurin reduction assay, a useful tool for assessment of heavy metal toxicity in acidic conditions. Environmental Monitoring and Assessment, 187, 1–11.
- Zeng, W., Liu, G., Ma, H., Zhao, D., Yang, Y., Liu, M., Mohammed, A., Zhao, C., Yang, Y., Xie, J. and Ding, C., 2020. Biochemical characterization of SARS-CoV-2 nucleocapsid protein. Biochemical and Biophysical Research Communications, 527(3), 618–623.
- Zhang, J. and Topp, E.M., 2012. Protein G, protein A and protein A-derived peptides inhibit the agitation induced aggregation of IgG. Molecular Pharmaceutics, 9(3), 622–628.
- Zhang, L., Lu, D. and Liu, Z., 2008. How native proteins aggregate in solution: A dynamic Monte Carlo simulation. Biophysical Chemistry, 133(1–3), 71–80.
- Zhang, S., Ye, C., Lin, H., Lv, L. and Yu, X., 2015. UV disinfection induces a VBNC state in Escherichia coli and Pseudomonas aeruginosa. Environmental Science and Technology, 49(3), 1721–1728.
- Zrimšek, P., Kunc, J., Kosec, M. and Mrkun, J., 2004. Spectrophotometric application of resazurin reduction assay to evaluate boar semen quality. International Journal of Andrology, 27(1), 57–62.
- Zucker, I., Lester, Y., Alter, J., Werbner, M., Yecheskel, Y., Gal-Tanamy, M. and Dessau, M., 2021. Pseudoviruses for the assessment of coronavirus disinfection by ozone. Environmental Chemistry Letters, 19, 1779–1785.

Appendix A

Sensory Test and Feedback on the Taste as well as Appearance

A sensory test was designed to compare the taste of artificially aged rice with the naturally aged rice samples. An amount of 150 gm of both artificially aged rice and naturally aged rice was taken for cooking in a rice cooker. The same amount of 280 mL of water was used for cooking each rice. A feedback form with a set of questions was made for this survey. Table A1 shows the questions that participants were asked to answer on a rating scale of 1 to 10. Questions were related to taste as well as the appearance of both artificially aged rice and naturally aged rice.

Table A1. Questionnaire for survey

	Question **(**Answer each question in a rating scale of 1 to 10**)**
Q1.	Sweetness? (0: Not at all sweet; 10: Very sweet)
Q2.	Appearance? (0: Very bad; 10: Very good)
Q3.	Softness? (0: Very hard; 10: Very soft)
Q4.	Overall experience? (0: Very bad; 10: Very good)

Response to questions in the sensory test

Questions asked in the test were related to the taste and appearance of both naturally aged rice and artificially aged rice, as listed in Table A1. A total 15 number of respondents participated in this test and no sensory booths were used. One spoon of each cooked rice was served to each participant. Arithmetic mean and standard deviation were obtained for each response. The average rating against Q1 was obtained as 6.14 ± 1.25 and 5.93 ± 1.28 points out of 10 for naturally aged and artificially aged rice, respectively. Respondents found naturally aged rice a little sweeter than artificially aged one. Against Q2, ratings obtained were 7.33 ± 1.19 and 7.8 ± 1.38 points for naturally and artificially aged rice, respectively. Participants liked the appearance of artificially aged rice than the other one. Q3 gained 6.8 ± 1.33 and 7.0 ± 1.32 ratings for naturally aged and artificially aged rice, respectively. Respondents felt artificially aged rice softer than naturally aged rice while eating. Ratings obtained by Q4 were 7.23 ± 1.33 and 7.33 ± 1.14 for naturally aged and artificially aged rice, respectively. Participants' overall experiences were better with artificially aged rice than with naturally aged rice. This sensory

test resulted in a better experience regarding taste and appearance in the case of artificially aged rice than naturally aged one. A detailed sensory test will be carried out in future research.

List of Publications from the Thesis

Journal Publications

1. Mahanta, N., Saxena, V., Pandey, L.M., Batra, P. and Dixit, U.S., 2021. Performance study of a sterilization box using a combination of heat and ultraviolet light irradiation for the prevention of COVID-19. **Environmental Research, 198,** 111309.
2. Mahanta, N., Sharma, S., Sharma, L.G., Pandey, L.M. and Dixit, U.S., 2022. Unfolding of the SARS-CoV-2 spike protein through infrared and ultraviolet-C radiation based disinfection. **International Journal of Biological Macromolecules, 221,** 71–82.
3. Mahanta, N. and Dixit, U.S., 2023. A Study on Degradation of N95 Respirator After Disinfecting it by Various Techniques. **Journal of The Institution of Engineers (India): Series C, 104(5),** 887–895.
4. Mahanta, N., Sharma, L.G., Pandey, L.M. and Dixit, U.S., 2024. Artificial aging of rice using a sterilization box equipped with infrared heating and ultraviolet-C radiation. **Journal of Food Process Engineering, 47(2)**, e14544.

Book Chapter

1. Mahanta, N., Dixit, U.S. and Davim, J.P., 2023. A Pedagogical Gadget for Teaching Heat Transfer. In: Dixit, U.S. et al. (eds.) **Engineering Pedagogy: A Collection of Articles in Honor of Prof. Amitabha Ghosh** (127–144). Singapore: Springer Nature Singapore.